Is the future of HPCSE quantum?

Matthias Möller | HPCSE 2026 | May 18-21, 2026 | Hotel Soláň

TU Delft

V0.1

Moore's law

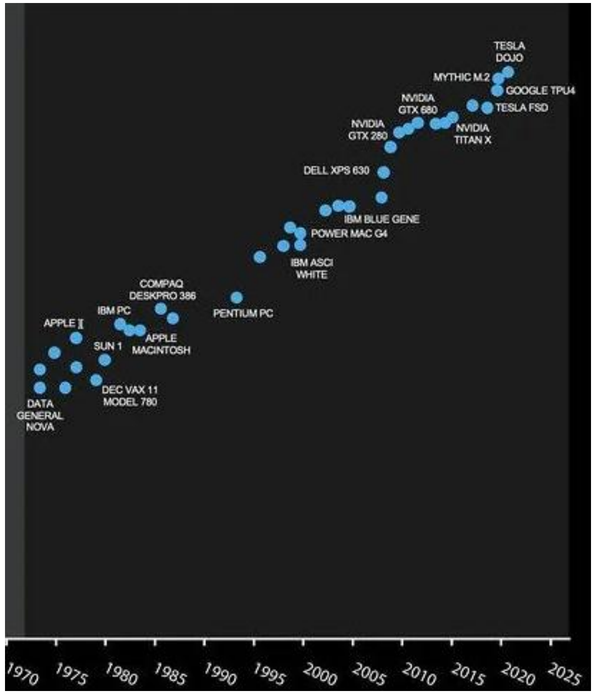
TESLA DOJO
MYTHIC M.2
GOOGLE TPU4
TESLA FSD
NVIDIA GTX 680
NVIDIA TITAN X
NVIDIA GTX 280
DELL XPS 630
IBM BLUE GENE
POWER MAC G4
IBM ASCI WHITE
PENTIUM PC
COMPAQ DESKPRO 386
IBM PC
APPLE II
APPLE MACINTOSH
SUN 1
DEC VAX 11 MODEL 780
DATA GENERAL NOVA
1970
1975
1980
1985
1990
1995
2000
2005
2010
2015
2020
2025

Moore's law

Enabled by changes in the computer technology

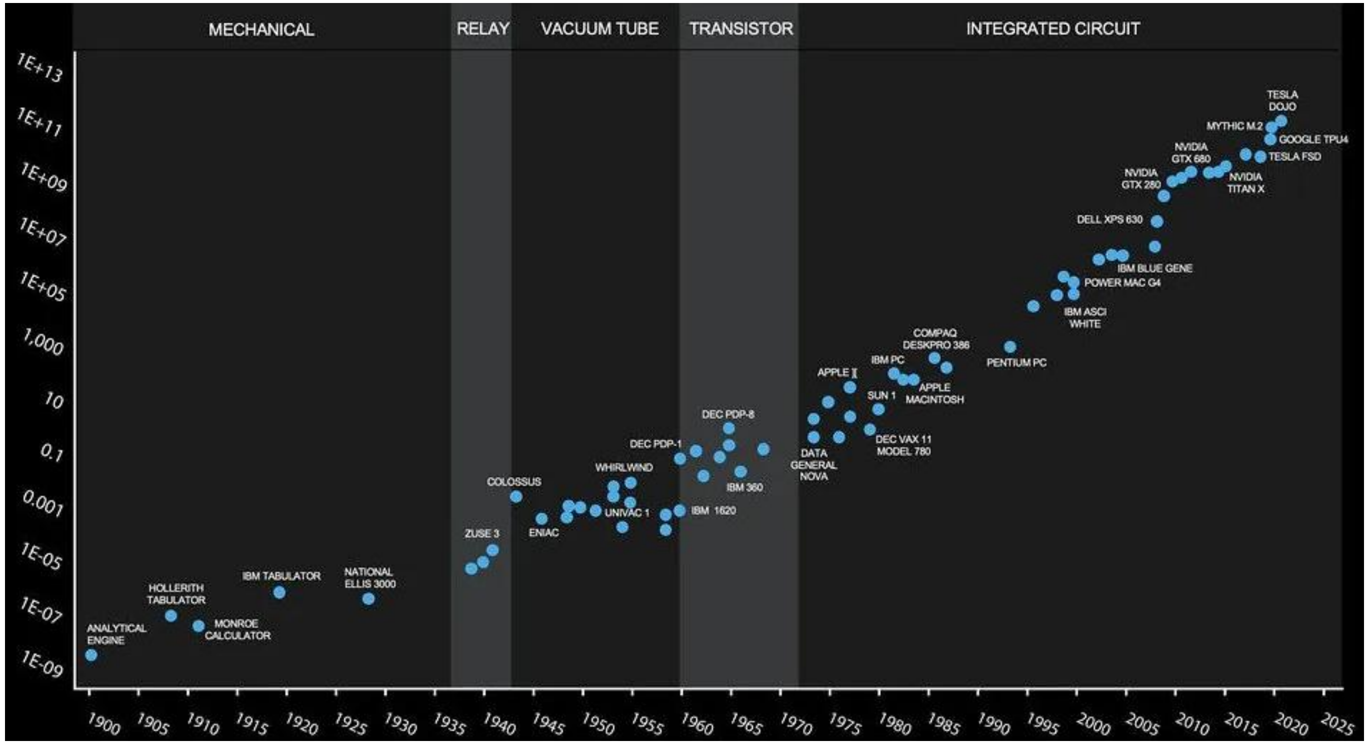

?

Enabled by technology improvements

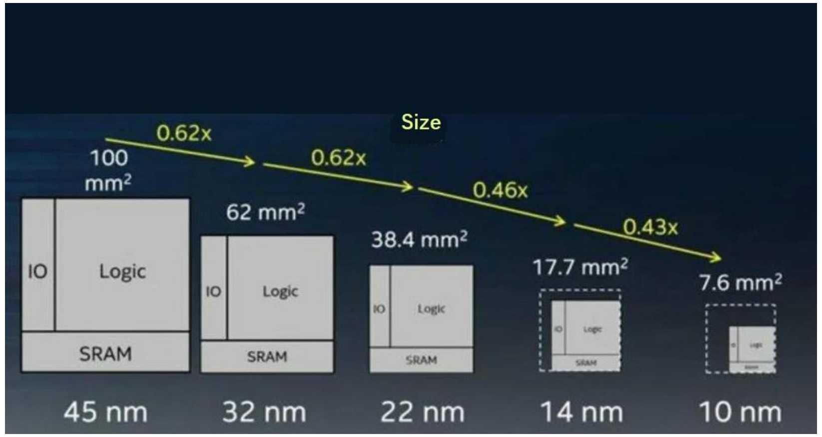

Left: https://www.unite.ai/mooreslaw/, right: https://www.utmel.com/blog/categories/integrated%20circuit/is-there-a-limit-to-the-chip-process-node

Components of a quantum ‘program’

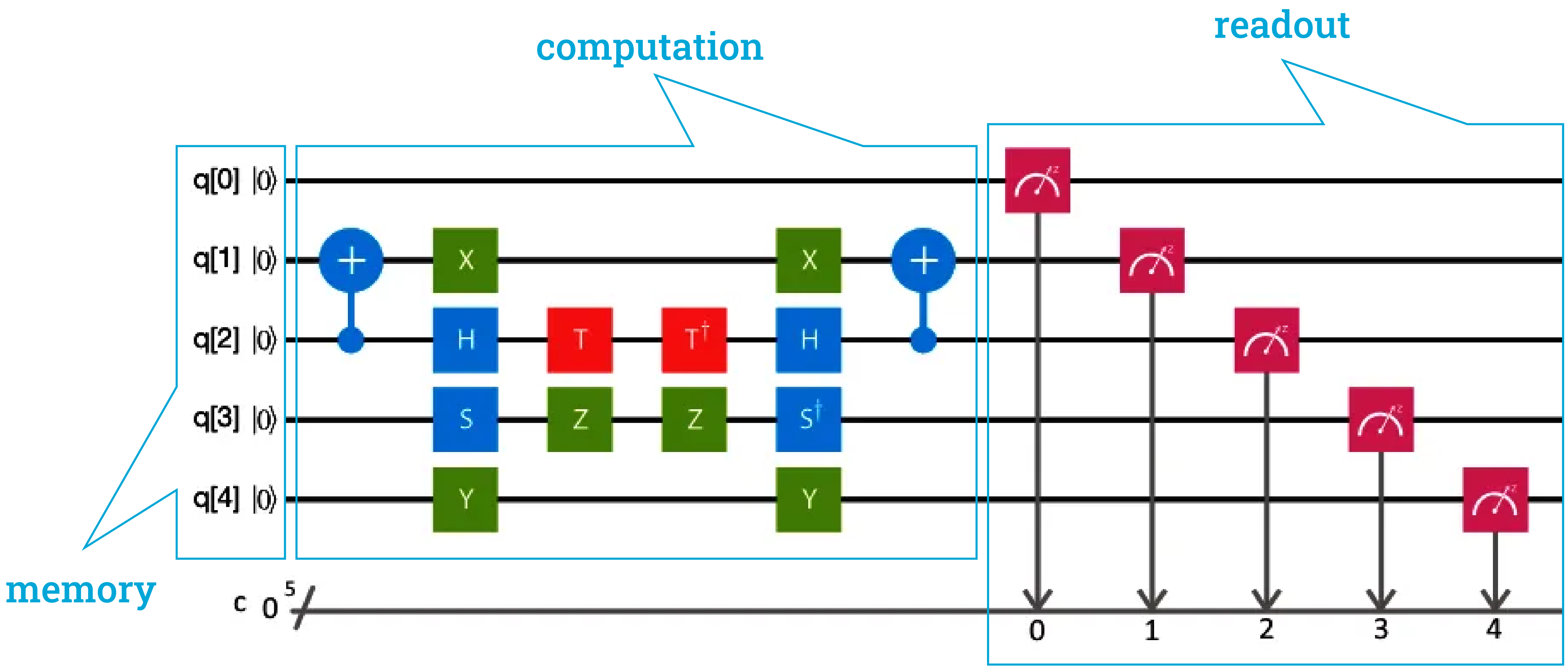

From bits to quantum bits

Classical bit

exclusive state 0 or 1

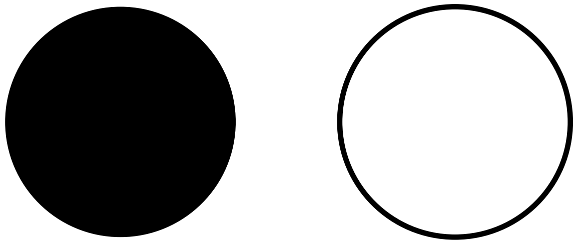

0 1

Quantum bit (qubits)

superposition of $|0\rangle$ and $|1\rangle$

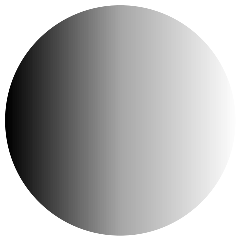

$$|\psi\rangle = \alpha_0|0\rangle + \alpha_1|1\rangle$$

Reading out quantum information

$$|\alpha_0|^2 + |\alpha_1|^2 = 1$$

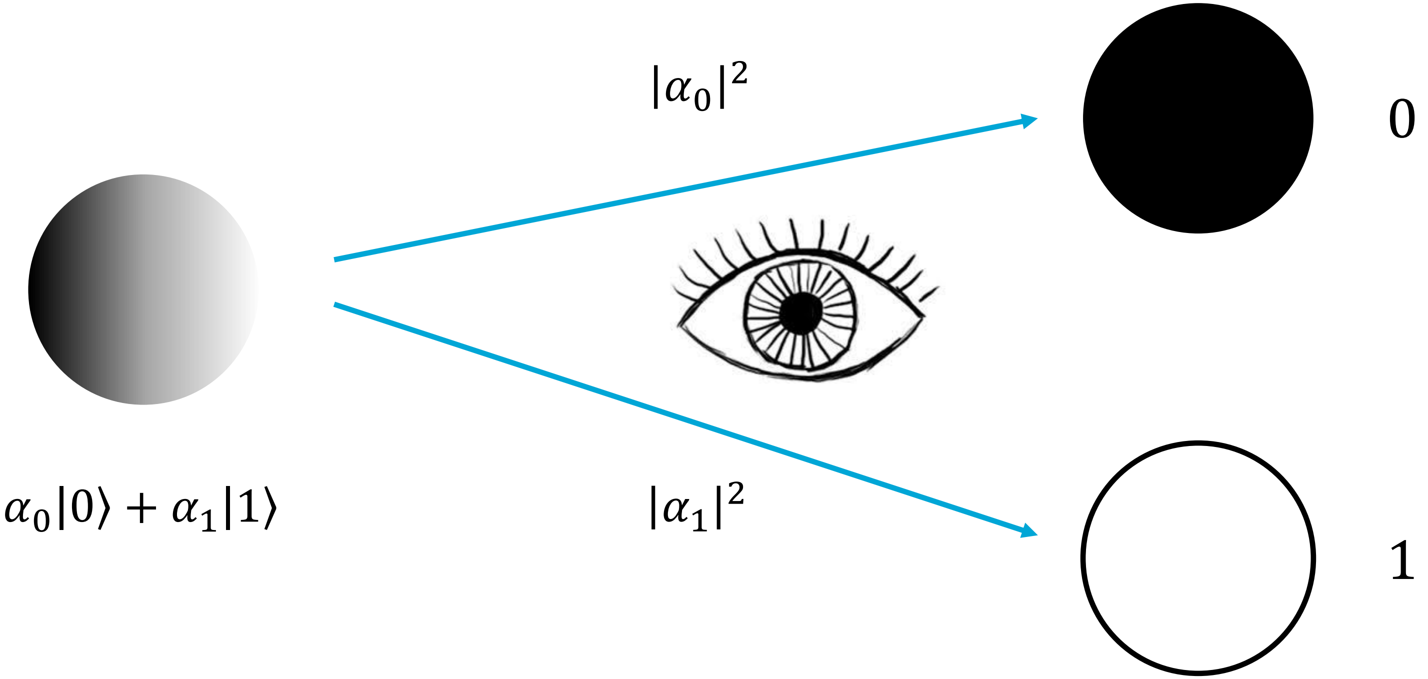

$$|\psi\rangle = \alpha_0|0\rangle + \alpha_1|1\rangle$$

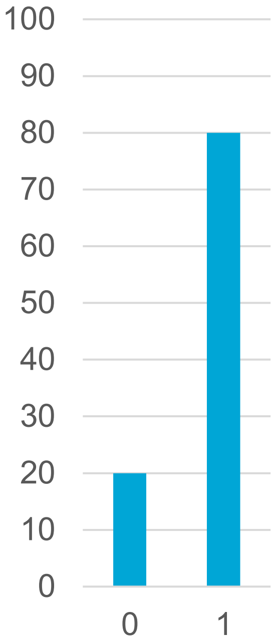

Superposition

$$|\alpha_0|^2 + \cdots + |\alpha_7|^2 = 1$$

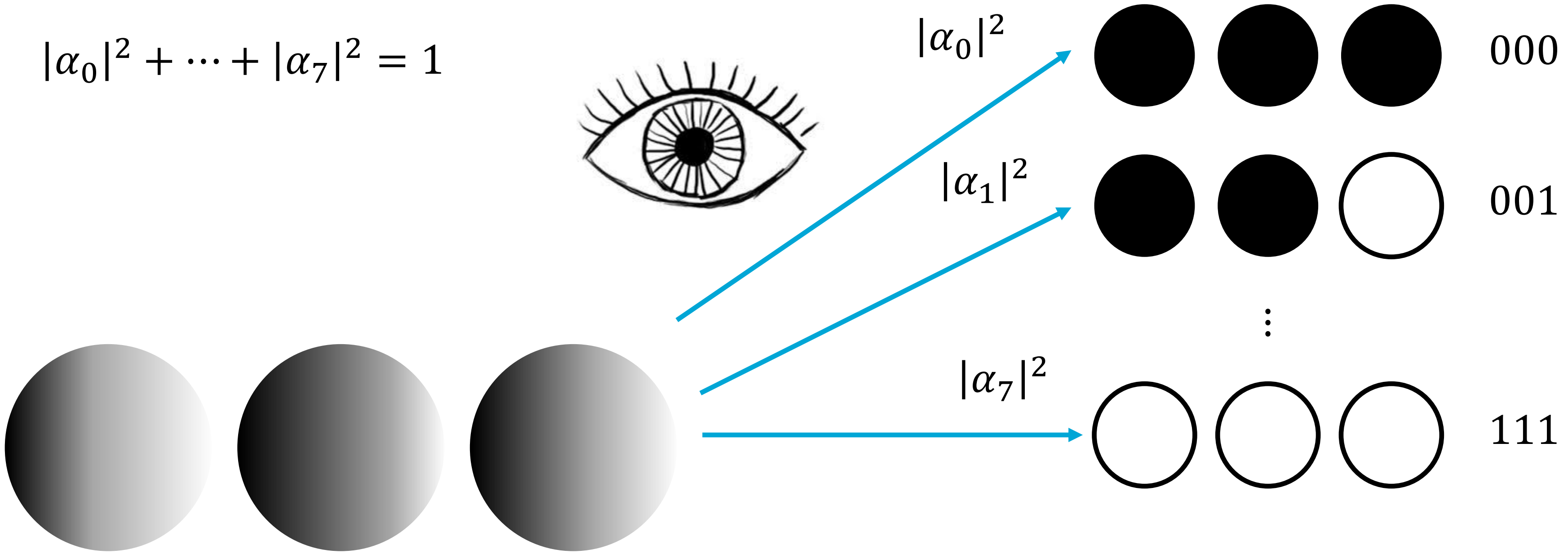

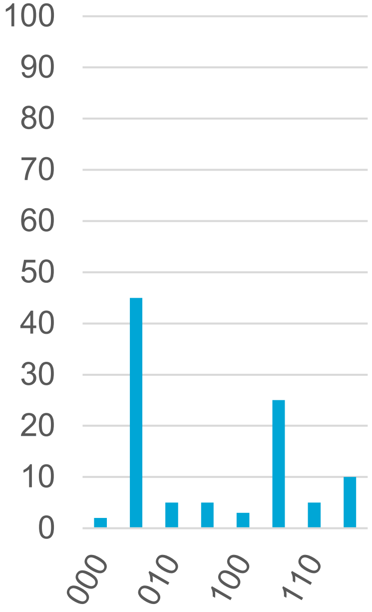

$$|\psi\rangle = \alpha_0|000\rangle + \alpha_1|001\rangle + \alpha_2|010\rangle + \alpha_3|011\rangle + \alpha_4|100\rangle + \alpha_5|101\rangle + \alpha_6|110\rangle + \alpha_7|111\rangle$$

n qubits can hold a **superposition** of 2^n values in their amplitudes $\alpha_i \in \mathbb{C}$; $|\alpha_i|^2$ is the **probability** of reading out the i-th basis state upon measurement

Entanglement

Product of two qubits (= separable quantum state)

$$|\psi\rangle = (\alpha_0|0\rangle + \alpha_1|1\rangle)\otimes(\beta_0|0\rangle + \beta_1|1\rangle)$$

$$= \alpha_0\beta_0|00\rangle + \alpha_0\beta_1|01\rangle + \alpha_1\beta_0|10\rangle + \alpha_1\beta_1|11\rangle$$

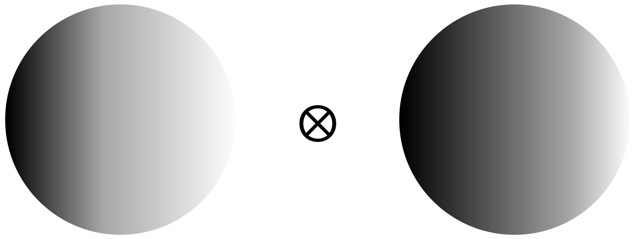

Non-separable (= entangled) quantum state

$$|\psi\rangle = \gamma_{00}|00\rangle + \gamma_{01}|01\rangle + \gamma_{10}|10\rangle + \gamma_{11}|11\rangle$$

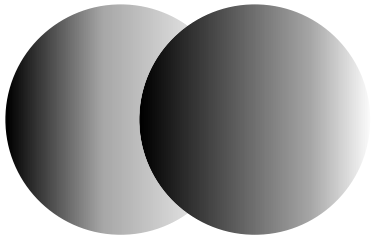

Quantum gates – the assembly of quantum computers

Example

$$|\psi\rangle = \mathrm{CNOT}(\mathrm{H}\otimes\mathrm{I})(|0\rangle\otimes|0\rangle)$$

$$\mathrm{H}|0\rangle = \frac{1}{\sqrt{2}}\begin{bmatrix}1 & 1\\ 1 & -1\end{bmatrix}\begin{pmatrix}0\\1\end{pmatrix}$$

$$= \frac{1}{\sqrt{2}}|0\rangle + \frac{1}{\sqrt{2}}|1\rangle$$

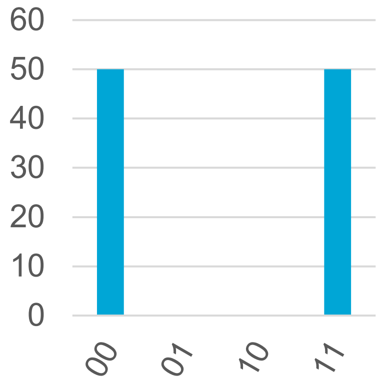

$$\mathrm{CNOT}|10\rangle = \begin{bmatrix}1 & 0 & 0 & 0\\ 0 & 1 & 0 & 0\\ 0 & 0 & 0 & 1\\ 0 & 0 & 1 & 0\end{bmatrix}\underbrace{\begin{bmatrix}0\\0\\1\\0\end{bmatrix}}_{|10\rangle} = \underbrace{\begin{bmatrix}0\\0\\0\\1\end{bmatrix}}_{|11\rangle}$$

Common pitfalls

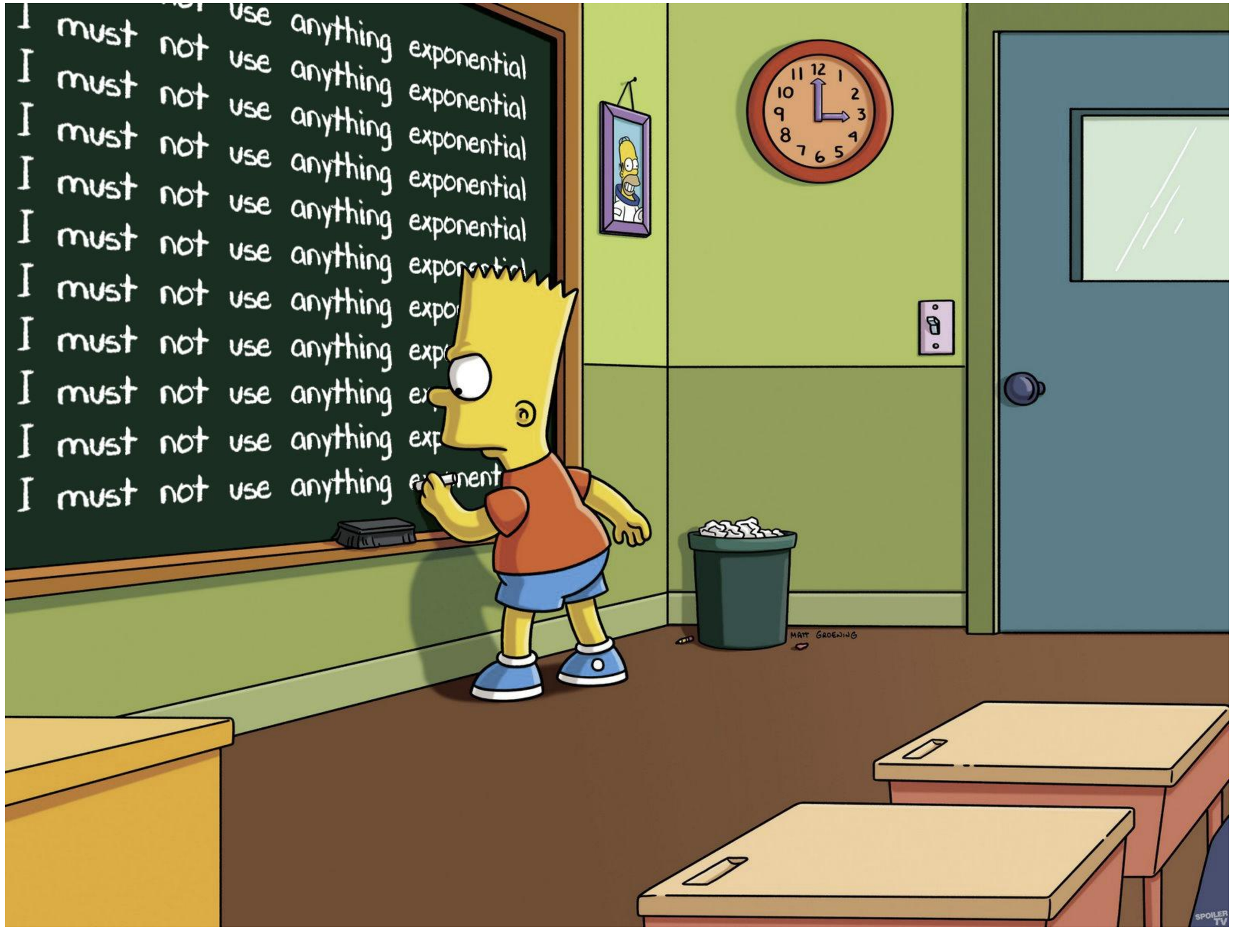

Quantum CFD Lab

Common pitfalls – exponentially large ‘programs’

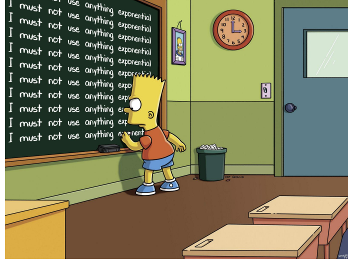

$$|\psi\rangle = U|0\rangle$$

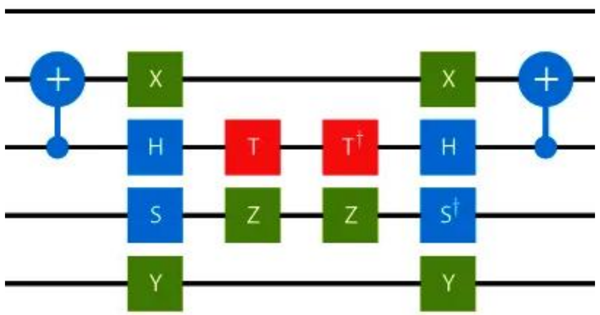

n qubits

$O(p^n)$ gates

Common pitfalls – exponentially many readouts

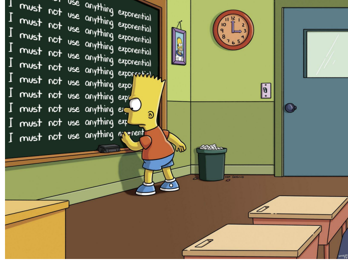

n qubits

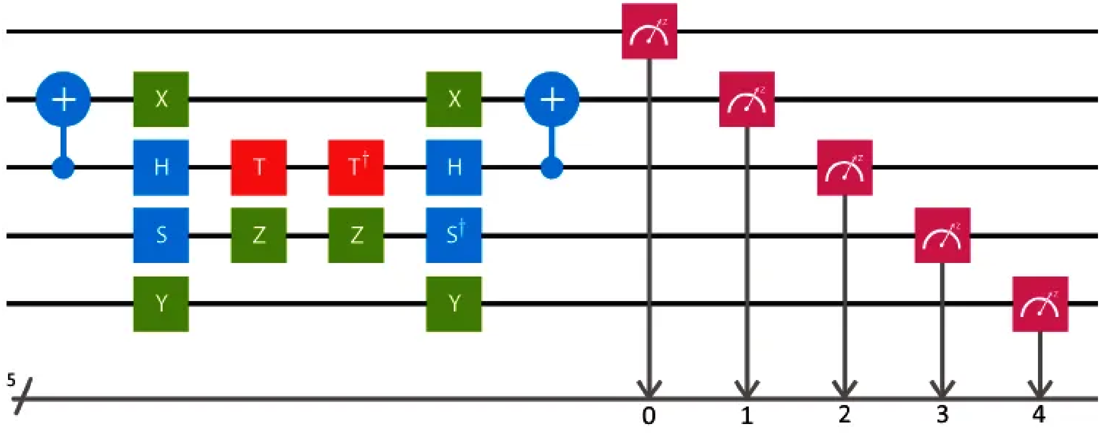

$O(p^n)$ measurements

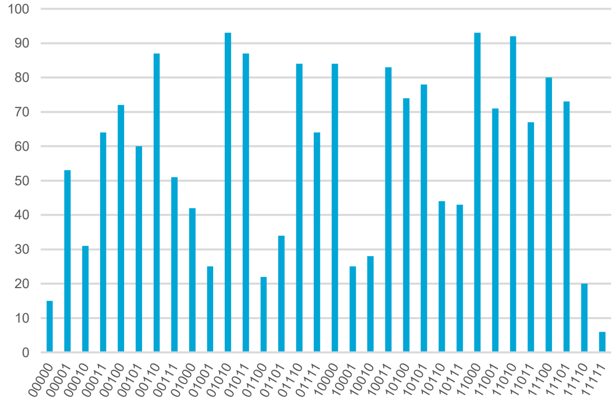

Common pitfalls – probabilistic successes

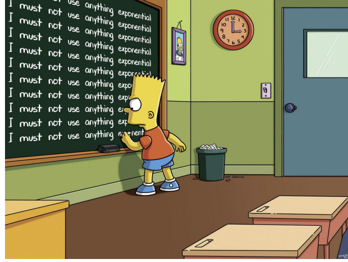

$$U|\psi\rangle|0\rangle = \sqrt{\delta}|\psi_{\text{good}}\rangle{\color{green}|0\rangle} + \sqrt{1-\delta}|\psi_{\text{bad}}\rangle{\color{red}|1\rangle}$$

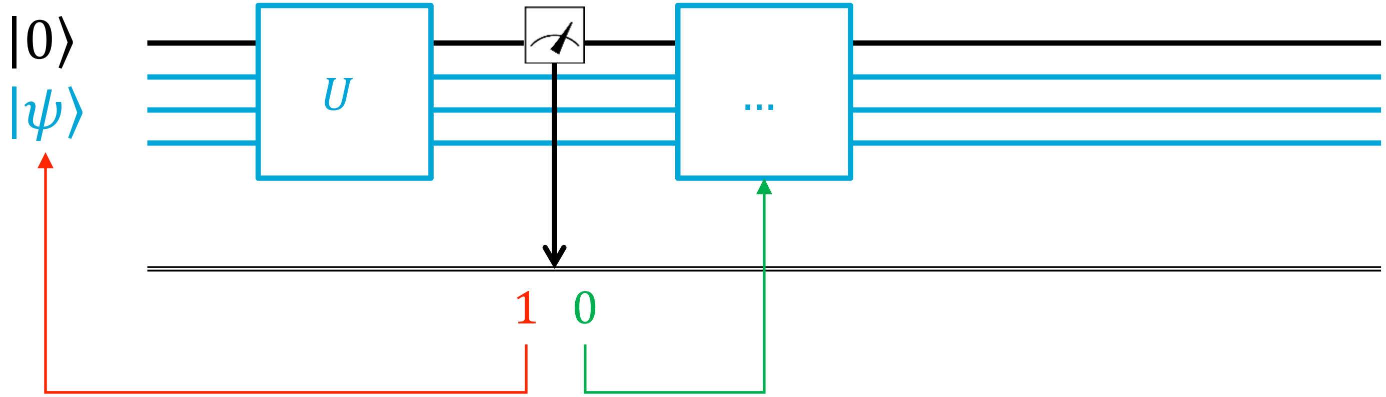

Common pitfalls – probabilistic successes

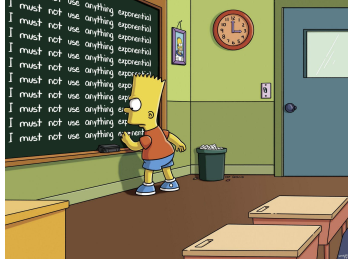

$$U^m|\psi\rangle|0\rangle = \sqrt{\delta}\big|\psi_{\text{good}}\big\rangle|0\rangle + \sqrt{1-\delta}|\psi_{\text{bad}}\rangle|1\rangle$$

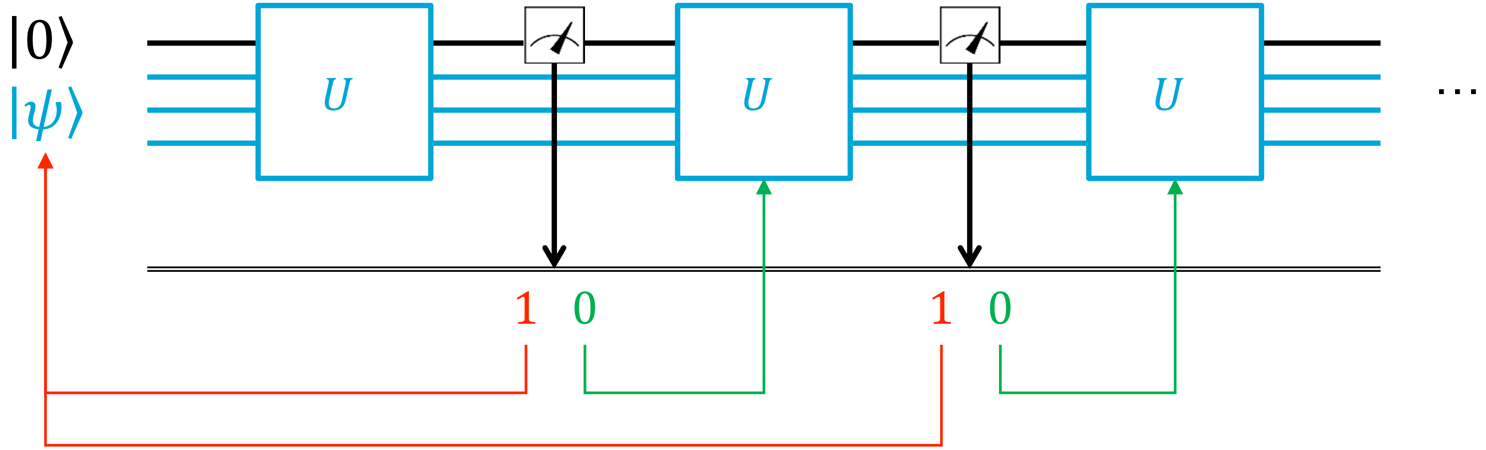

Common pitfalls – probabilistic successes

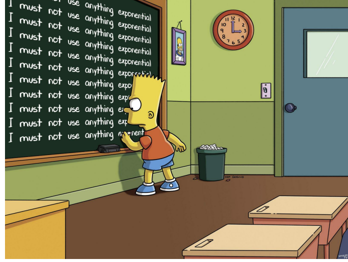

$$U^m|\psi\rangle|0\rangle = \sqrt{\delta}|\psi_{\text{good}}\rangle|0\rangle + \sqrt{1-\delta}|\psi_{\text{bad}}\rangle|1\rangle$$

m	$\delta = 0.9$	$\delta = 0.99$	$\delta = 0.999$
10	0.349	0.904	0.990
100	$2.66 \cdot 10^{-5}$	0.366	0.905
1,000	$1.75 \cdot 10^{-48}$	$4.32 \cdot 10^{-5}$	0.368
10,000	n/a	$2.52 \cdot 10^{-44}$	$4.52 \cdot 10^{-5}$

Take-home lessons

$$|0\rangle + \sum_{i=1}^{2^n-1} 0|i\rangle \xrightarrow{\text{unitary operations}} \sum_{i=0}^{2^n-1} \alpha_i|i\rangle \xrightarrow{\text{measurement}} i \text{ with probability } |\alpha_i|^2$$

If quantum computing shall become the future of HPCSE we need to …

- … identify **applications** that cannot be solved (efficiently) with classical computers
- … develop **algorithms** that exploit the strengths of quantum computers (and avoid their limitations)
- … (most probably) change the **workflows** that were designed for classical computers

Application #1: Computational fluid dynamics

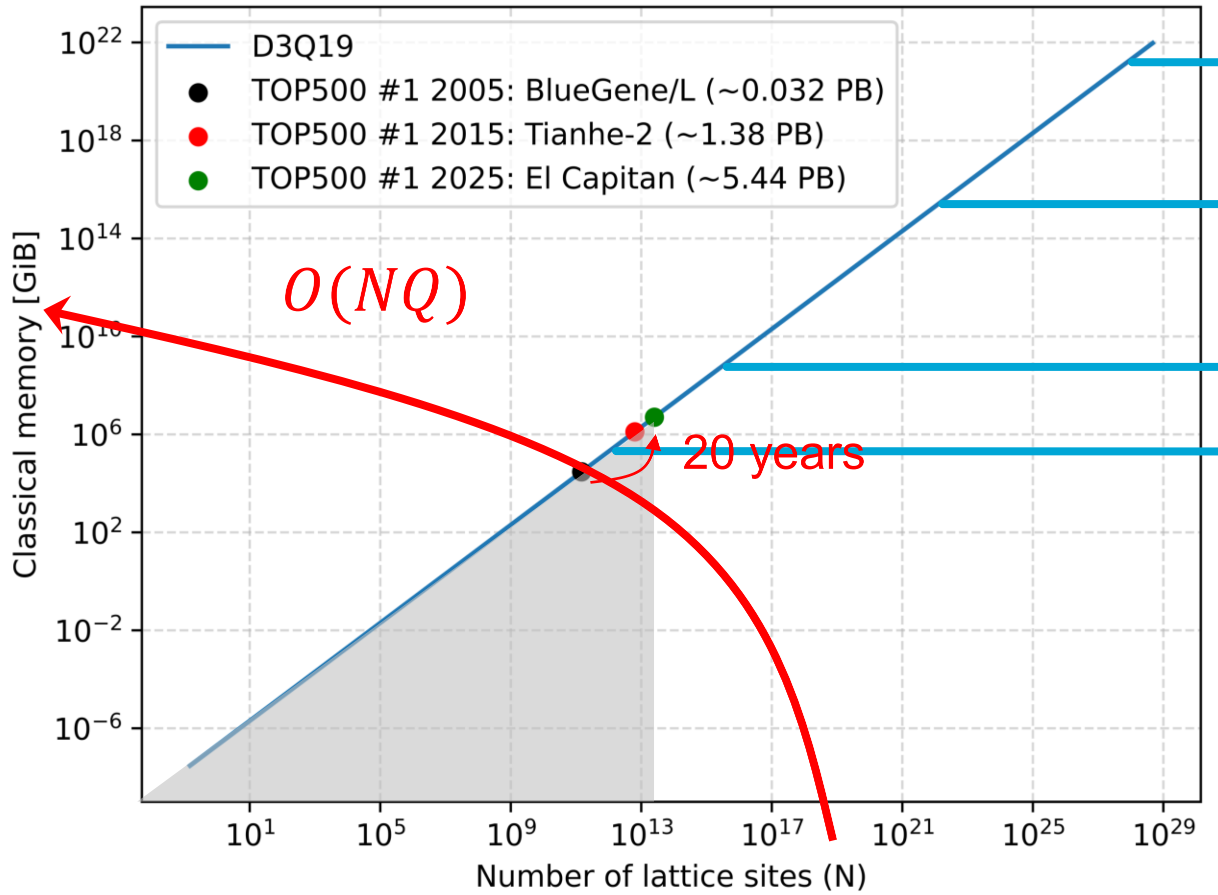

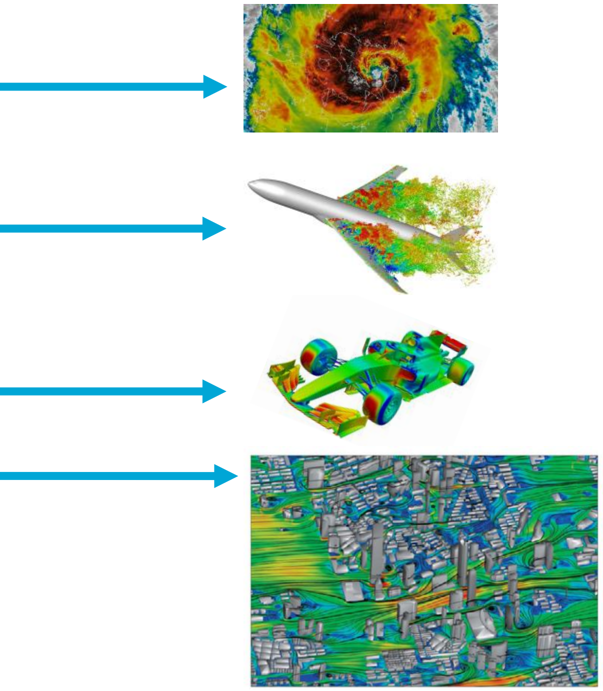

Urban wind flow simulation of Shenzhen city (LBM + LES)

DOI: 10.1137/23M1600797

Application #1: Computational fluid dynamics

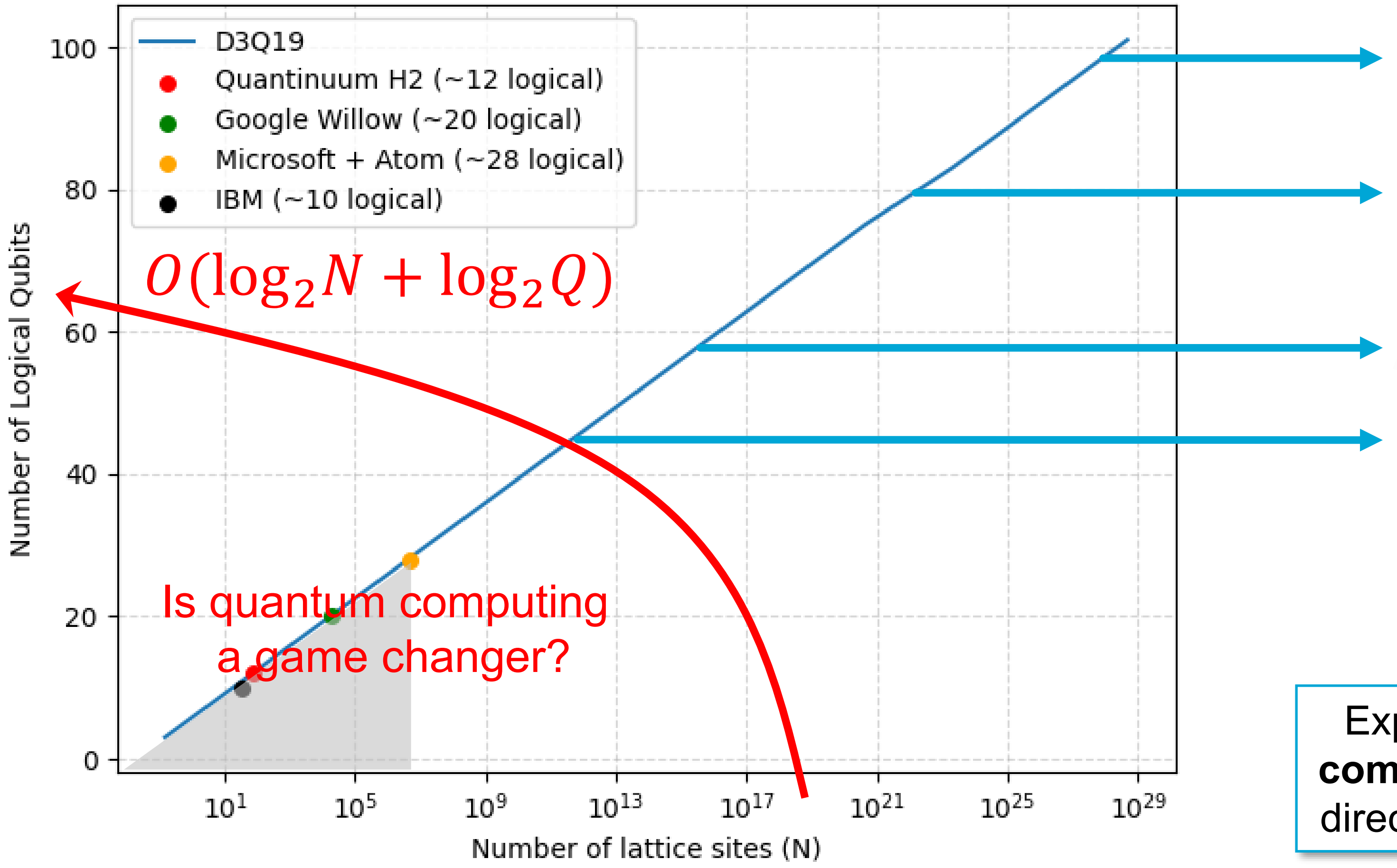

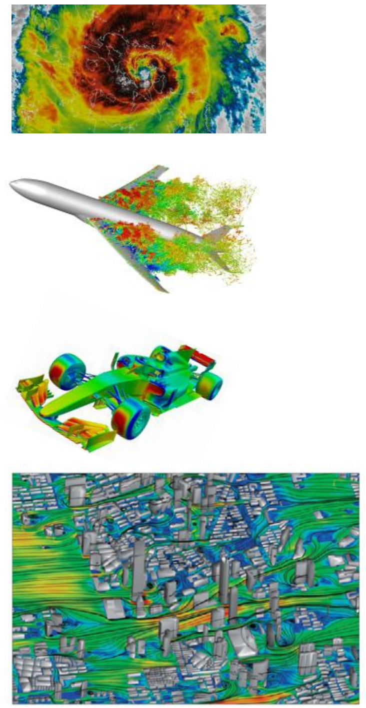

Exploit **exponential data compression** in large-scale direct numerical simulations

Application #2: Design optimization (not just for CFD)

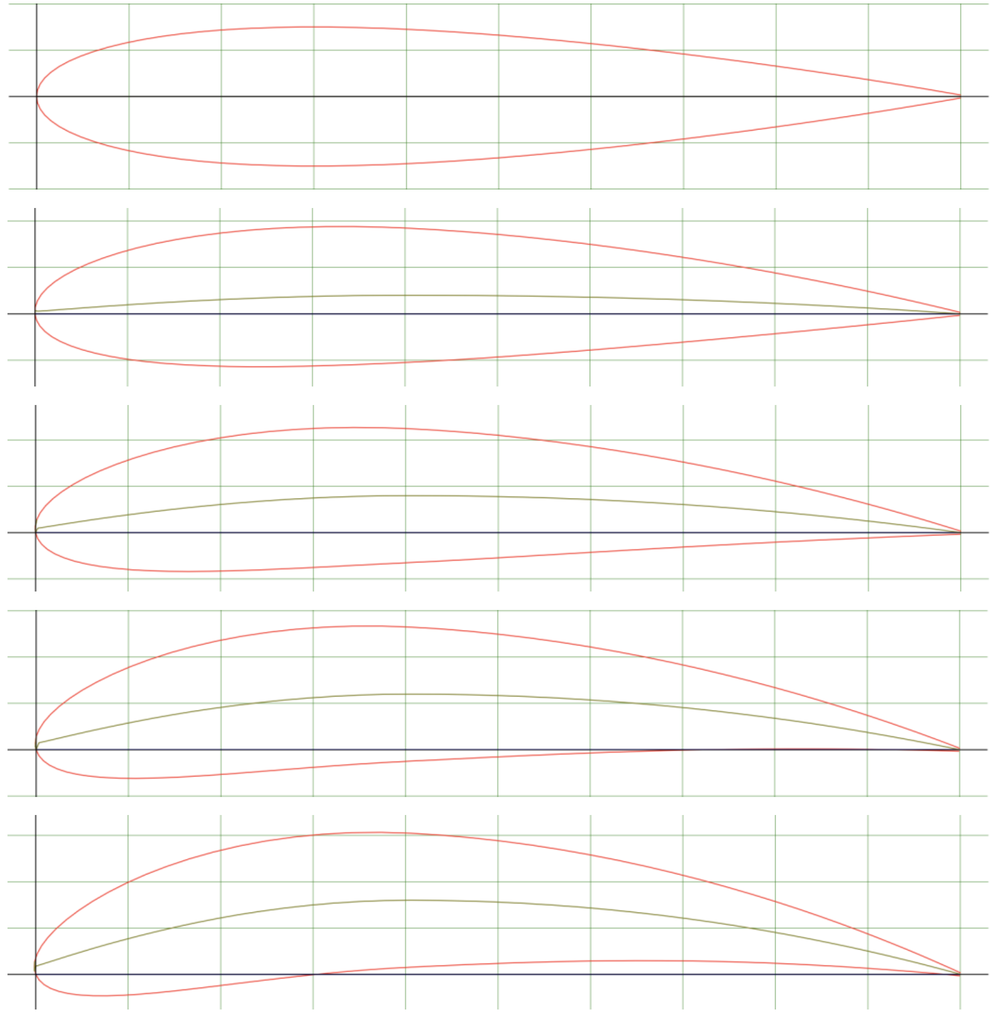

Generated with airfoiltools.com

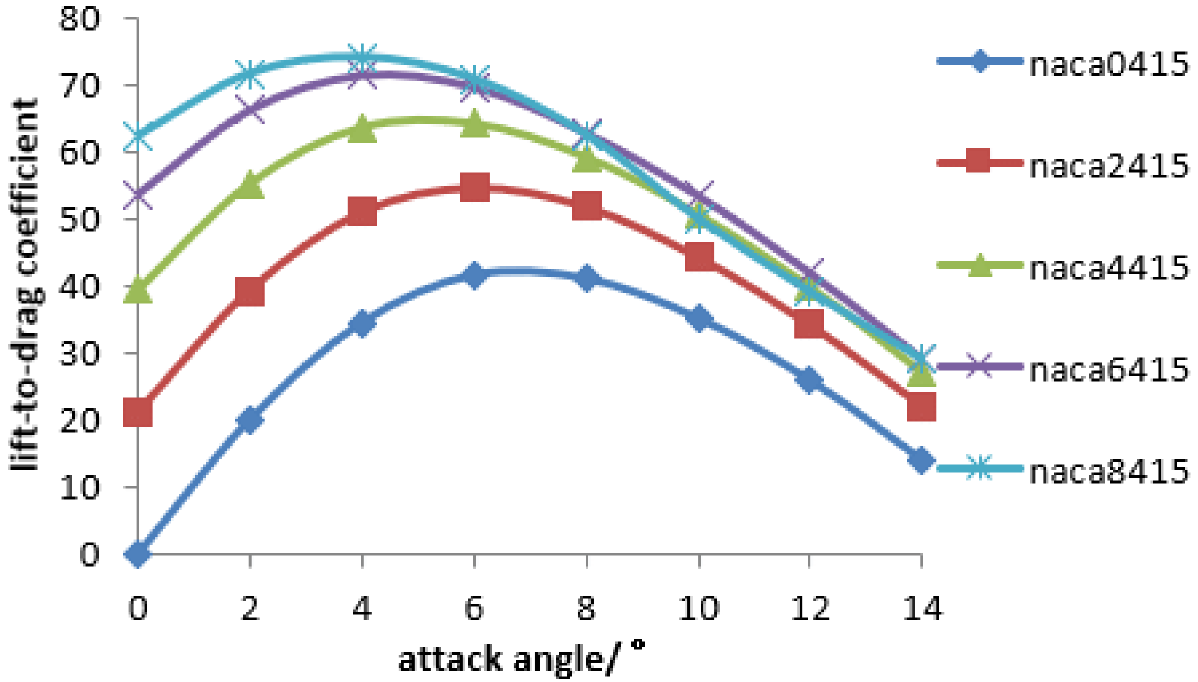

DOI: 10.1088/1742-6596/1519/1/012020

Exploit **quadratic speedup of quantum search algorithms** in design optimization

Boltzmann equation (BE)

$$\varrho(\boldsymbol{x},t) = \int f(\boldsymbol{x},\boldsymbol{v},t)\,d\boldsymbol{v}$$

$$\varrho\boldsymbol{u}(\boldsymbol{x},t) = \int \boldsymbol{v}f(\boldsymbol{x},\boldsymbol{v},t)\,d\boldsymbol{v}$$

effect of external forces

$$\frac{\partial f}{\partial t} + \boldsymbol{v}\cdot\nabla_x f + \boldsymbol{a}\cdot\nabla_v f = -\frac{1}{\tau}(f - f^{\mathrm{eq}})$$

free streaming

redistribution by collision

distribution function

$$f(\boldsymbol{x},\boldsymbol{v},t) \quad \left[\frac{\mathrm{kg\ s^3}}{\mathrm{m^6}}\right]$$

From BE to the lattice Boltzmann method (LBM)

$$\frac{\partial f}{\partial t} + \boldsymbol{v} \cdot \nabla f = \Omega$$

discretize in velocity space → discretize in space and time

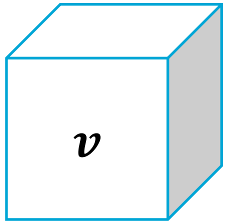

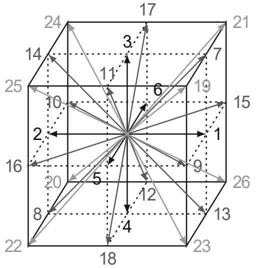

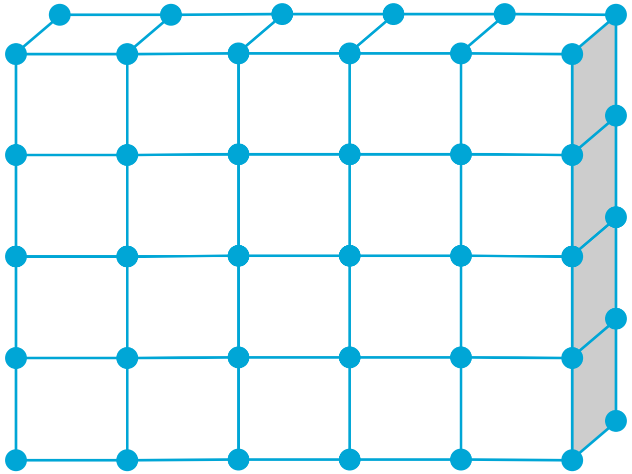

$f(\boldsymbol{x}, \boldsymbol{v}, t)$ → $f_\alpha(\boldsymbol{x}, t) = f(\boldsymbol{x}, \boldsymbol{e}_\alpha, t)$

$f_\alpha(\boldsymbol{x}_i, t^n)$

LBM

$$\frac{\partial f_\alpha}{\partial t} + \boldsymbol{e}_\alpha \cdot \nabla f_\alpha = \Omega_\alpha$$

$$f_\alpha^*(\boldsymbol{x}_i, t^n) = f_\alpha(\boldsymbol{x}_i, t^n) + \Delta t \Omega_\alpha(\boldsymbol{x}_i, t^n)$$

collision of all f_α at grid point $\boldsymbol{x}_i$

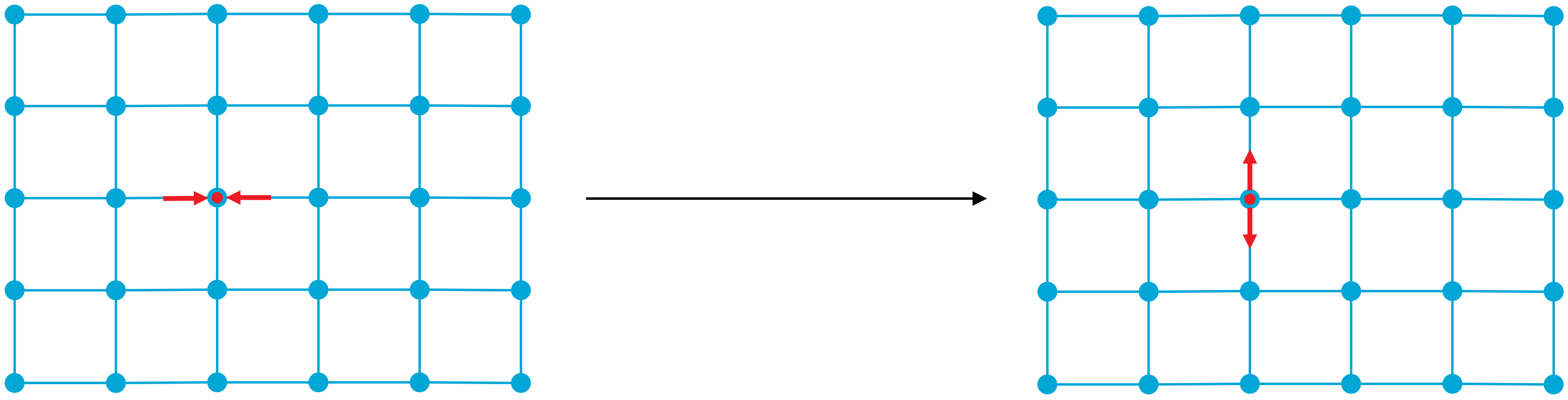

LBM

$$\frac{\partial f_\alpha}{\partial t} + \boldsymbol{e}_\alpha \cdot \nabla f_\alpha = \Omega_\alpha$$

$$f_\alpha(\boldsymbol{x}_i + \boldsymbol{e}_\alpha \Delta t, t^n + \Delta t) = f_\alpha^*(\boldsymbol{x}_i, t^n)$$

streaming of all f_α along direction $\boldsymbol{e}_\alpha$

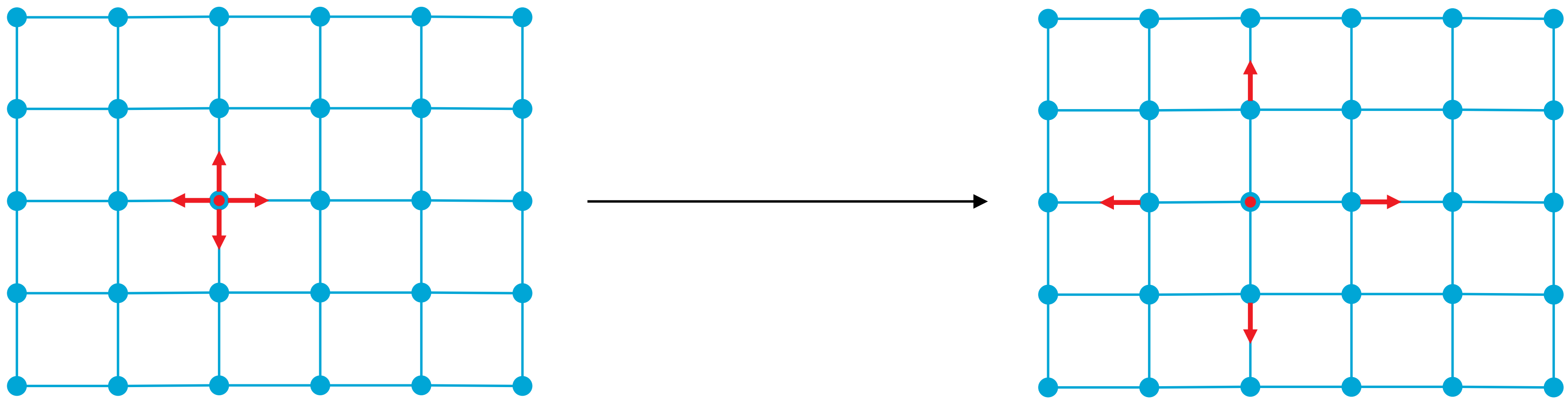

LBM

$$\frac{\partial f_\alpha}{\partial t} + \boldsymbol{e}_{\boldsymbol{\alpha}} \cdot \nabla f_\alpha = \Omega_\alpha$$

reflection or bounce-back boundary

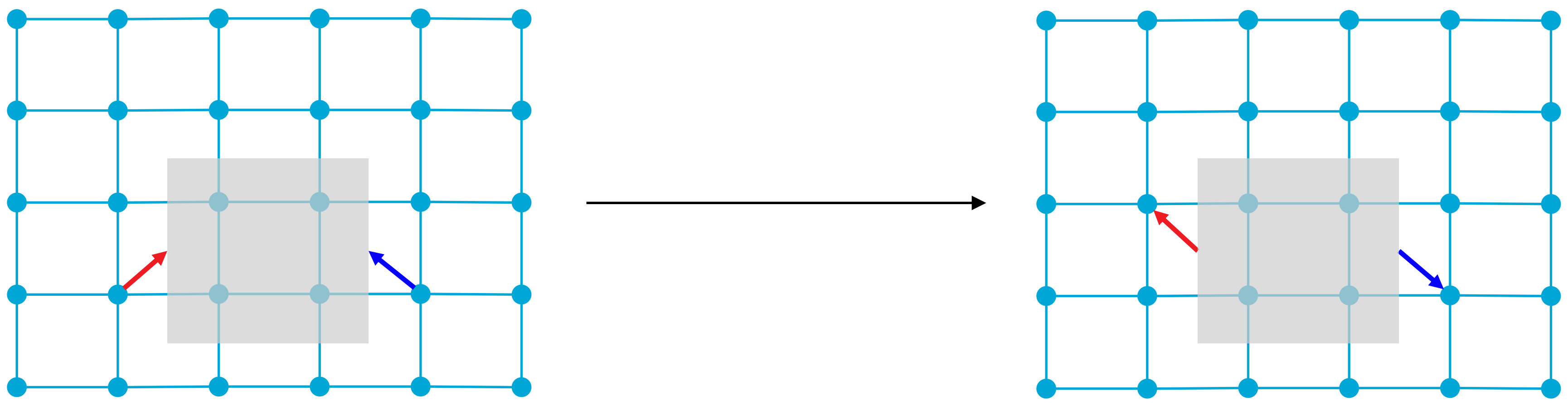

LBM

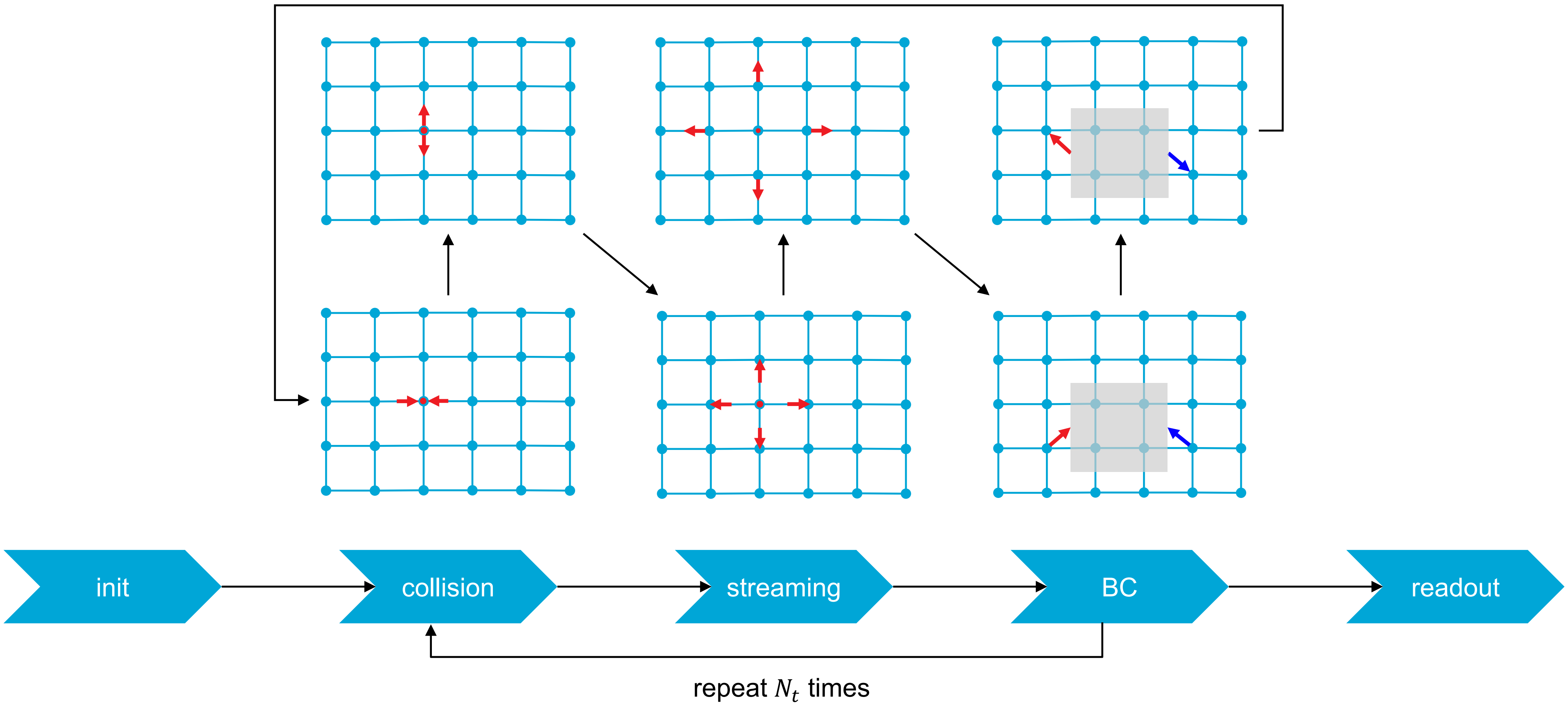

Advantages of LBM over other flow models

1. Update **moments** and **equilibrium distribution functions**

$$\varrho = \sum_\alpha f_\alpha\,, \qquad \boldsymbol{u} = \frac{1}{\varrho}\sum_\alpha f_\alpha \boldsymbol{e}_\alpha\,, \qquad f_\alpha^{\text{eq}} = w_\alpha \varrho \left(1 + \frac{\boldsymbol{u}\cdot\boldsymbol{e}_\alpha}{c_s^2} + \frac{(\boldsymbol{u}\cdot\boldsymbol{e}_\alpha)^2}{2c_s^4} - \frac{\boldsymbol{u}\cdot\boldsymbol{u}}{2c_s^4}\right)$$

2. **Collide**

$$f_\alpha^*(\boldsymbol{x}_i, t^n) = f_\alpha(\boldsymbol{x}_i, t^n) - \frac{\Delta t}{\tau}\left(f_\alpha(\boldsymbol{x}_i, t^n) - f_\alpha^{\text{eq}}(\boldsymbol{x}_i, t^n)\right)$$

nonlinear & local 🚫

3. **Stream**

↕ decoupled ✅

$$f_\alpha(\boldsymbol{x}_i + \boldsymbol{c}_\alpha \Delta t, t^n + \Delta t) = f_\alpha^*(\boldsymbol{x}_i, t^n)$$

linear & global ✅

4. Apply **boundary conditions**
5. Repeat

Data encoding

Classical register

$$f[N_v][N_x][N_y] \qquad N_v = 9, N_x = N_y = 8$$

$$f[\alpha][i][j] \;\mapsto\; f_\alpha(x_i, y_j)$$

Quantum register

$$|v\rangle \otimes |x\rangle \otimes |y\rangle, \qquad n_v = \lceil \log_2 9 \rceil = 4, n_x = n_y = 3$$

$$|\psi\rangle = \sum_{\alpha,i,j} \gamma_{\alpha ij} |\boldsymbol{e}_\alpha\rangle |i\rangle |j\rangle, \qquad \gamma_{\alpha ij} \propto \sqrt{f_\alpha(x_i, y_j)}$$

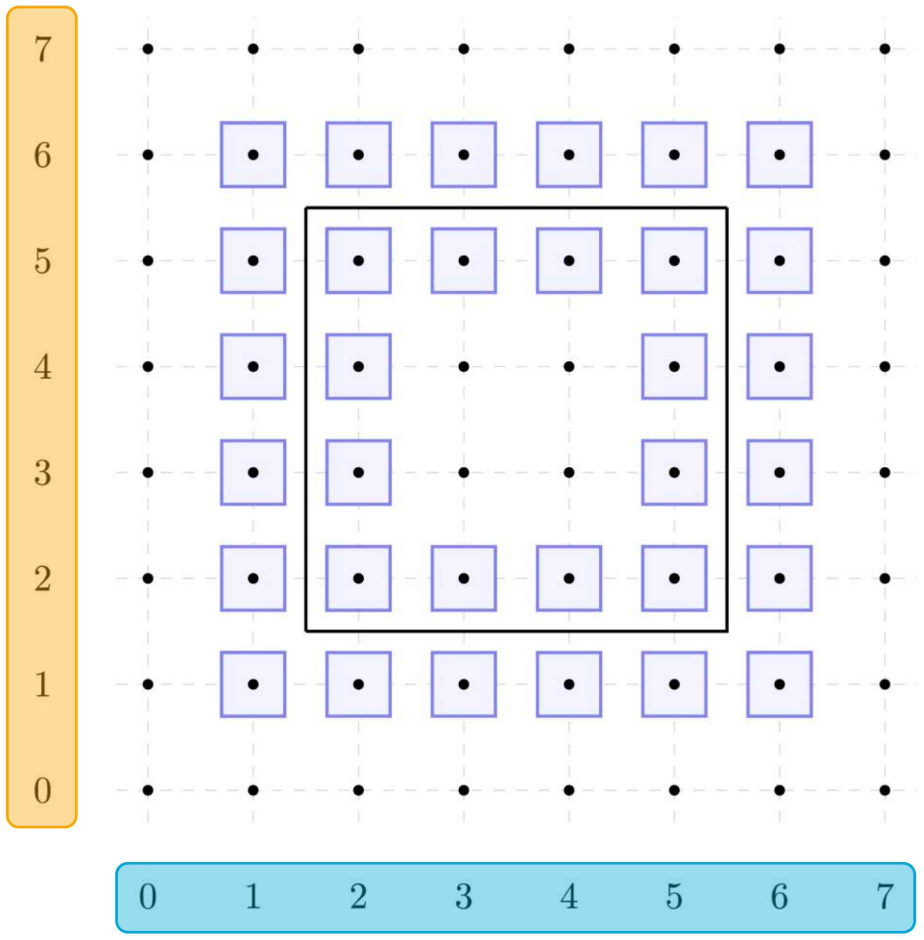

Data encoding

Classical register

$$f[N_v][N_x][N_y] \qquad N_v = 9, N_x = N_y = 8$$

$$f[\alpha][i][j] \;\mapsto\; f_\alpha(x_i, y_j)$$

Quantum register

$$|v\rangle \otimes |x\rangle \otimes |y\rangle, \qquad n_v = \lceil \log_2 9 \rceil = 4, n_x = n_y = 3$$

$$|\psi\rangle = \sum_{\alpha,i,j} \gamma_{\alpha i j} |\boldsymbol{e}_\alpha\rangle |i\rangle |j\rangle, \qquad \gamma_{\alpha i j} \propto \sqrt{f_\alpha(x_i, y_j)}$$

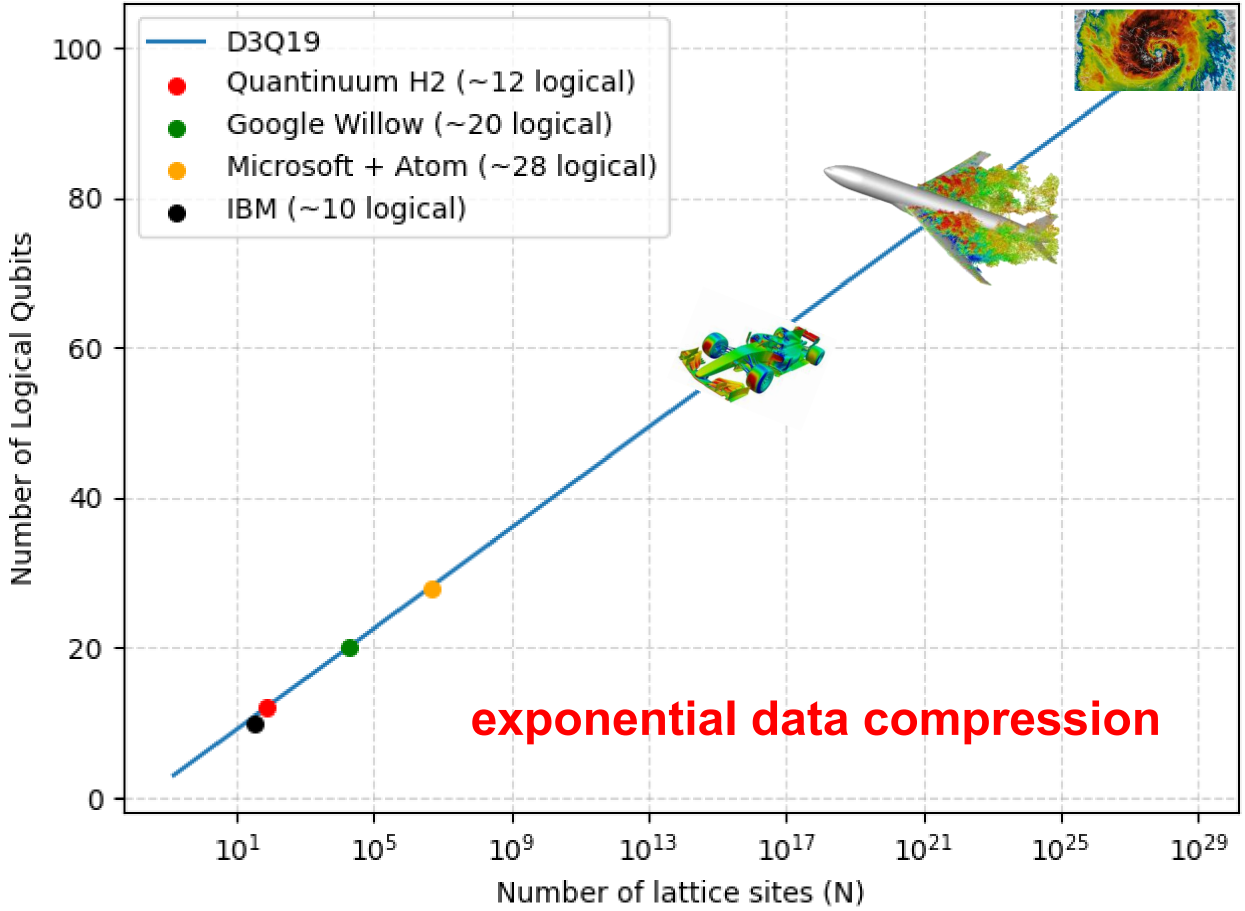

Sketch of the streaming operation

Our streaming primitive is based on **Draper's quantum adder** ("Addition on a Quantum Computer" '98) which is an in-place quantum adder for two integer values that works without auxiliary qubits

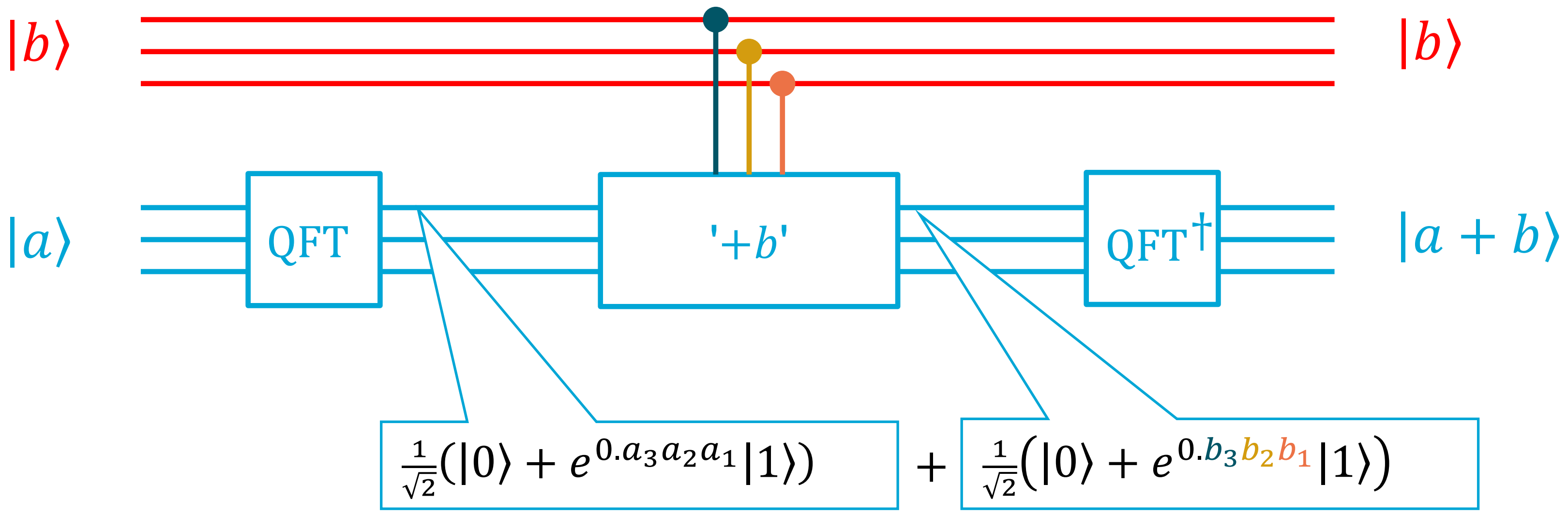

Sketch of the streaming operation

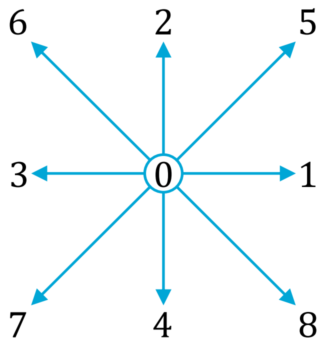

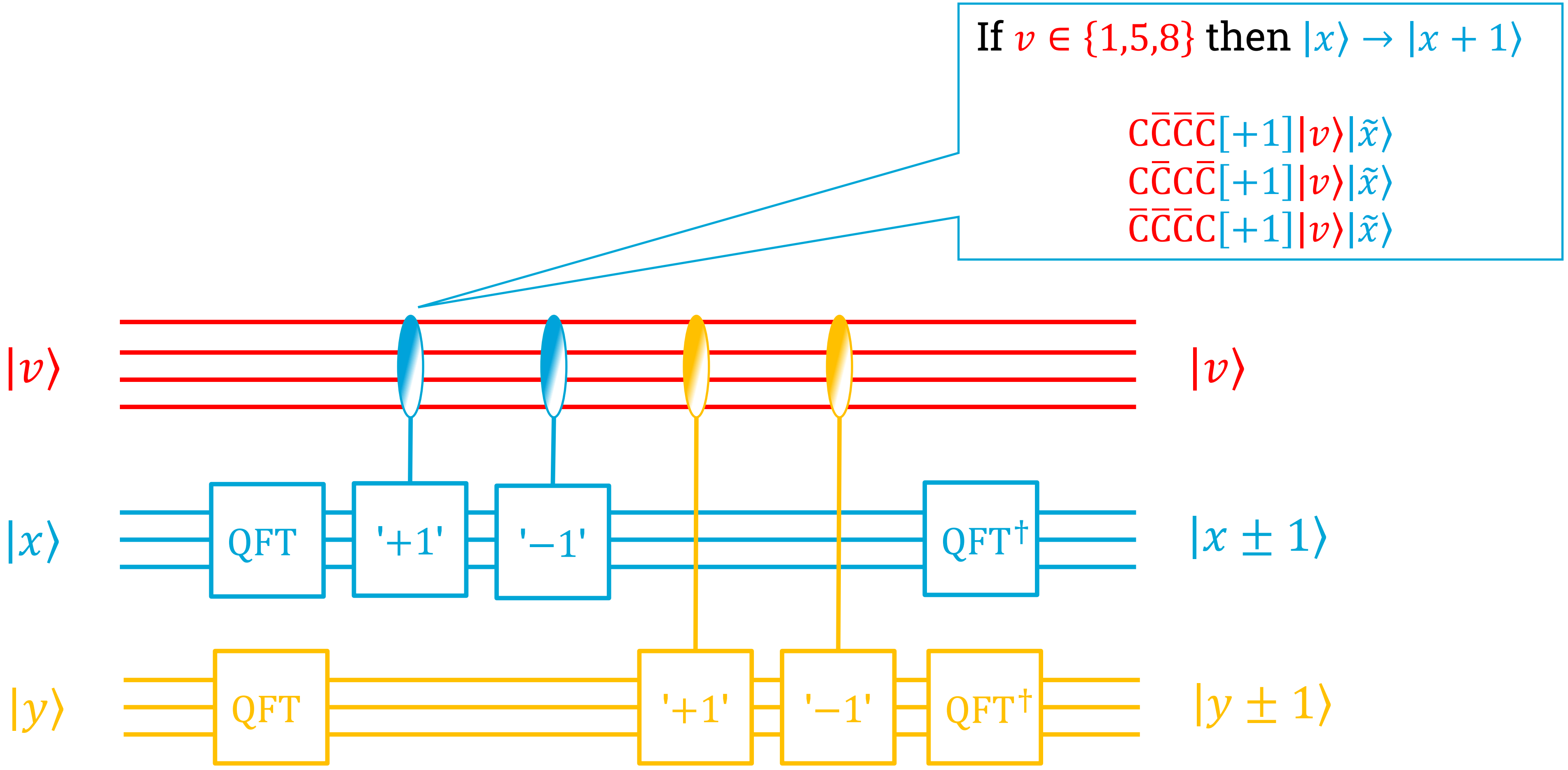

M. Schalkers, MM, *Efficient and fail-safe quantum algorithm for the transport equation*. JCP 502, 2024

Specular reflection / bounce back boundary conditions

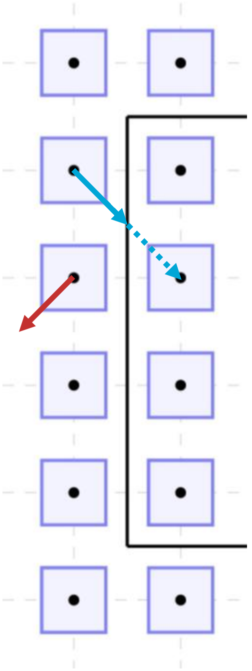

For all quantum states $|x\ y\ \ ????\rangle$ in the first inner layer of an obstacle

1. Place data back into flow domain

$$|x\ y\ \ ????\rangle \xrightarrow{\text{CCCC}[\pm 1]} |x \pm 1\ y \pm 1\ \ ????\rangle$$

2. Change velocity direction

$$|x \pm 1\ y \pm 1\ \ ????\rangle \xrightarrow{\text{Perm}} |x \pm 1\ y \pm 1\ \ ?'?'?'?'\rangle$$

Obstacle detection

- *Quantum comparator*

M. Schalkers, MM, *Efficient and fail-safe quantum algorithm for the transport equation*. JCP 502, 2024

Three grand challenges in quantum LBM

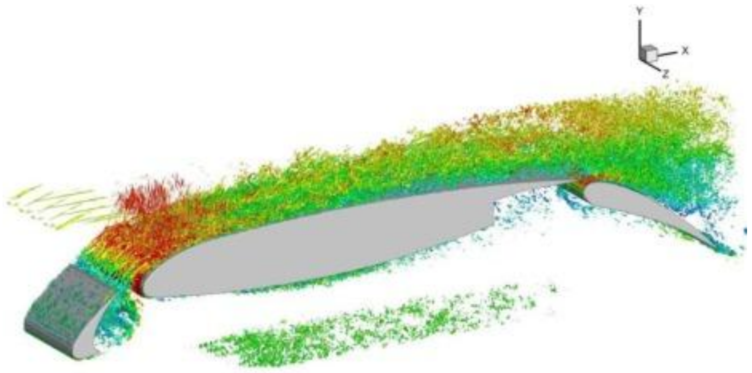

Complex geometries

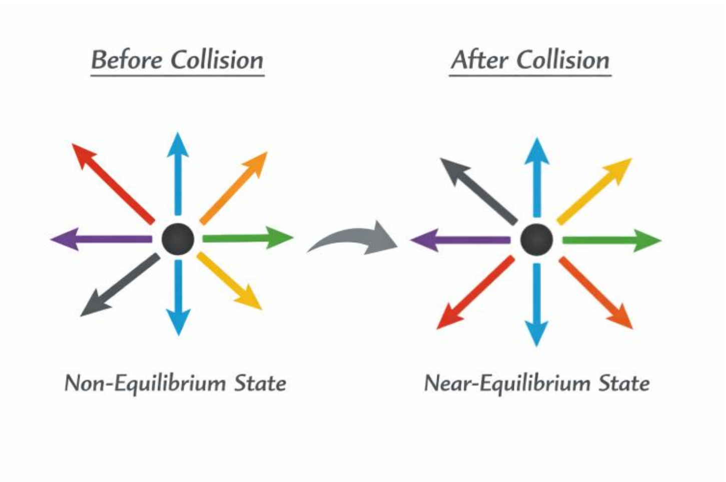

Nonlinear dynamics

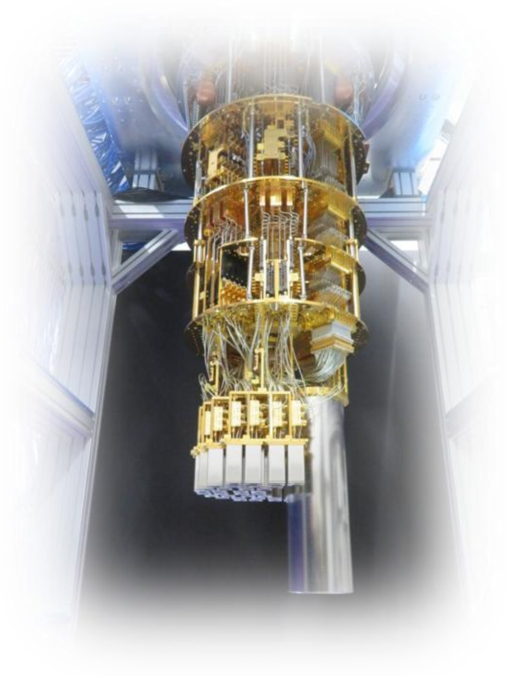

Running on NISQ hardware

Zone-agnostic boundary conditions

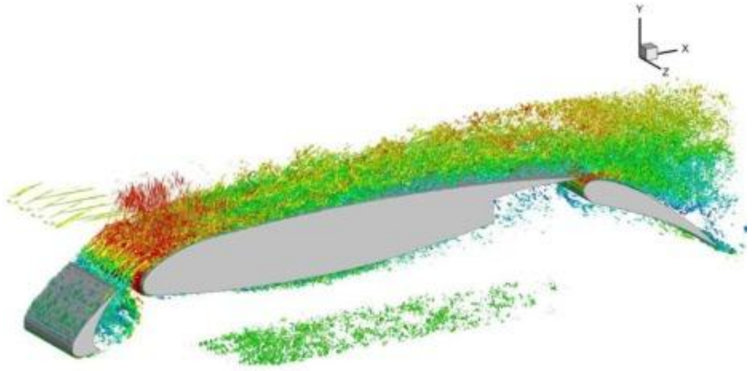

Complex geometries

C. Georgescu, MM, *Efficient implementation of complex geometries in quantum lattice Boltzmann methods*. In preparation

Collision à la Bhatnagar-Gross-Krook (BGK)

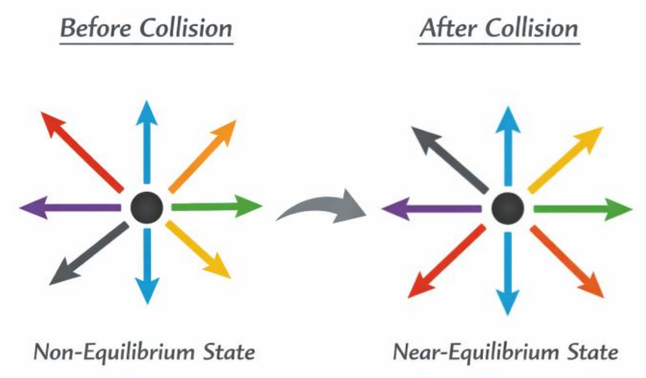

Nonlinear dynamics

linear nonlinear

$$f_\alpha^* = (1-\omega) f_\alpha + \omega w_\alpha \varrho \left(1 + \frac{\boldsymbol{u}\cdot\boldsymbol{e}_\alpha}{c_s^2} + \frac{(\boldsymbol{u}\cdot\boldsymbol{e}_\alpha)^2}{2c_s^4} - \frac{\boldsymbol{u}\cdot\boldsymbol{u}}{2c_s^4} \right)$$

- ignore collision → collisionless QLBM
- ignore nonlinear term → linearized QLBM
- approximate nonlinear term → QLBM

Surrogate quantum circuits

Learn a low-depth, unitary **approximation** of the BGK operator that mimics its physical properties

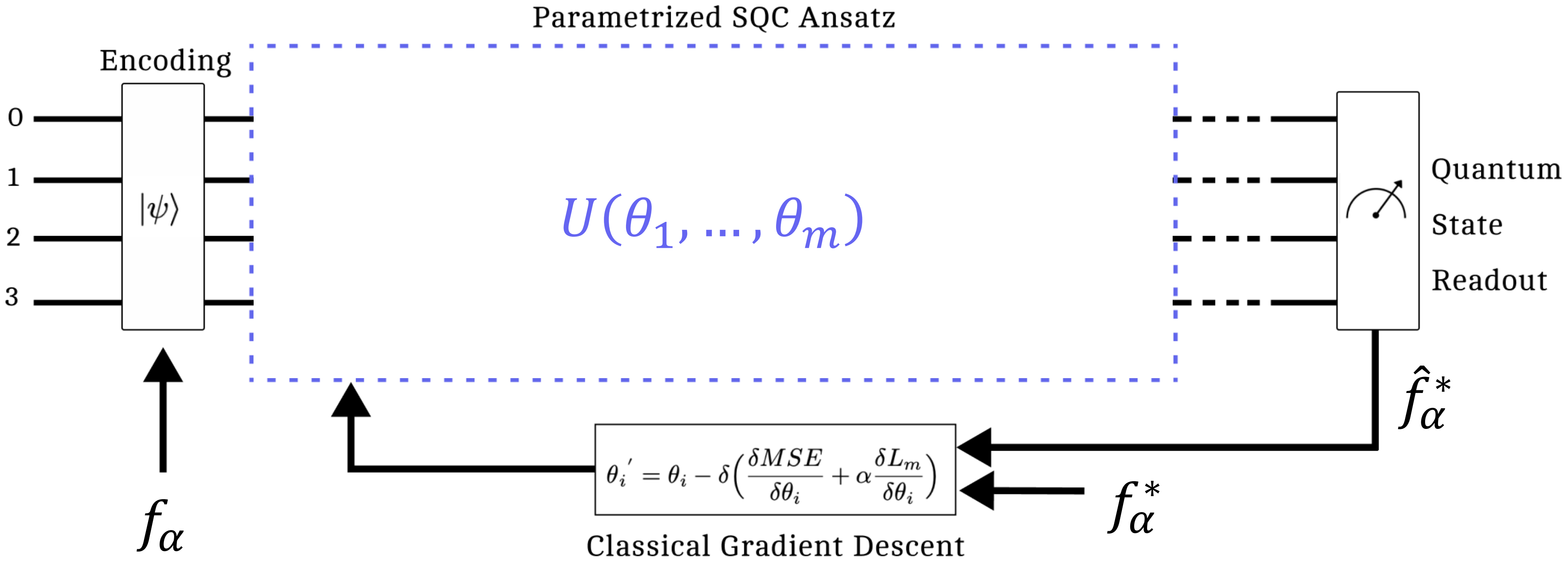

M. Lacatus, MM, Surrogate quantum circuit design for the lattice Boltzmann collision operator*, IJNME 127(4):e70286, 2026*

Physical properties of the BGK operator for D_2Q_9

Mass conservation

$$|\psi\rangle = \frac{1}{\sqrt{\rho}} \sum_{\alpha} \sqrt{f_\alpha} |\boldsymbol{e}_\alpha\rangle, \qquad \rho = \sum_{\alpha} f_\alpha$$

Momentum conservation

Enforced weakly in the loss function

Scale invariance

$$\Omega(\lambda \cdot f_\alpha) = \lambda \cdot \Omega(f_\alpha), \qquad \lambda > 0$$

	Discrete velocity	Velocity basis state
f_0	$(0,0)$	$\|0000\rangle$
f_1	$(1,0)$	$\|0001\rangle$
f_2	$(0,1)$	$\|0010\rangle$
f_3	$(-1,0)$	$\|0100\rangle$
f_4	$(0,-1)$	$\|1000\rangle$
f_5	$(1,1)$	$\|0011\rangle$
f_6	$(-1,1)$	$\|0110\rangle$
f_7	$(-1,-1)$	$\|1100\rangle$
f_8	$(1,-1)$	$\|1001\rangle$

The remaining 7 basis states are unused and are assigned to the $(0,0)$ velocity state, effectively contributing to the population f_0, to ensure mass conservation

Physical properties of the BGK operator for D_2Q_9

D_8 equivariance

D_2Q_9 lattice is invariant under the dihedral group D_8, i.e., the full symmetry group of a square ($r = 90°$ **rotation** and s is a **reflection**):

$$D_8 = [I, r, r^2, r^3, s, rs, r^2s, r^3s]$$

BGK operator **commutes** with all group elements:

$$\Omega(\sigma \circ f_\alpha) = \sigma \circ \Omega(f_\alpha) \quad \forall \sigma \in D_8$$

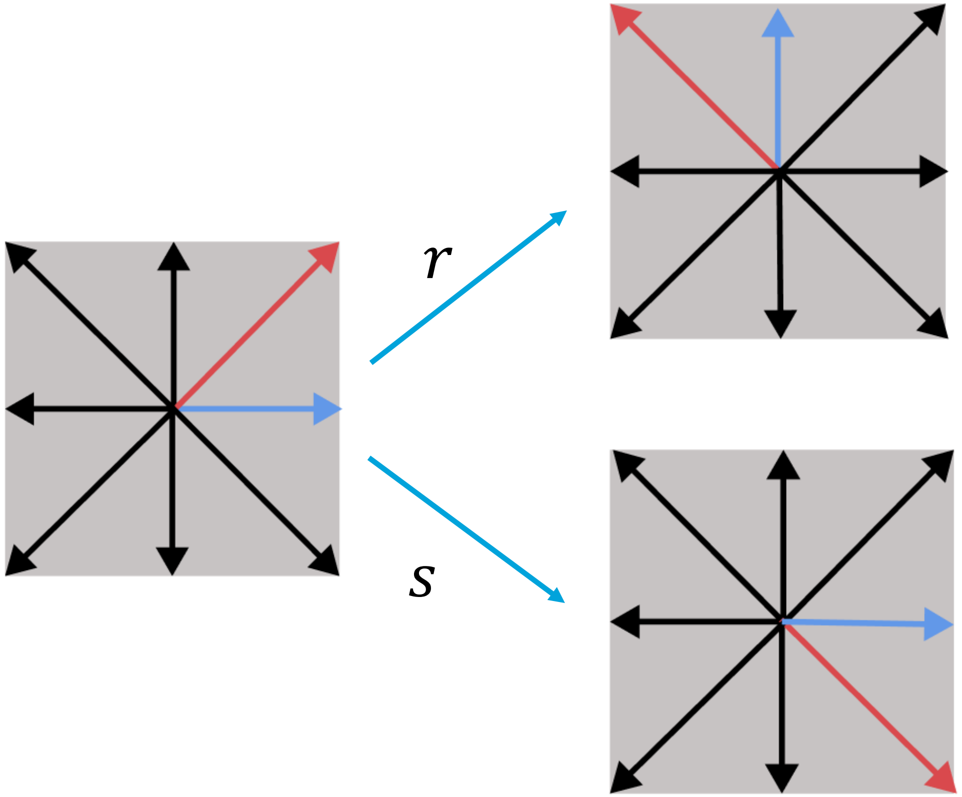

Construction of the SQC

No entanglement

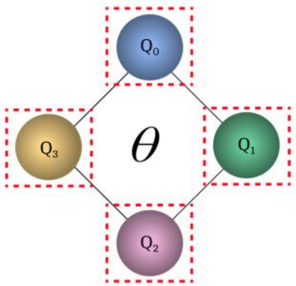

Axial entanglement

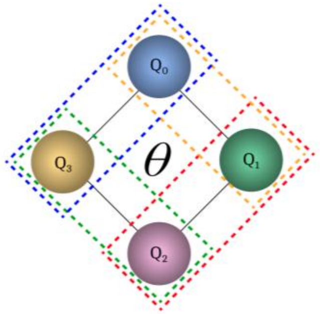

Diagonal entanglement

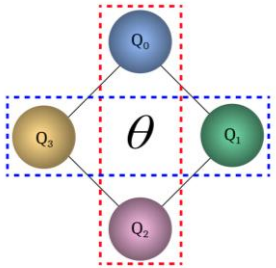

Single-qubit rotation layers

$$R_x(\theta)^{\otimes 4}$$

$$R_z(\theta)^{\otimes 4}$$

Ising XX & ZZ entangling layers

$$\text{Ising}_{xx} = \exp\left(-\frac{i\theta}{2}\sigma_x \otimes \sigma_x\right)$$

$$\text{Ising}_{zz} = \exp\left(-\frac{i\theta}{2}\sigma_z \otimes \sigma_z\right)$$

M. Lacatus, MM, Surrogate quantum circuit design for the lattice Boltzmann collision operator, *IJNME 127(4):e70286, 2026*

Training of the SQC

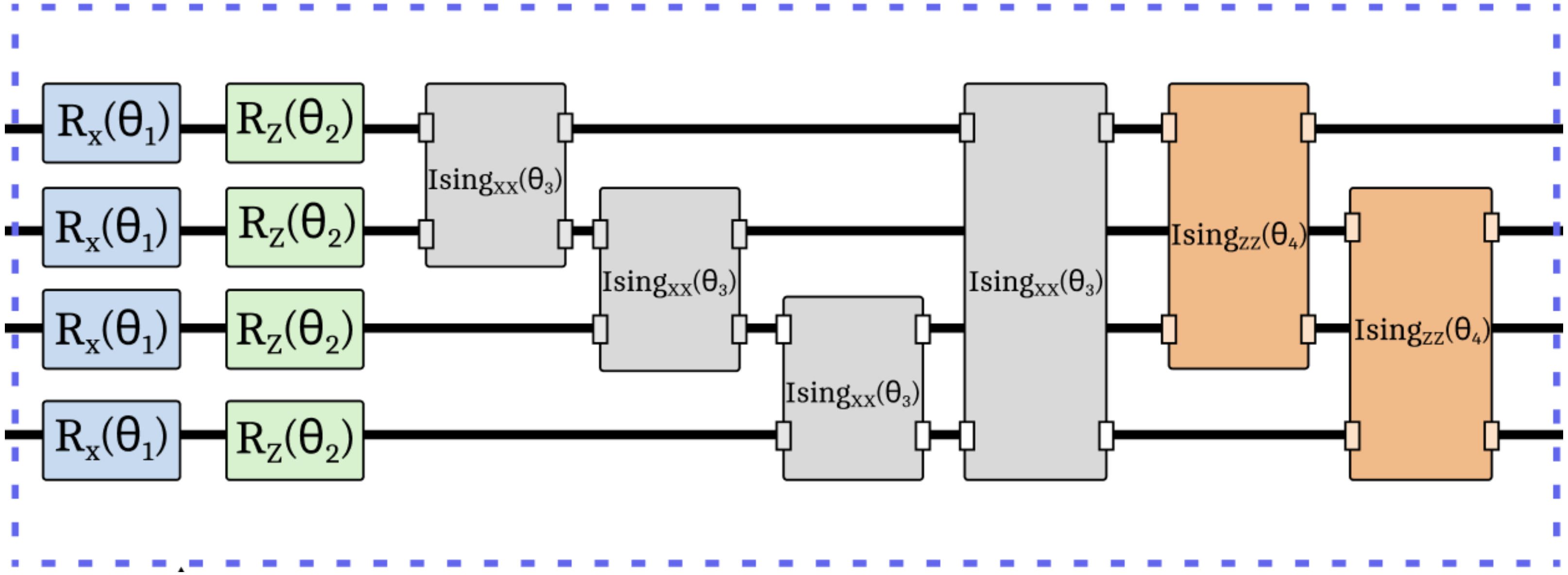

M. Lacatus, MM, Surrogate quantum circuit design for the lattice Boltzmann collision operator*, IJNME 127(4):e70286, 2026*

M. Lacatus, MM: Surrogate Quantum Circuit Design for the Lattice Boltzmann Collision Operator. arXiv: 2507.12256

Training of the SQC

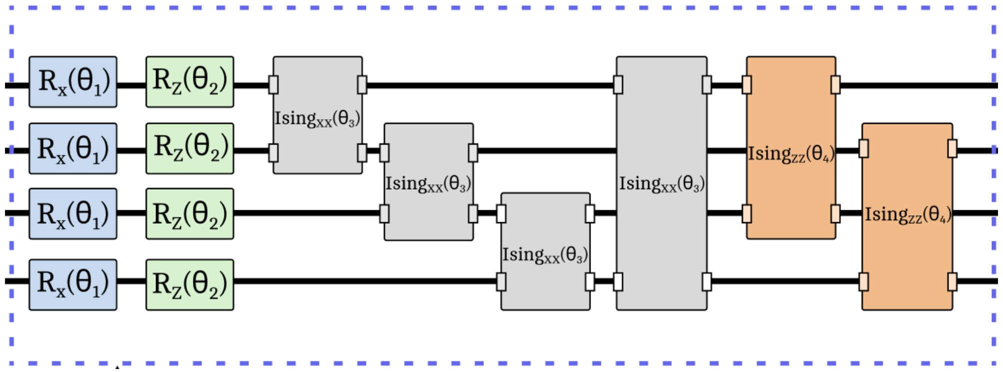

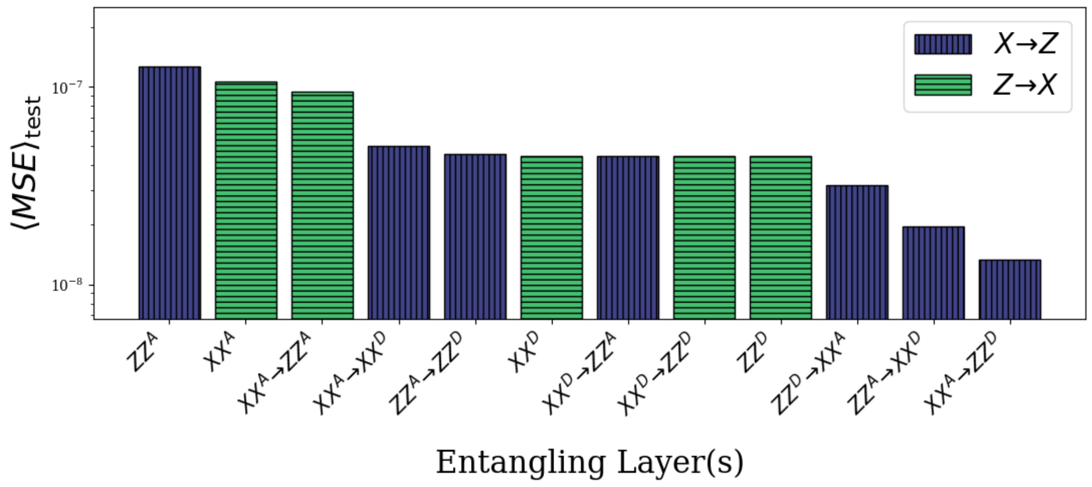

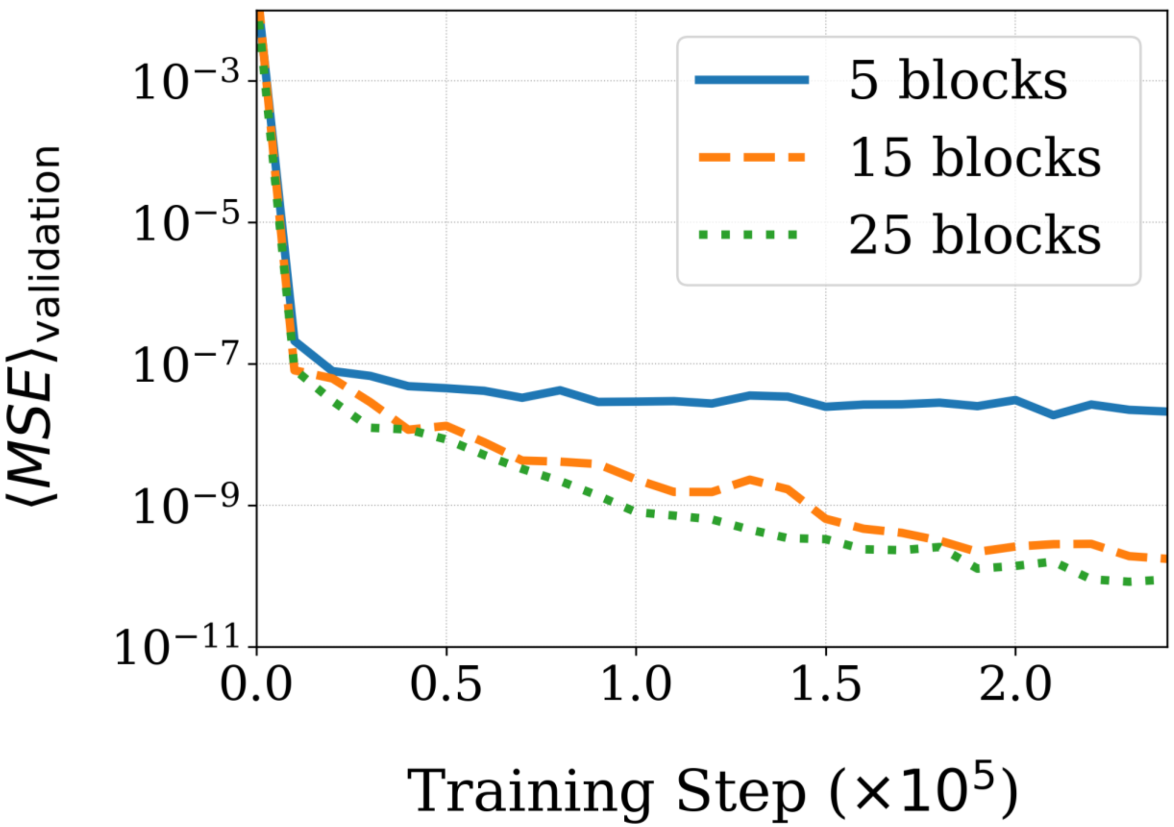

M. Lacatus, MM, Surrogate quantum circuit design for the lattice Boltzmann collision operator, *IJNME 127(4):e70286, 2026*

Application of the SQC

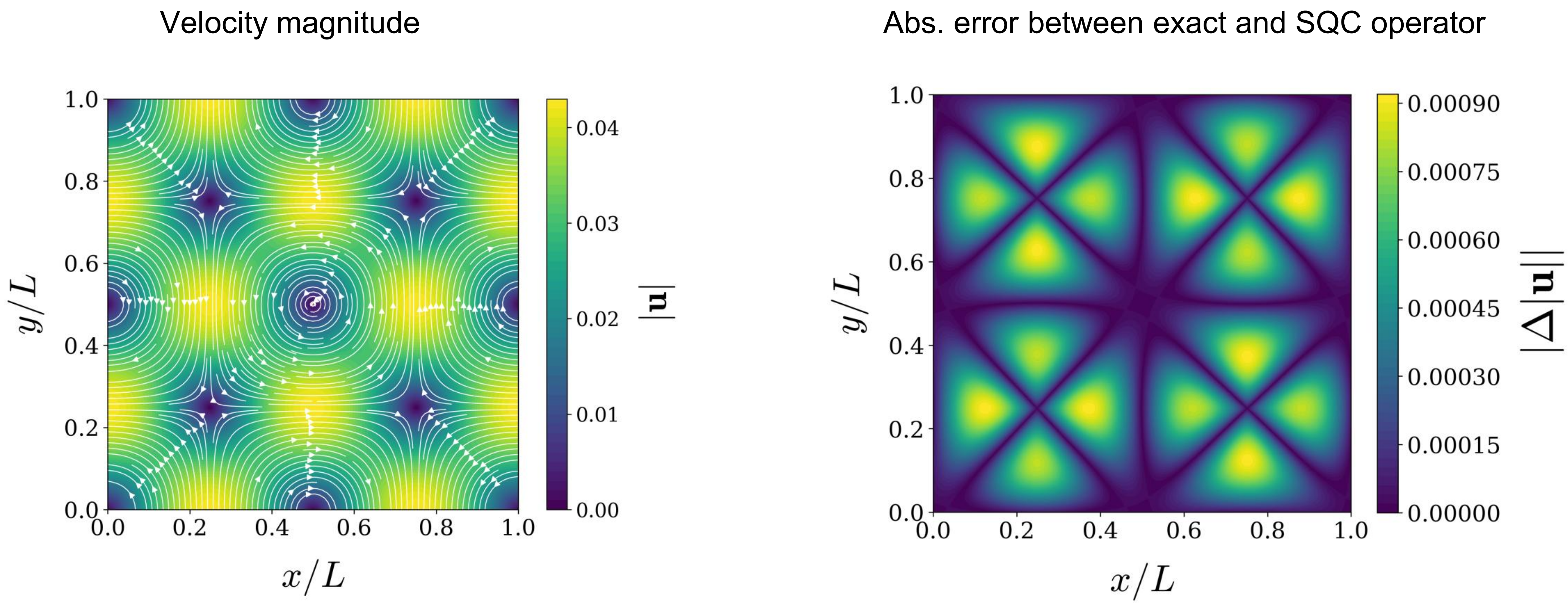

Taylor-Green vortex decay: 64x64 grid, Re=50

M. Lacatus, MM, Surrogate quantum circuit design for the lattice Boltzmann collision operator*, IJNME 127(4):e70286, 2026*

Application of the SQC

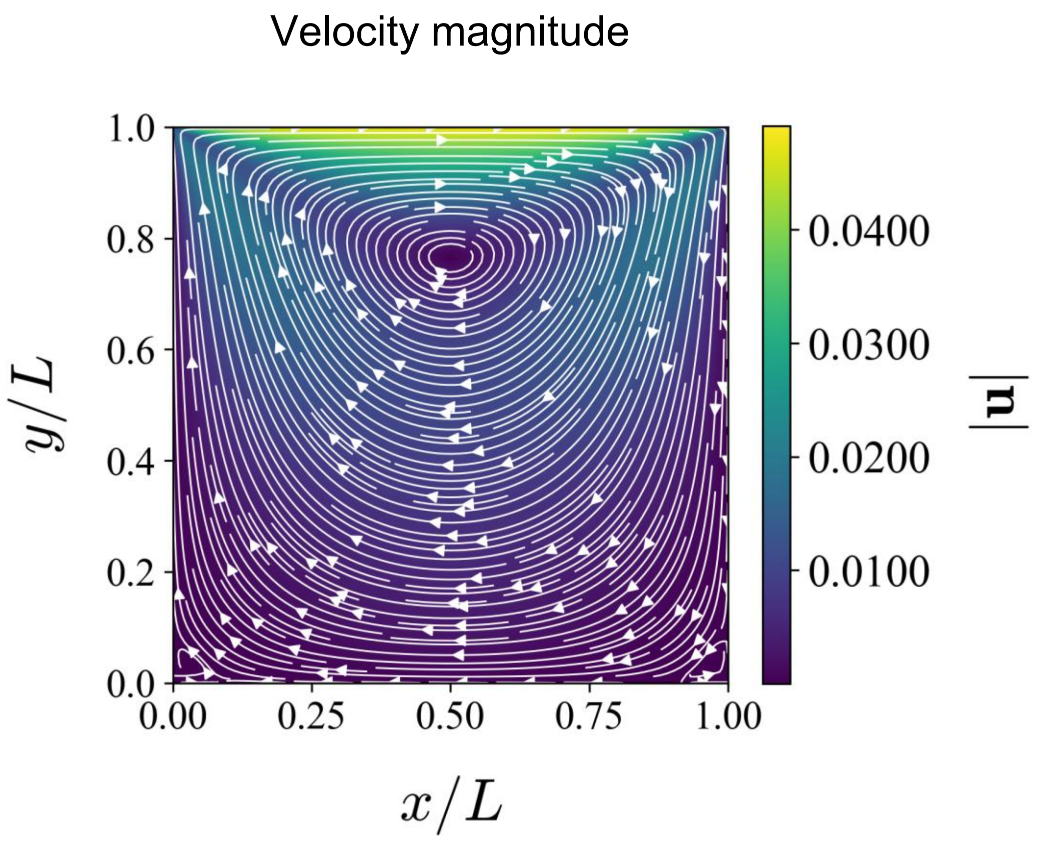

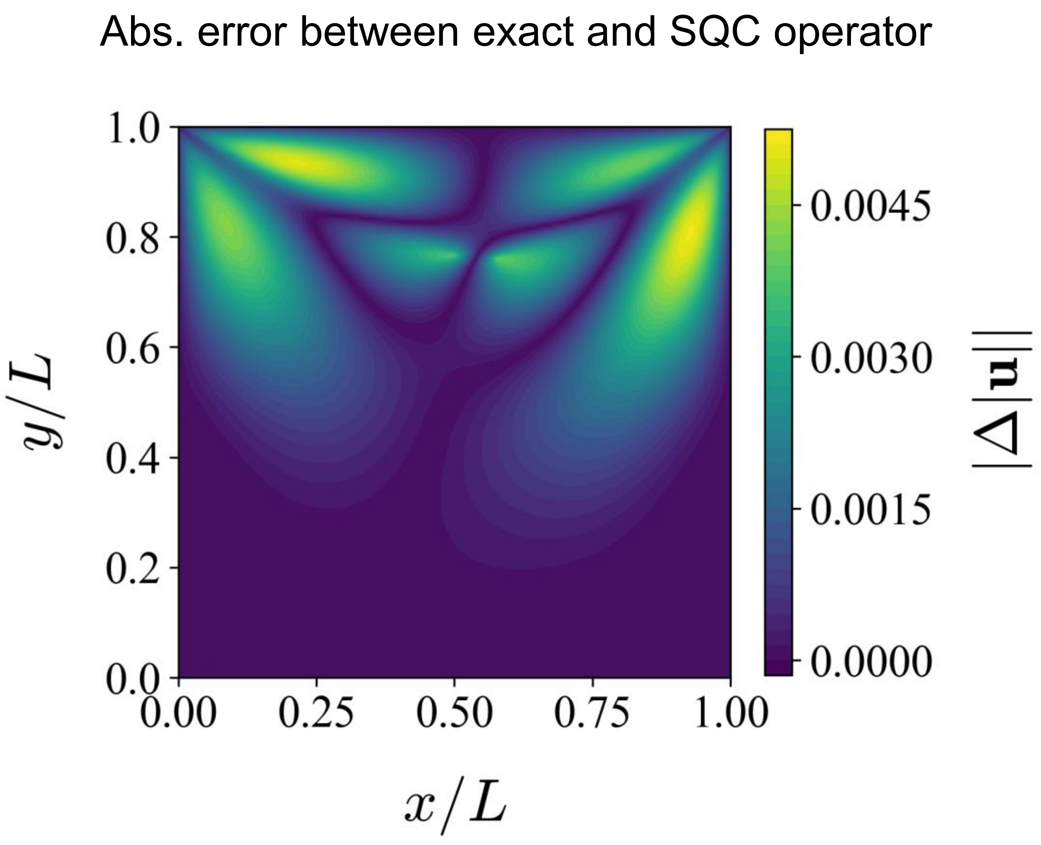

Lid-driven cavity: 64x64 grid, Re=50

M. Lacatus, MM, Surrogate quantum circuit design for the lattice Boltzmann collision operator*, IJNME 127(4):e70286, 2026*

Application of the SQC

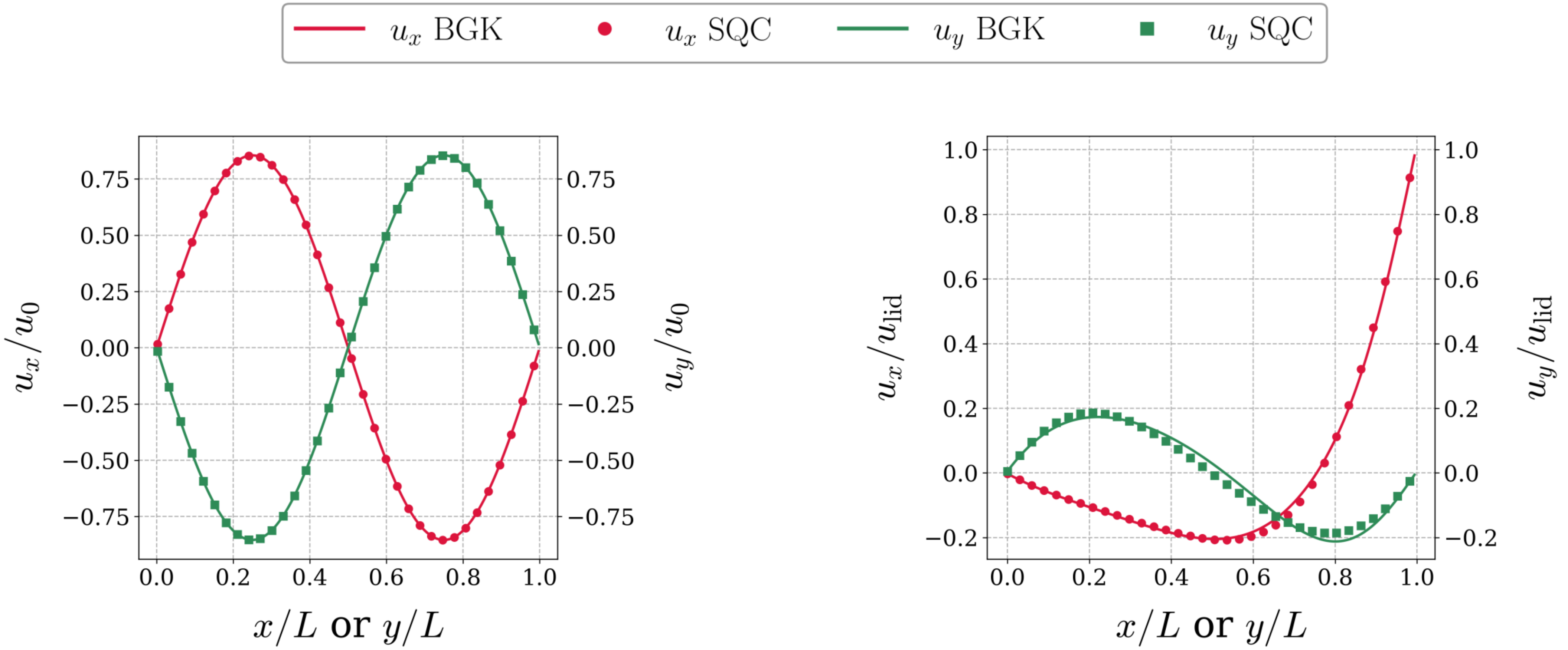

Taylor-Green vortex decay

Lid driven cavity

M. Lacatus, MM, Surrogate quantum circuit design for the lattice Boltzmann collision operator, *IJNME 127(4):e70286, 2026*

Application of the SQC

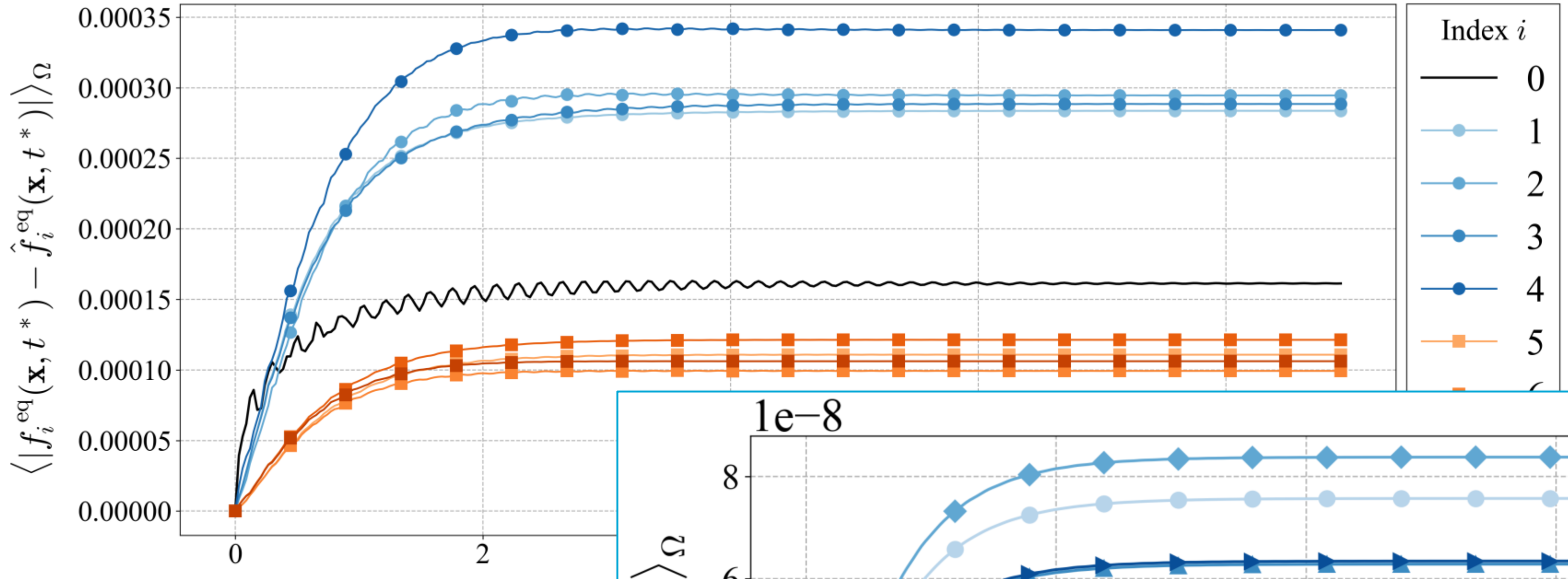

Lid driven cavity: Time evolut

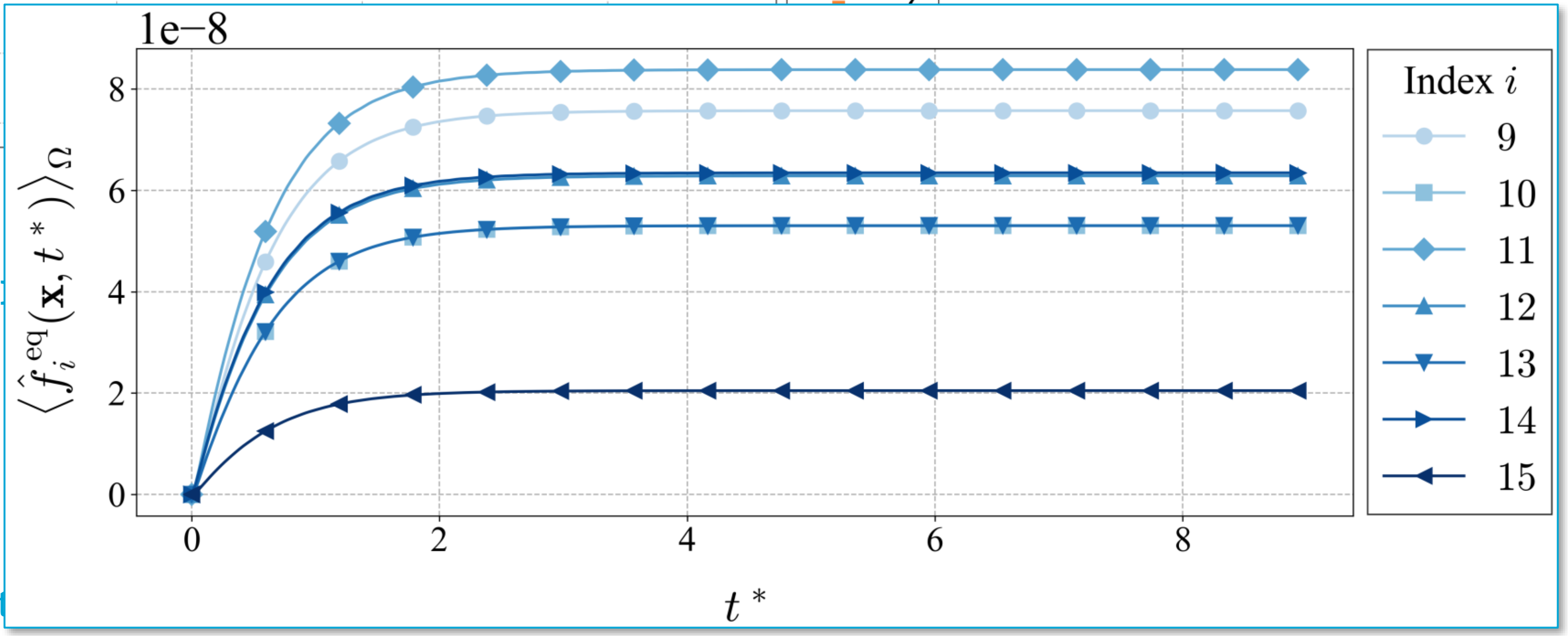

M. Lacatus, MM, Surrogate quant

Nonlinearity through measurement

- f_α^{eq} is **nonlinear** in $\boldsymbol{u}$

$$w_\alpha \varrho \left(1 + \frac{\boldsymbol{u}\cdot\boldsymbol{e}_\alpha}{c_s^2} + \frac{(\boldsymbol{u}\cdot\boldsymbol{e}_\alpha)^2}{2c_s^4} - \frac{\boldsymbol{u}\cdot\boldsymbol{u}}{2c_s^4}\right)$$

- f_α^{lin} is **linear** in $\boldsymbol{u}$

$$w_\alpha \varrho \left(1 + \frac{\boldsymbol{u}\cdot\boldsymbol{e}_\alpha}{c_s^2}\right)$$

- $\hat{f}_\alpha^{\text{eq}}$ is computed by a unitary

$$U(\Theta)\frac{1}{\sqrt{\rho}}\Sigma_\alpha \sqrt{f_\alpha}|\boldsymbol{e}_\alpha\rangle$$

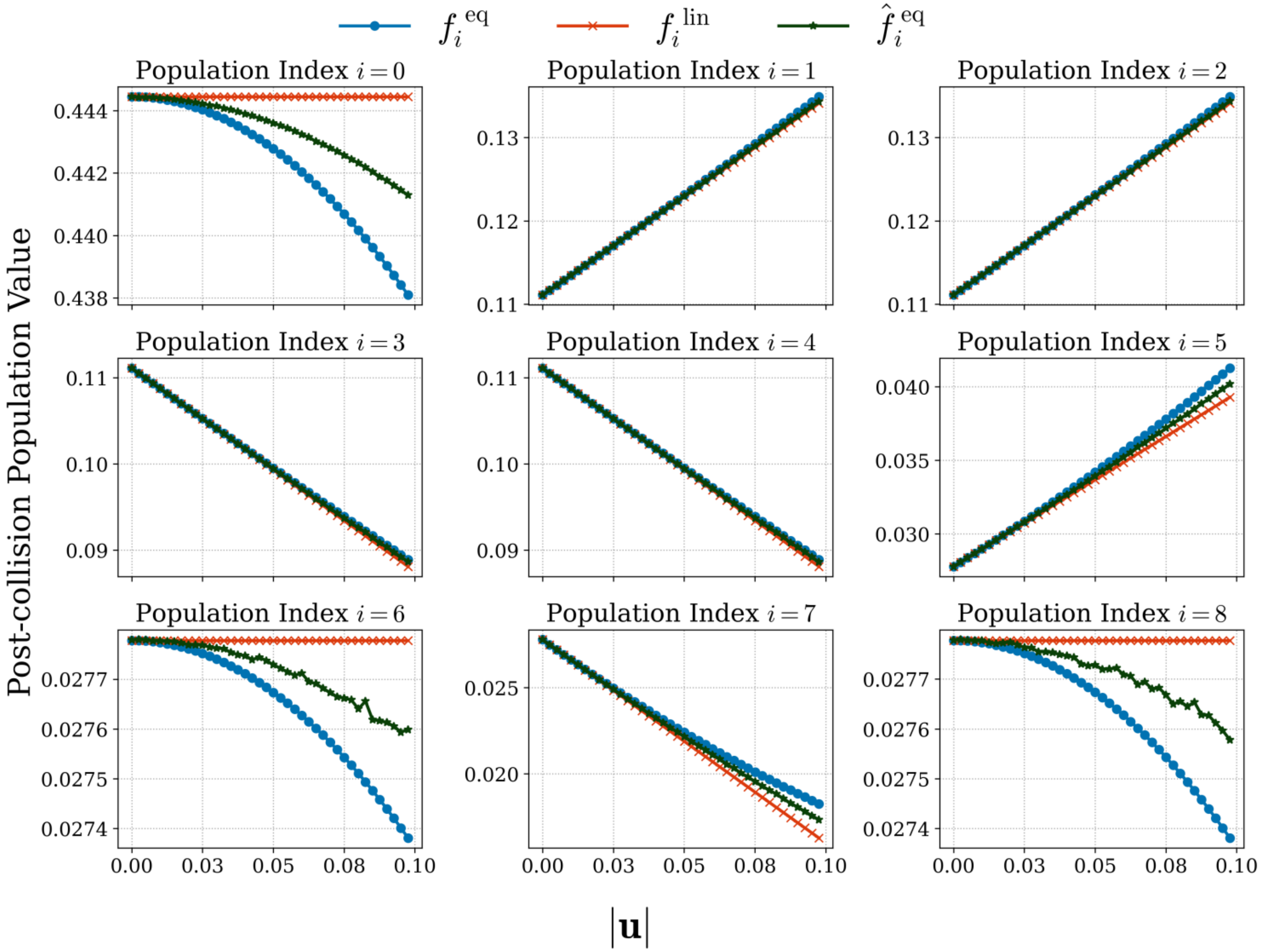

M. Lacatus, MM, Surrogate quantum circuit design for the lattice Boltzmann collision operator, IJNME 127(4):e70286, 2026

Nonlinearity through measurement

- f_α^{eq} is **nonlinear** in $\boldsymbol{u}$

$$w_\alpha \varrho \left(1 + \frac{\boldsymbol{u}\cdot\boldsymbol{e}_\alpha}{c_s^2} + \frac{(\boldsymbol{u}\cdot\boldsymbol{e}_\alpha)^2}{2c_s^4} - \frac{\boldsymbol{u}\cdot\boldsymbol{u}}{2c_s^4}\right)$$

- f_α^{lin} is **linear** in $\boldsymbol{u}$

$$w_\alpha \varrho \left(1 + \frac{\boldsymbol{u}\cdot\boldsymbol{e}_\alpha}{c_s^2}\right)$$

- $\hat{f}_\alpha^{\text{eq}}$ is computed by a unitary

$$U(\Theta)\frac{1}{\sqrt{\rho}}\sum_\alpha \sqrt{f_\alpha}\,|\boldsymbol{e}_\alpha\rangle$$

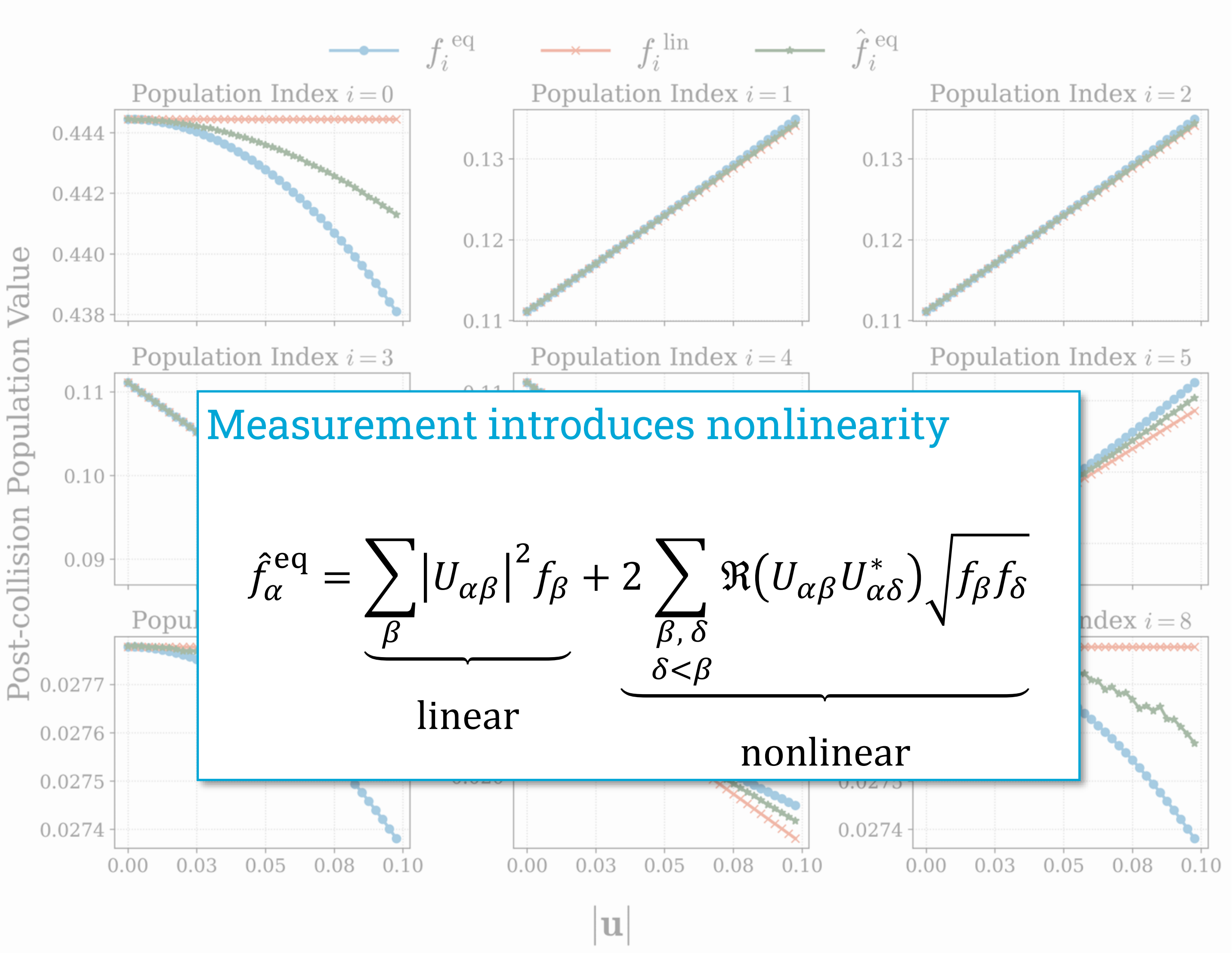

Measurement introduces nonlinearity

$$\hat{f}_\alpha^{\text{eq}} = \underbrace{\sum_\beta |U_{\alpha\beta}|^2 f_\beta}_{\text{linear}} + \underbrace{2\sum_{\substack{\beta,\delta\\ \delta<\beta}} \Re\left(U_{\alpha\beta}U_{\alpha\delta}^*\right)\sqrt{f_\beta f_\delta}}_{\text{nonlinear}}$$

M. Lacatus, MM, Surrogate quantum circuit design for the lattice Boltzmann collision operator, *IJNME 127(4):e70286, 2026*

Running on NISQ hardware

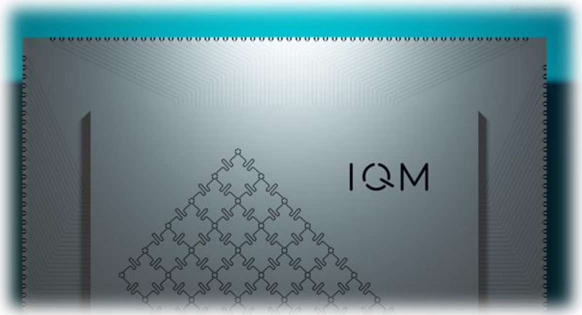

QPU	IQM Crystal 20	IQM Crystal 54
Qubit count	20	54
1Q fidelity	99.92%	99.93%
2Q fidelity	99.51%	99.5%
Q-volume	32	64
CLOPS	2600	2550
Q-score	15	24

Sim

initialization

IQM20

- R: 1, CZ: 0, shots: 100.000, trials: 6

IQM54

- R: 1, CZ: 0, shots: 100.000, trials: 6

Running on NISQ hardware

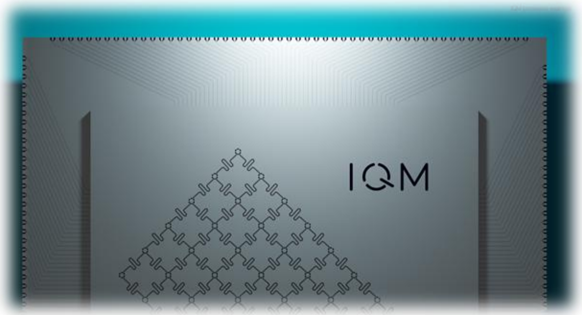

QPU	IQM Crystal 20	IQM Crystal 54
Qubit count	20	54
1Q fidelity	99.92%	99.93%
2Q fidelity	99.51%	99.5%
Q-volume	32	64
CLOPS	2600	2550
Q-score	15	24

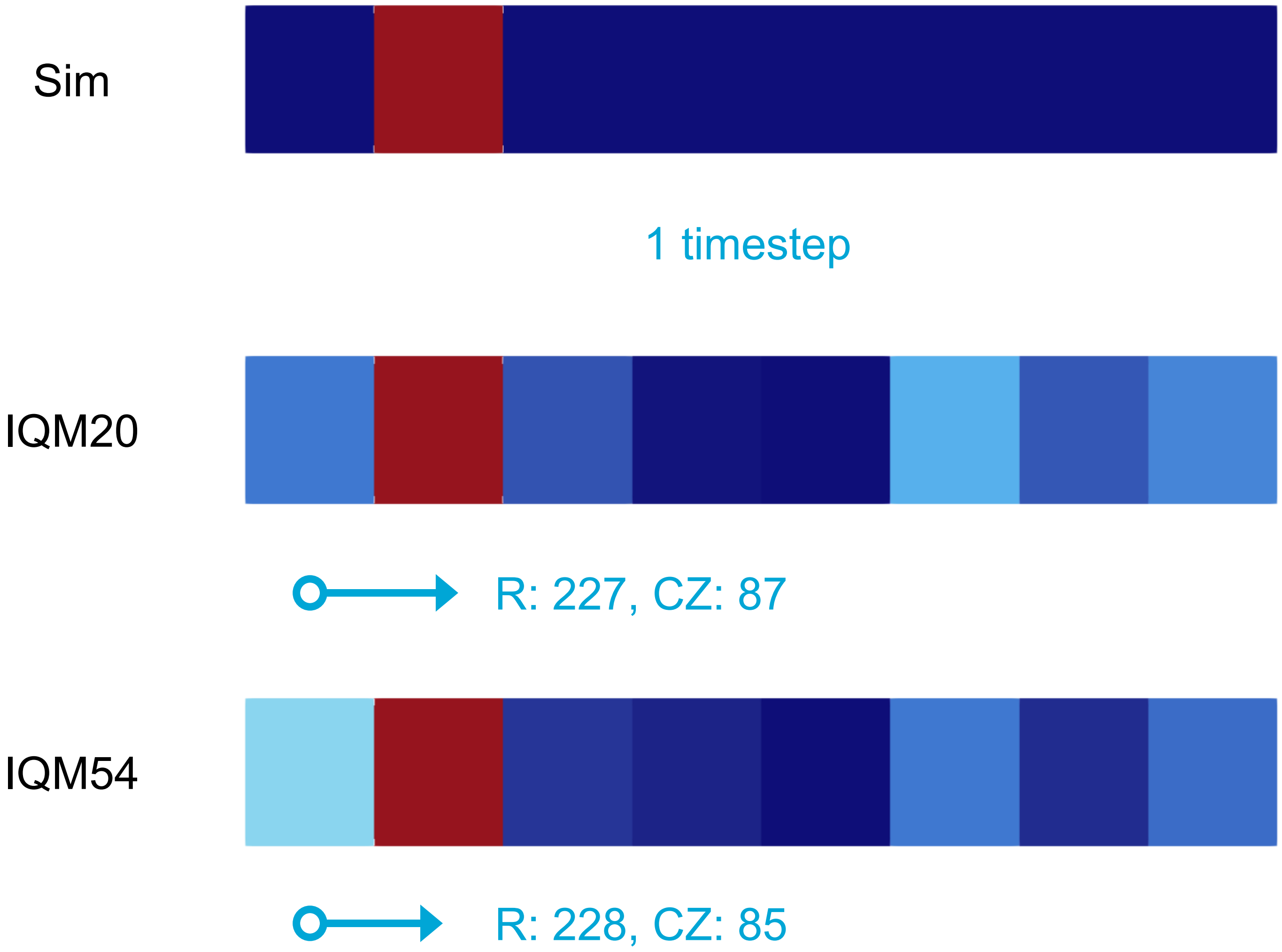

Running on NISQ hardware

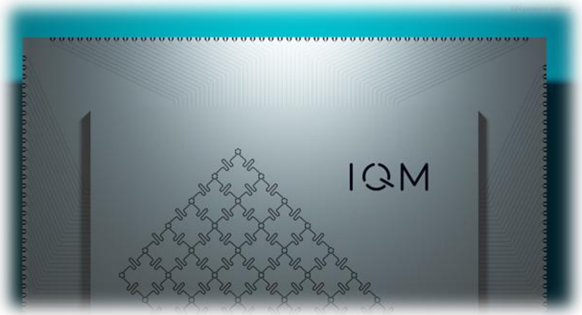

QPU	IQM Crystal 20	IQM Crystal 54
Qubit count	20	54
1Q fidelity	99.92%	99.93%
2Q fidelity	99.51%	99.5%
Q-volume	32	64
CLOPS	2600	2550
Q-score	15	24

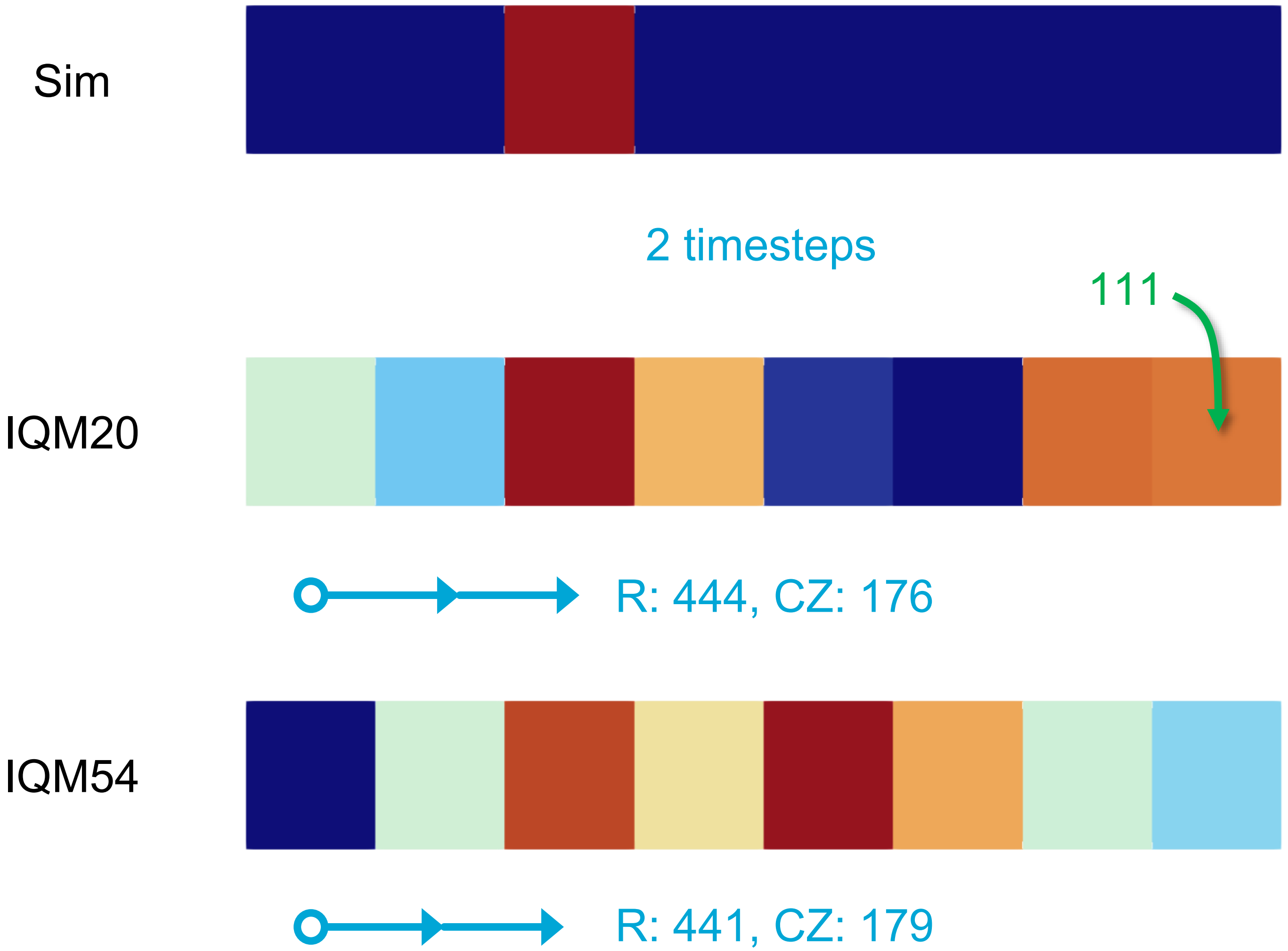

Running on NISQ hardware

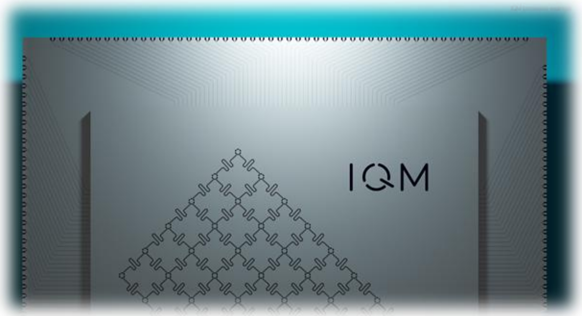

QPU	IQM Crystal 20	IQM Crystal 54
Qubit count	20	54
1Q fidelity	99.92%	99.93%
2Q fidelity	99.51%	99.5%
Q-volume	32	64
CLOPS	2600	2550
Q-score	15	24

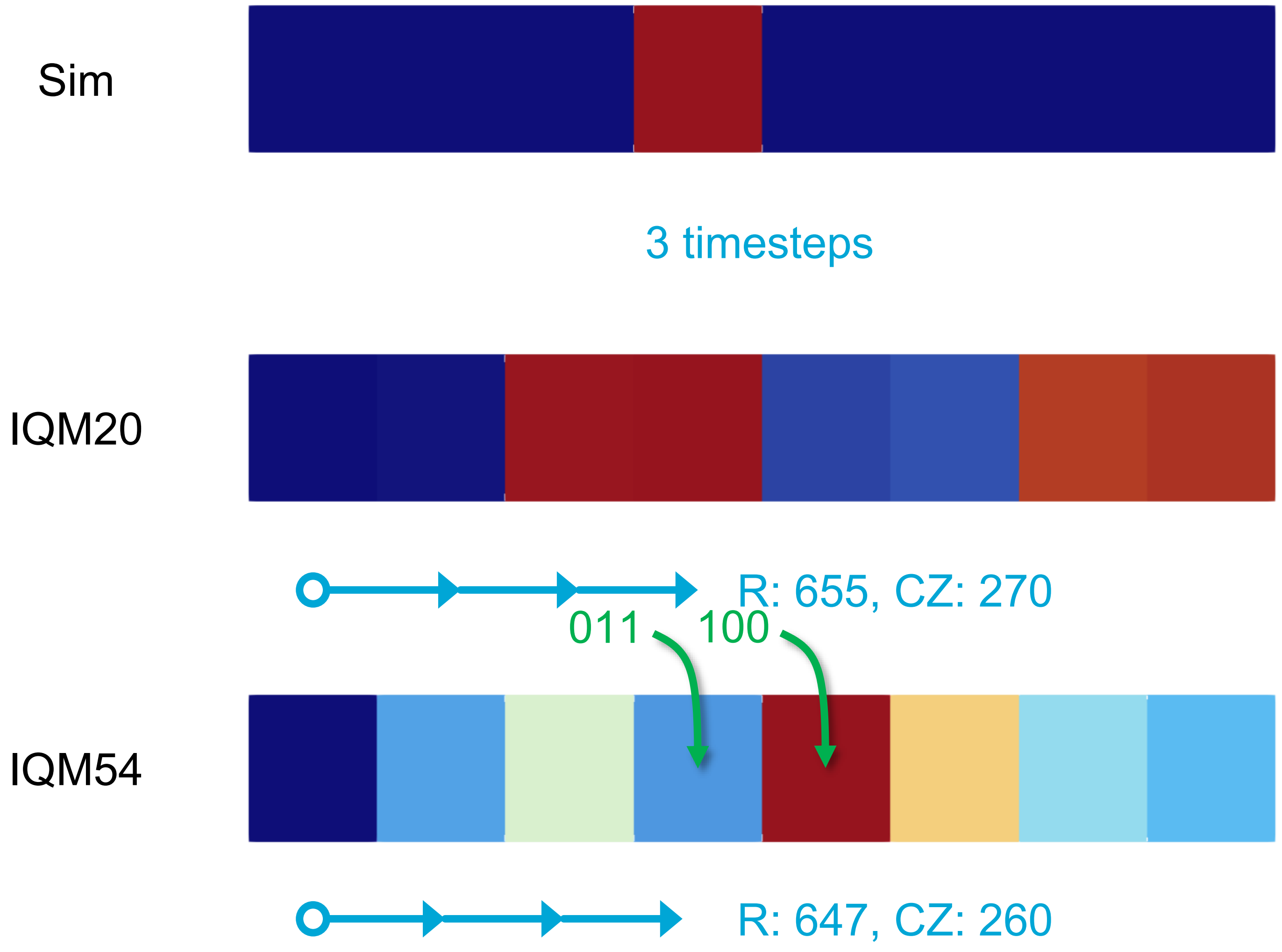

Running on NISQ hardware

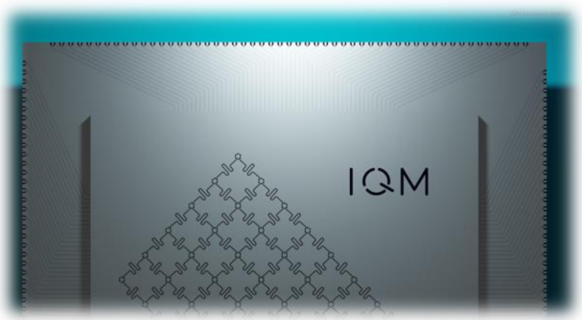

QPU	IQM Crystal 20	IQM Crystal 54
Qubit count	20	54
1Q fidelity	99.92%	99.93%
2Q fidelity	99.51%	99.5%
Q-volume	32	64
CLOPS	2600	2550
Q-score	15	24

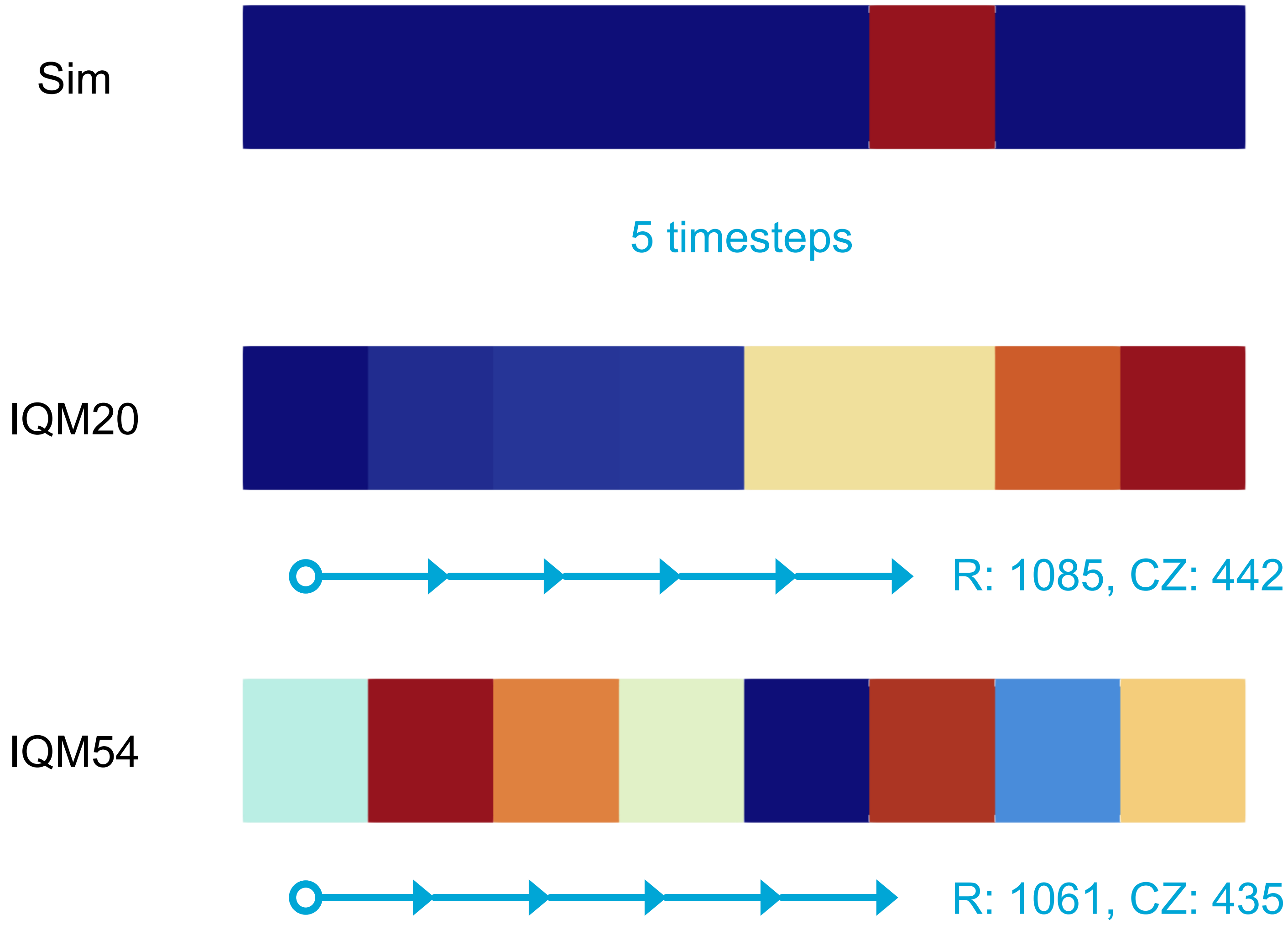

Running on NISQ hardware

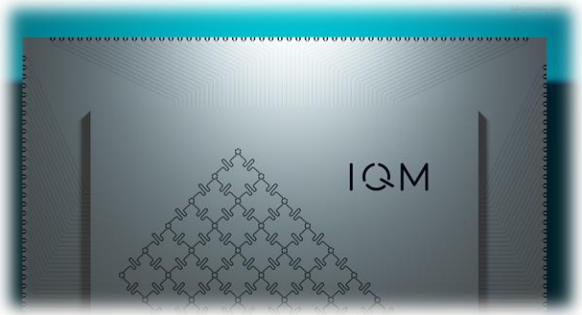

QPU	IQM Crystal 20	IQM Crystal 54
Qubit count	20	54
1Q fidelity	99.92%	99.93%
2Q fidelity	99.51%	99.5%
Q-volume	32	64
CLOPS	2600	2550
Q-score	15	24

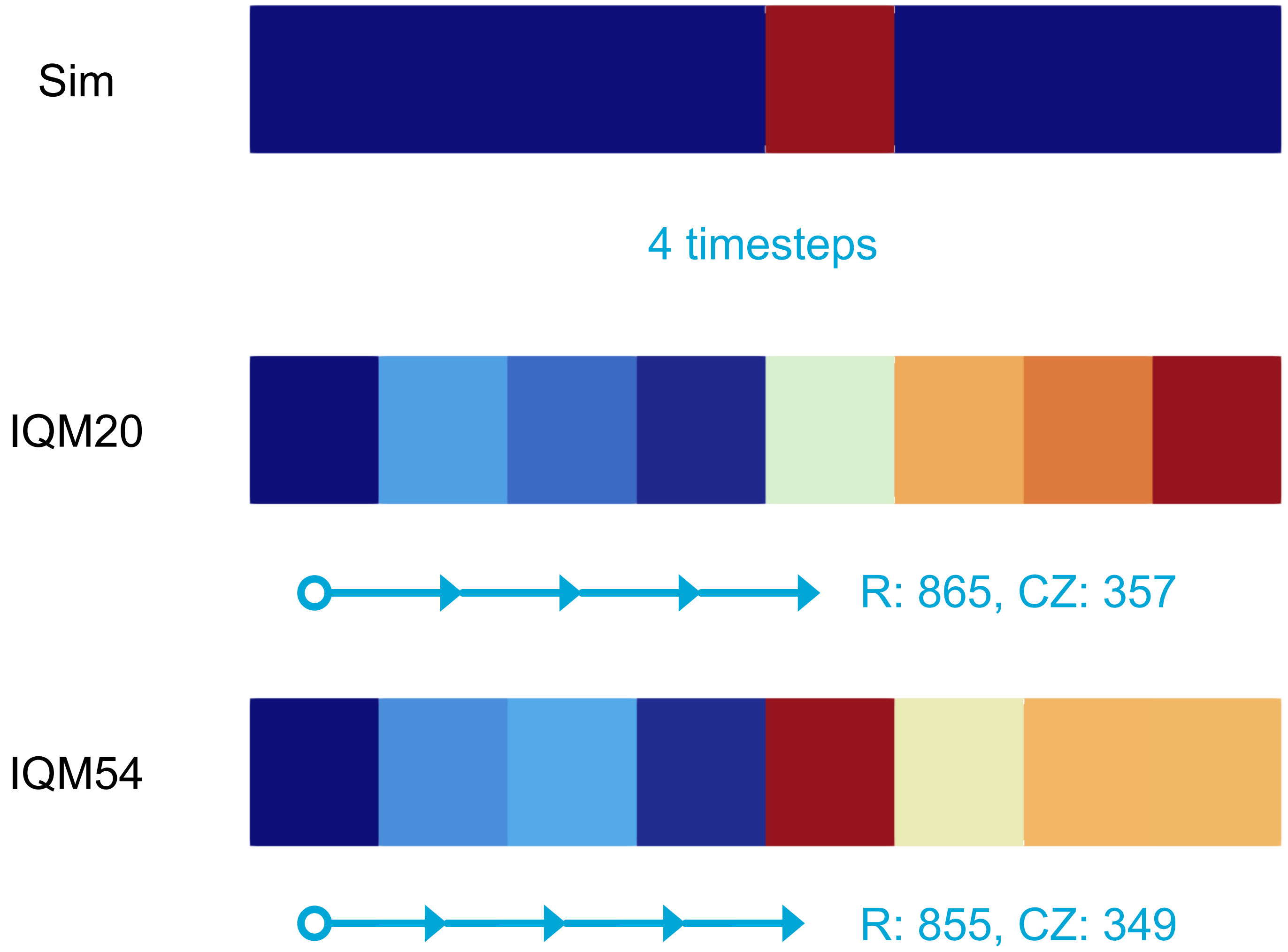

Quantum-enhanced design optimization

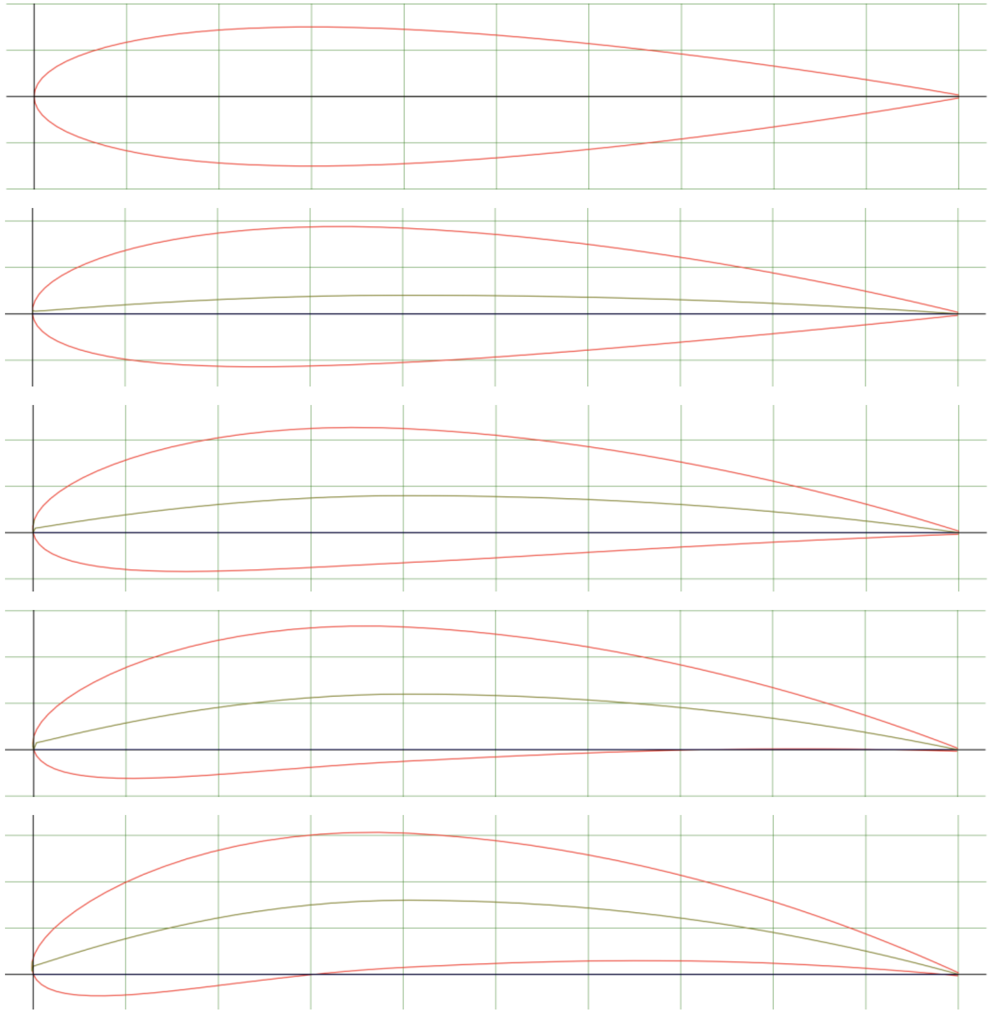

Generated with airfoiltools.com

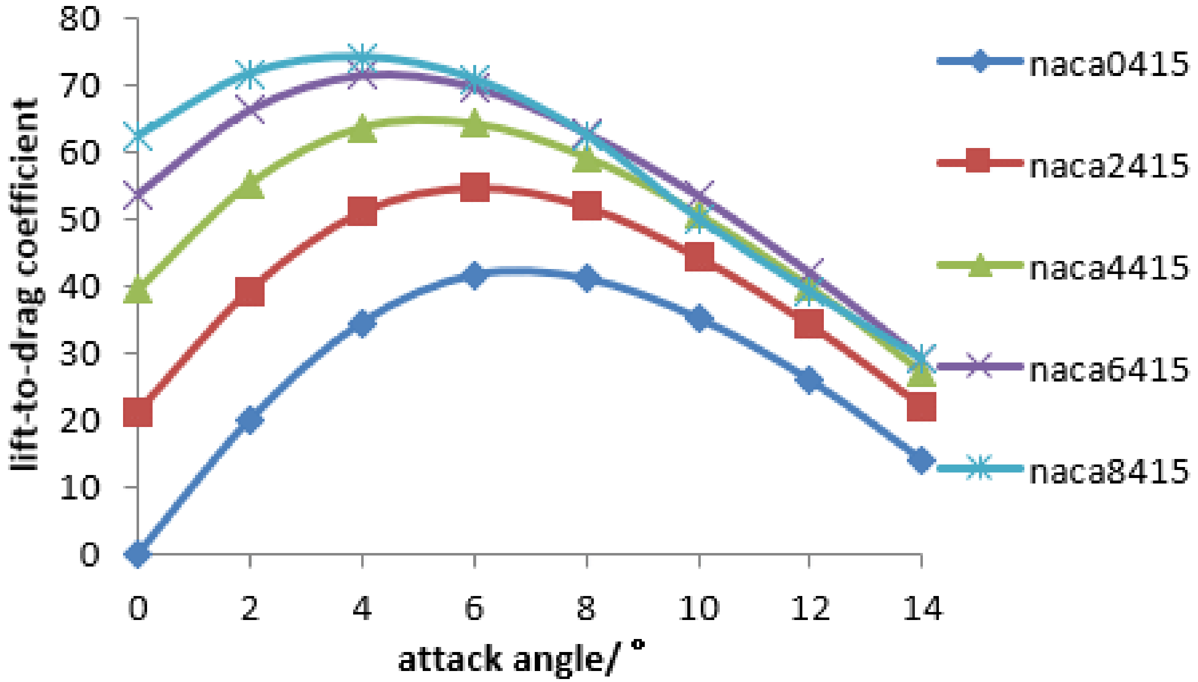

DOI: 10.1088/1742-6596/1519/1/012020

Exploit **quadratic speedup of quantum search algorithms** in design optimization

Quantum-enhanced design optimization

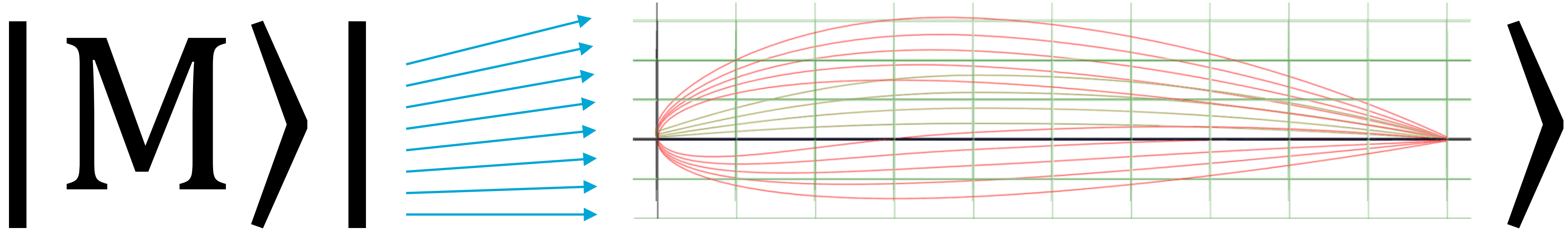

C. Georgescu, MM, Quantum Search in Superposed Quantum Lattice Gas Automata and Lattice Boltzmann Systems, *arXiv: 2510.14062*

Quantum-enhanced design optimization

$|7\rangle|$ → 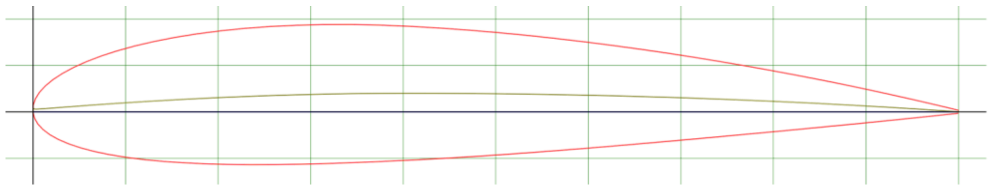 $\rangle$

C. Georgescu, MM, Quantum Search in Superposed Quantum Lattice Gas Automata and Lattice Boltzmann Systems, *arXiv: 2510.14062*

Quantum-enhanced design optimization

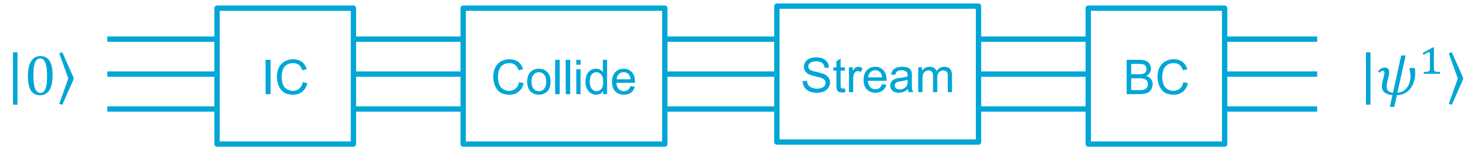

C. Georgescu, MM, Quantum Search in Superposed Quantum Lattice Gas Automata and Lattice Boltzmann Systems, *arXiv: 2510.14062*

Quantum-enhanced design optimization

Dürr-Høyer minimum-finding algorithm

Finds optimal configuration with $\sqrt{N}$ queries (N queries classically) → **quadratic speedup**

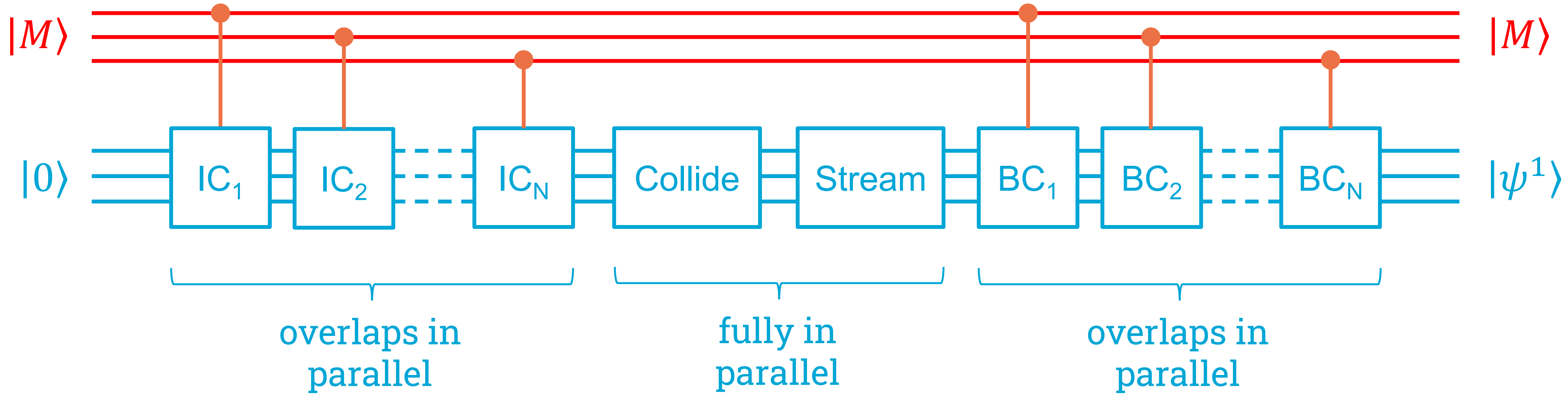

C. Georgescu, MM, Quantum Search in Superposed Quantum Lattice Gas Automata and Lattice Boltzmann Systems, *arXiv: 2510.14062*

End-to-end implementation

<u>Goal</u>: Find the initial configuration for which the relative density in the right half-plane is largest

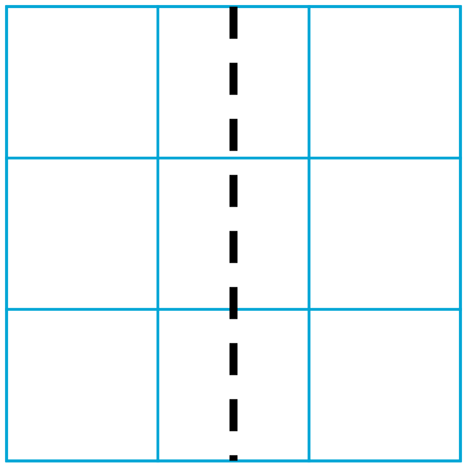

$x > 0.5$

End-to-end implementation

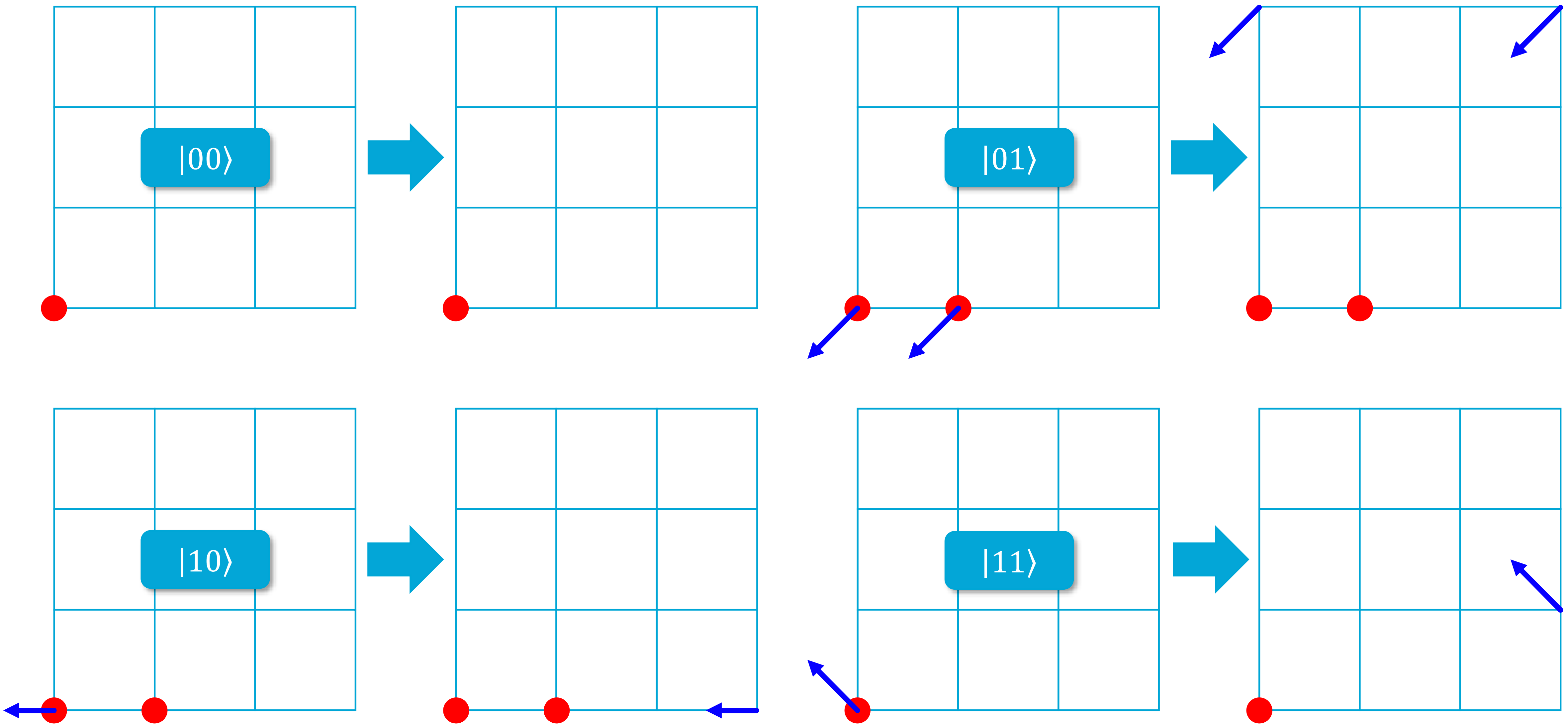

End-to-end implementation

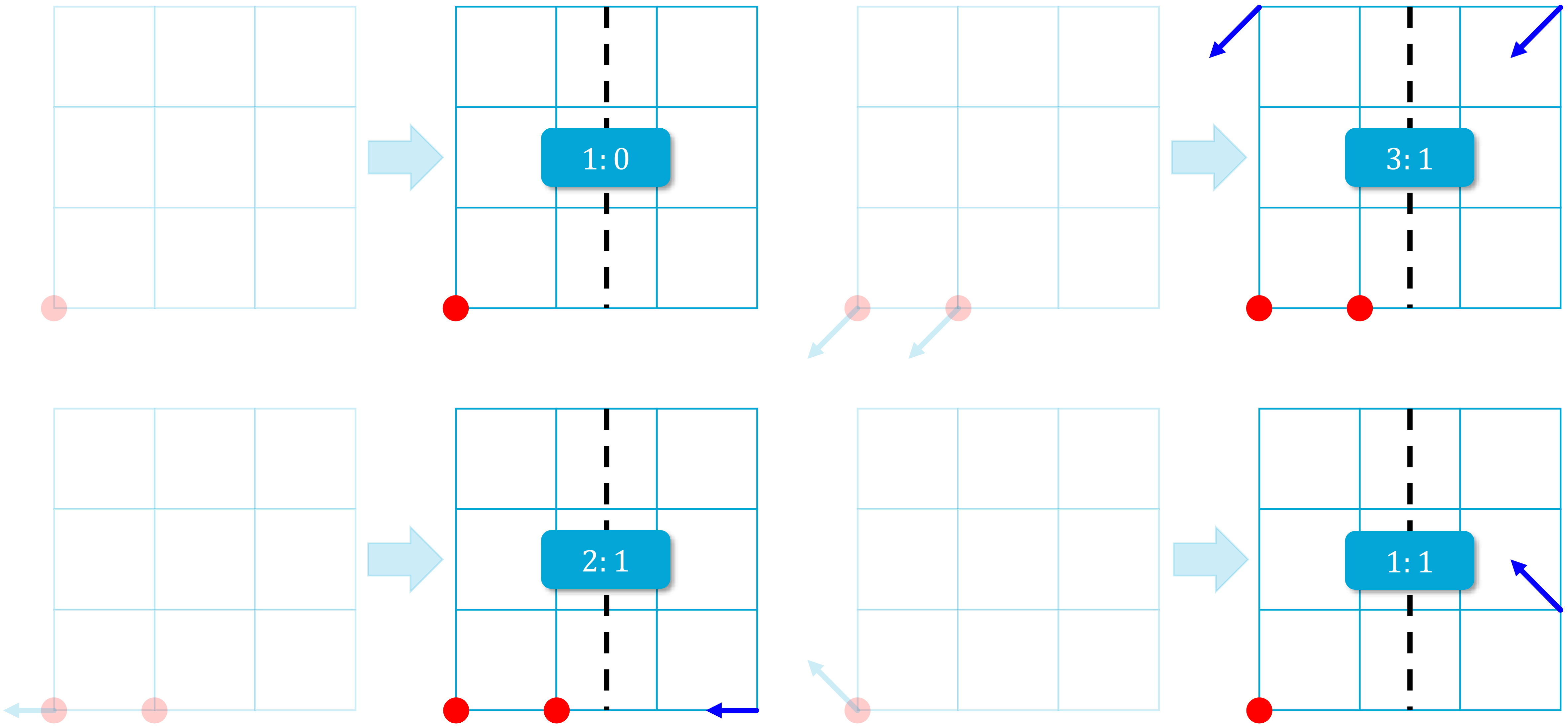

End-to-end implementation

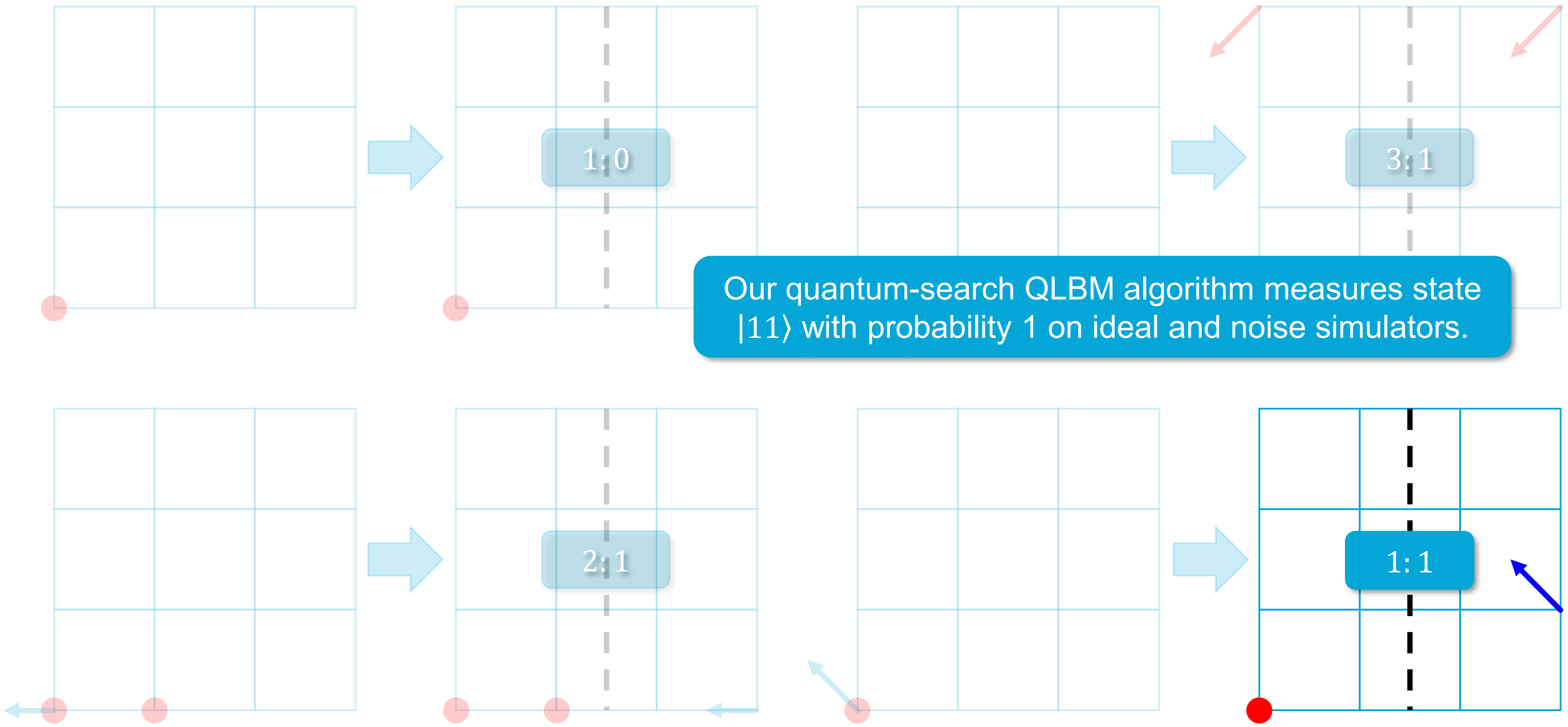

Our quantum-search QLBM algorithm measures state $|11\rangle$ with probability 1 on ideal and noise simulators.

Take-home lessons, continued

If quantum computing shall become the future of HPCSE we need to ...

- … identify **applications** that cannot be solved efficiently with classical computers
- … develop **algorithms** that exploit the strengths of quantum computers (and avoid their limitations)
- … (most probably) change the **workflows** that were designed for classical computers

Application:	large-scale direct numerical simulation of fluid dynamics
Algorithm:	quantum lattice Boltzmann method
Workflow:	quantum-accelerated design optimization workflow

Is this enough to make quantum the future of HPCSE? We will see ...

Applied Quantum Methods in Computational Science and Engineering

September 14-17, 2026 Delft, NL

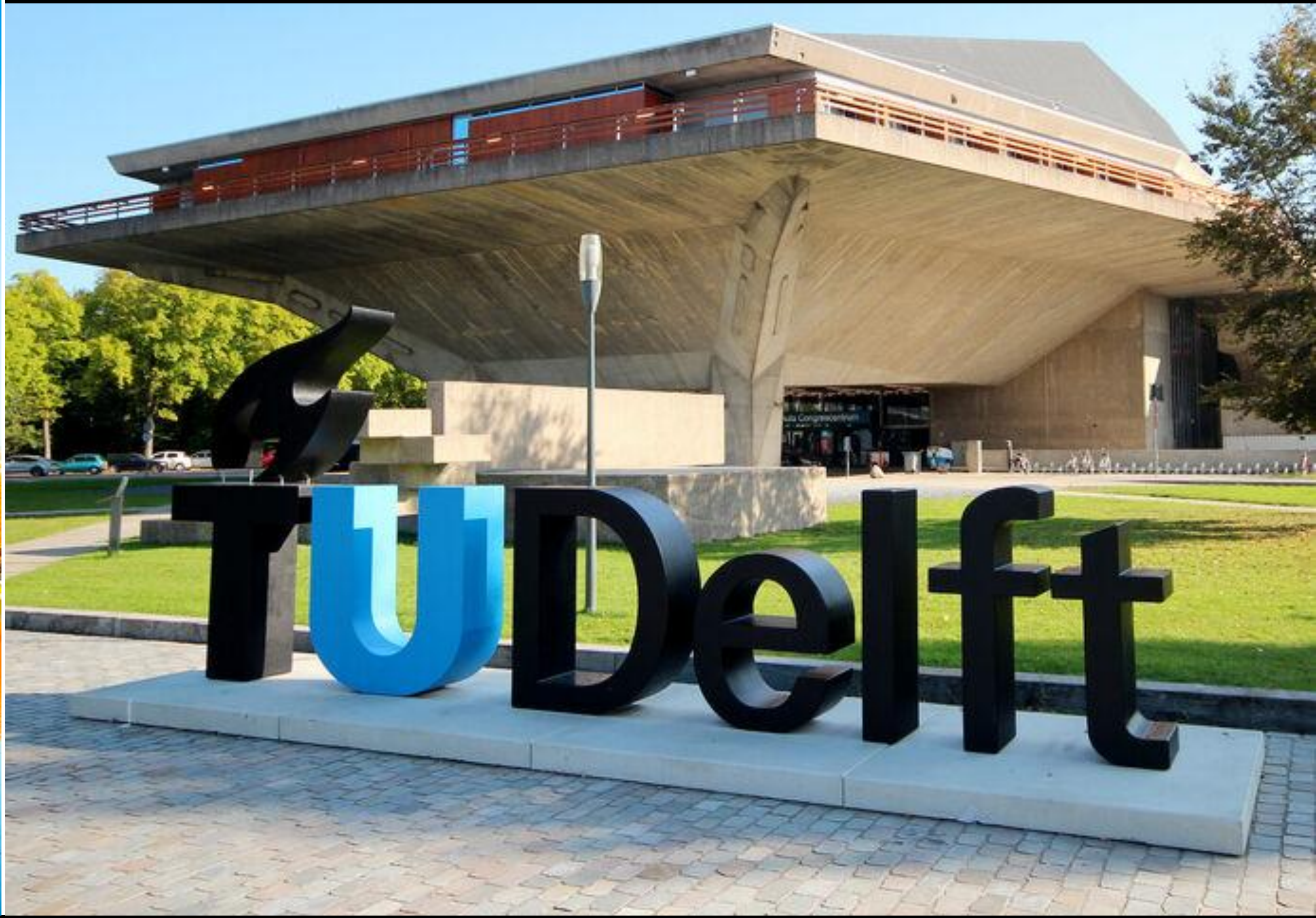

Applied Quantum Methods in Computational Science and Engineering

September 14-17, 2026 Delft, NL

We have open positions, please contact me

M.Moller@tudelft.nl

Acknowledgement

C. Georgescu, M. Lacatus, M. Schalkers, N. Hosters, S. Berger, E. Duong, ...

Fujitsu Limited, RVO NL

Physics-informed neural networks (PINNs)

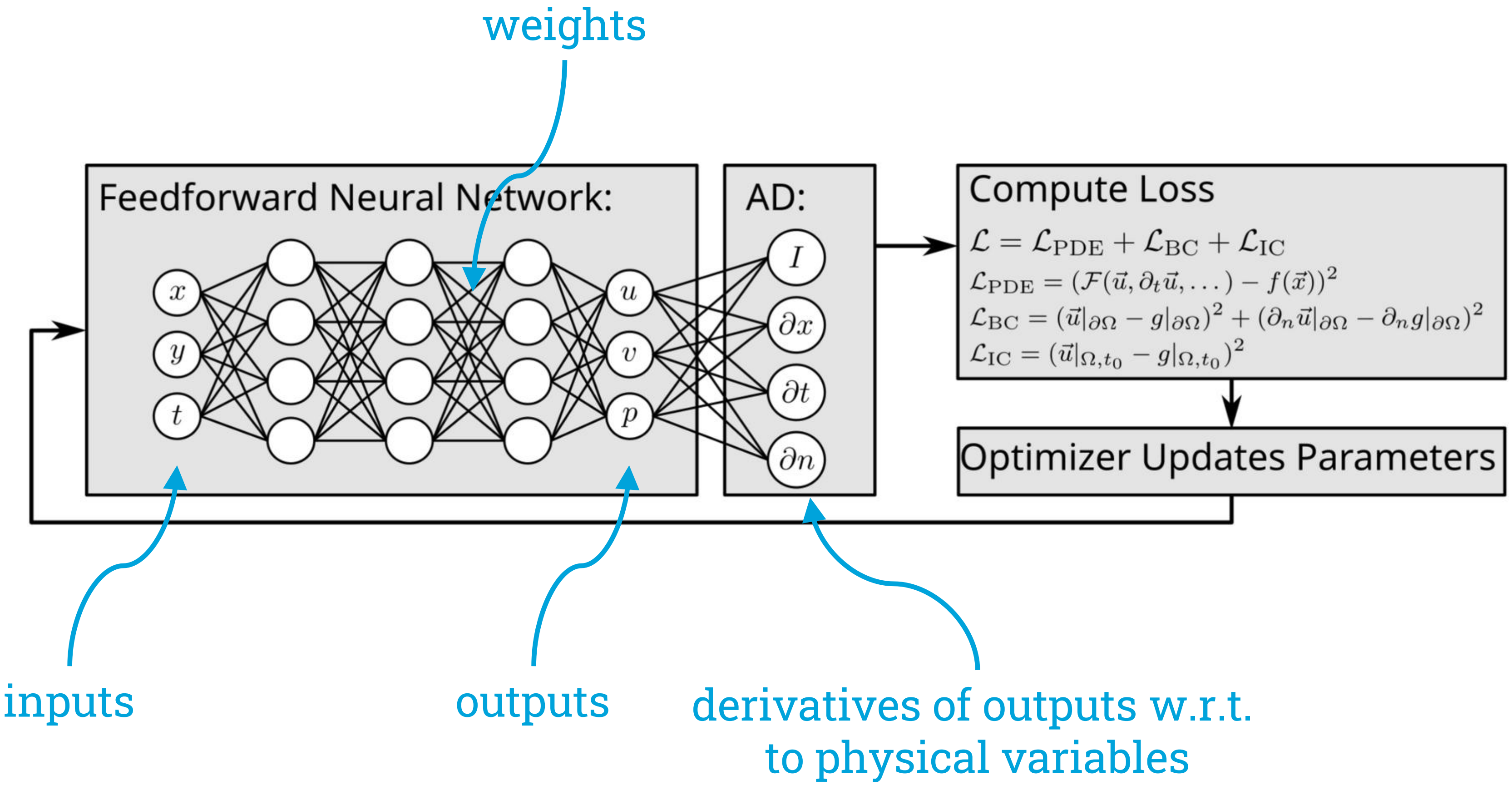

Quantum physics-informed neural networks (QPINNs)

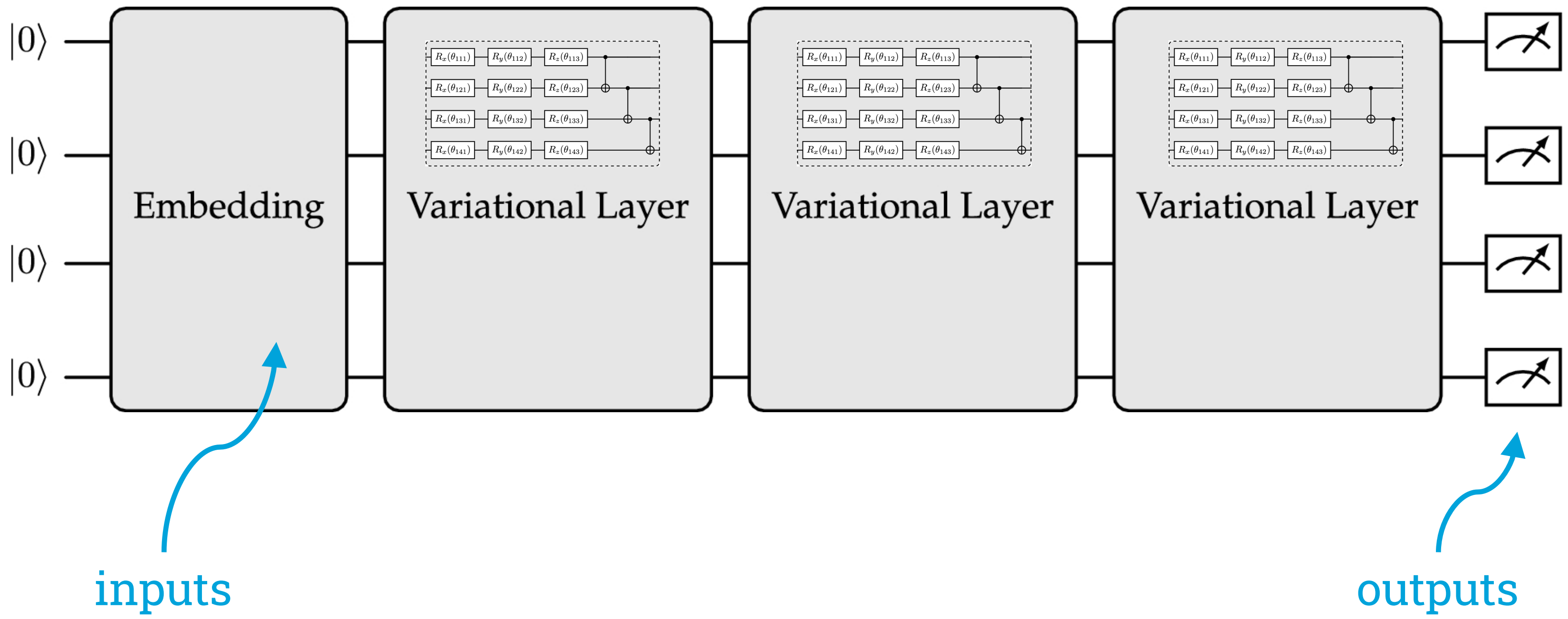

Quantum physics-informed neural networks (QPINNs)

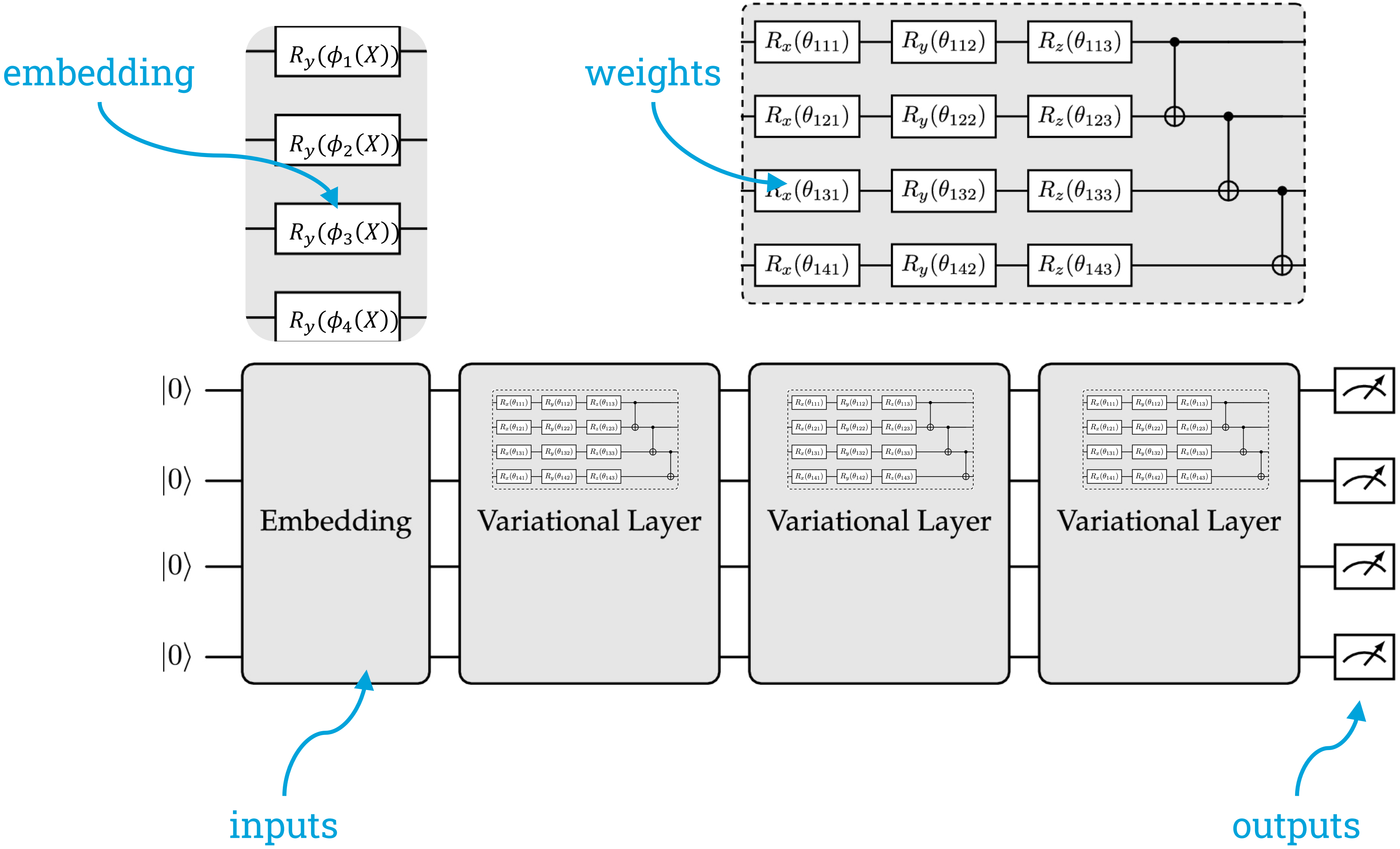

Quantum physics-informed neural networks (QPINNs)

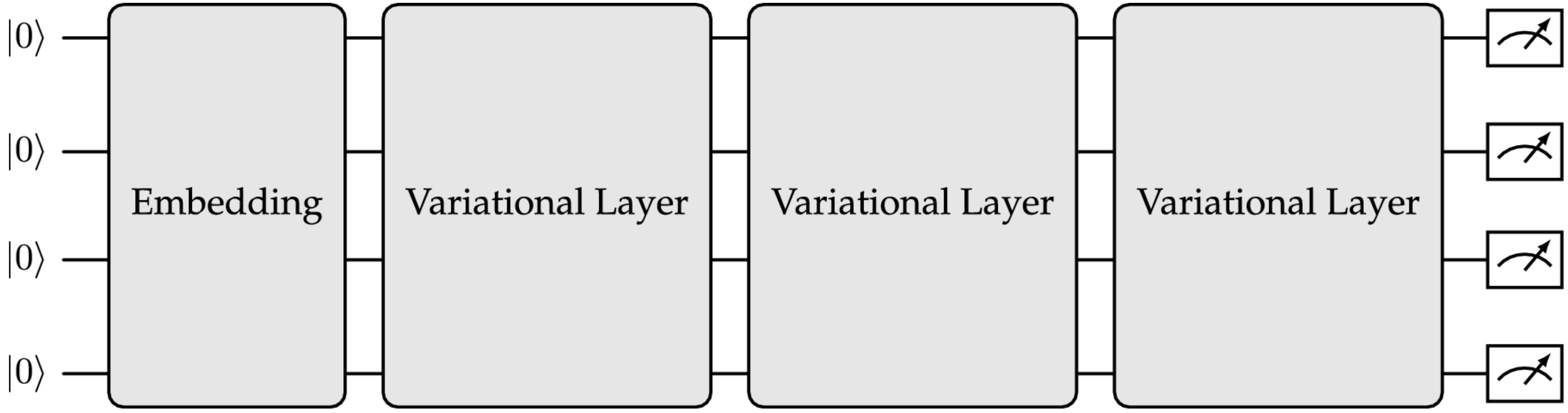

basis

$\{b_i(X)\}$

coefficients

$\{c_{ij}(\Theta)\}$

$$f(X,\Theta) = \sum_{i,j} c_{ij} b_i^\dagger(X) b_j(X)$$

Our approach: Trainable embedding (TE-QPINNs)

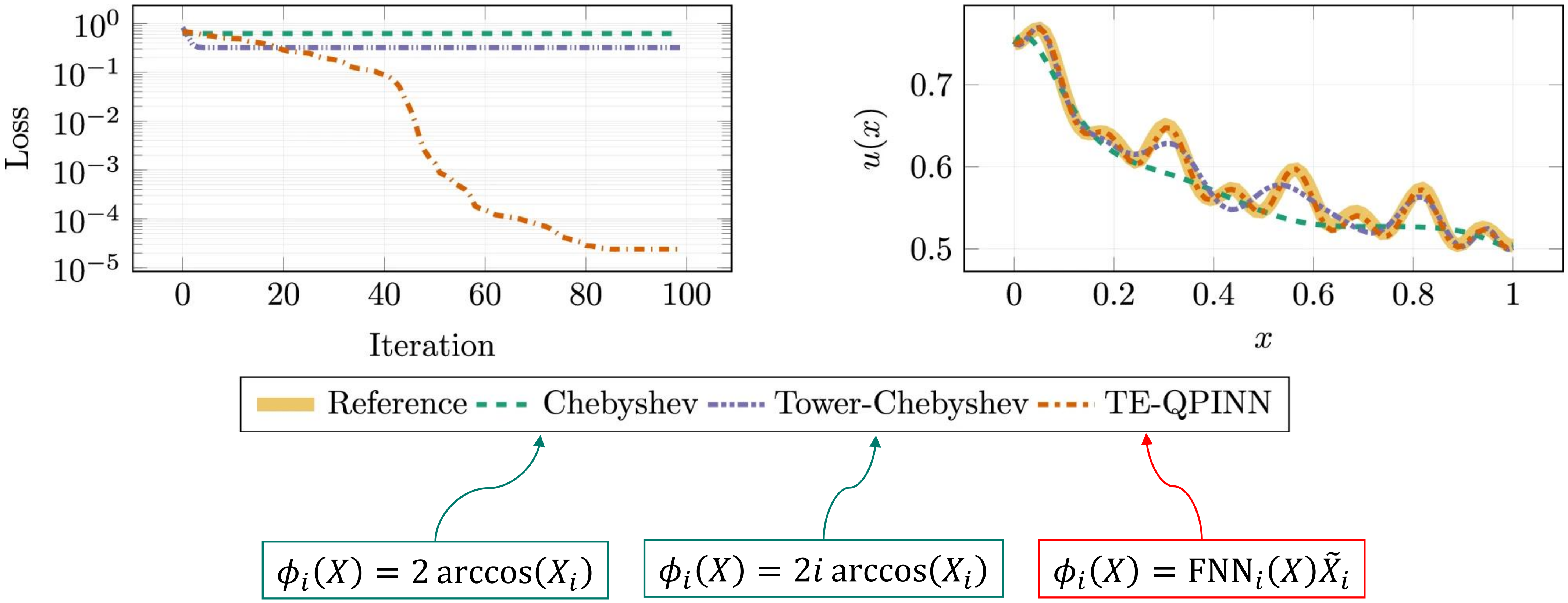

S. Berger et al., Trainable embedding quantum physics informed neural networks for solving nonlinear PDEs, *Sci. Rep. 15 (2025)*

TE-QPINNs applied to Burger's equation

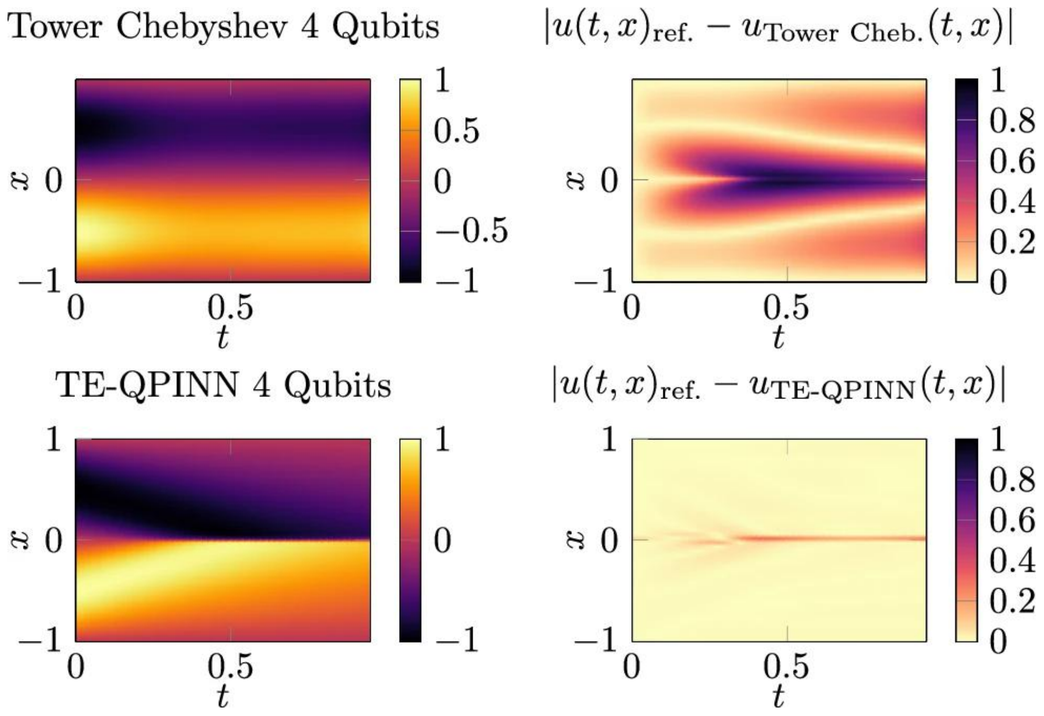

exact solution

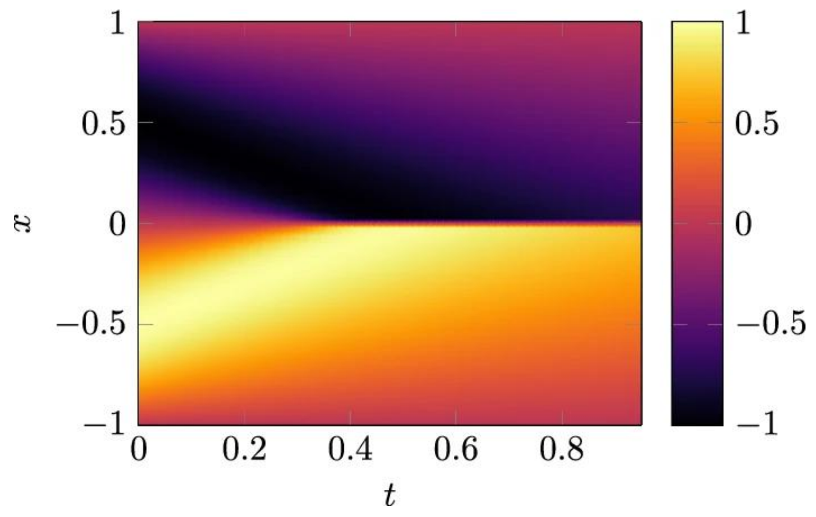

S. Berger et al., Trainable embedding quantum physics informed neural networks for solving nonlinear PDEs, *Sci. Rep. 15 (2025)*

TE-QPINNs applied to Burger's equation

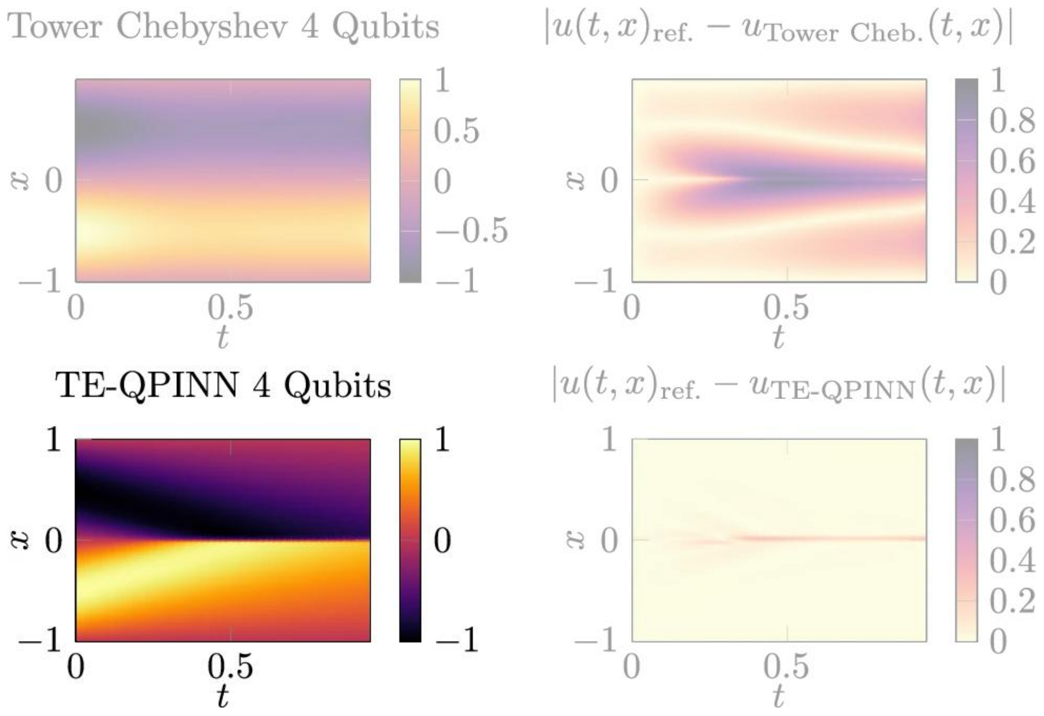

basis functions

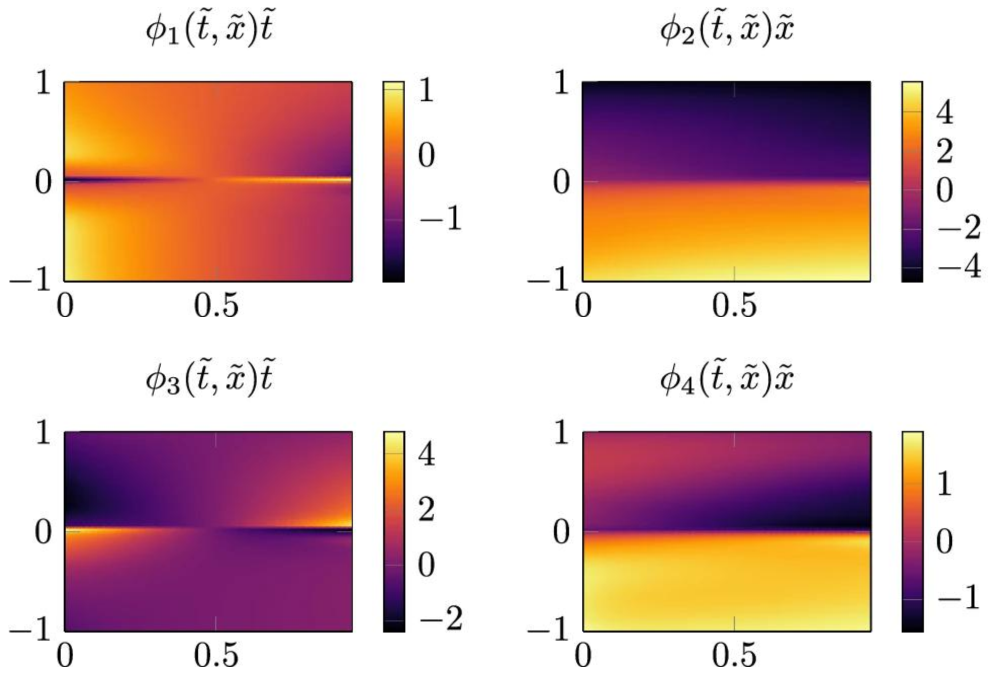

S. Berger et al., Trainable embedding quantum physics informed neural networks for solving nonlinear PDEs, *Sci. Rep. 15 (2025)*

TE-QPINNs applied to Burger's equation

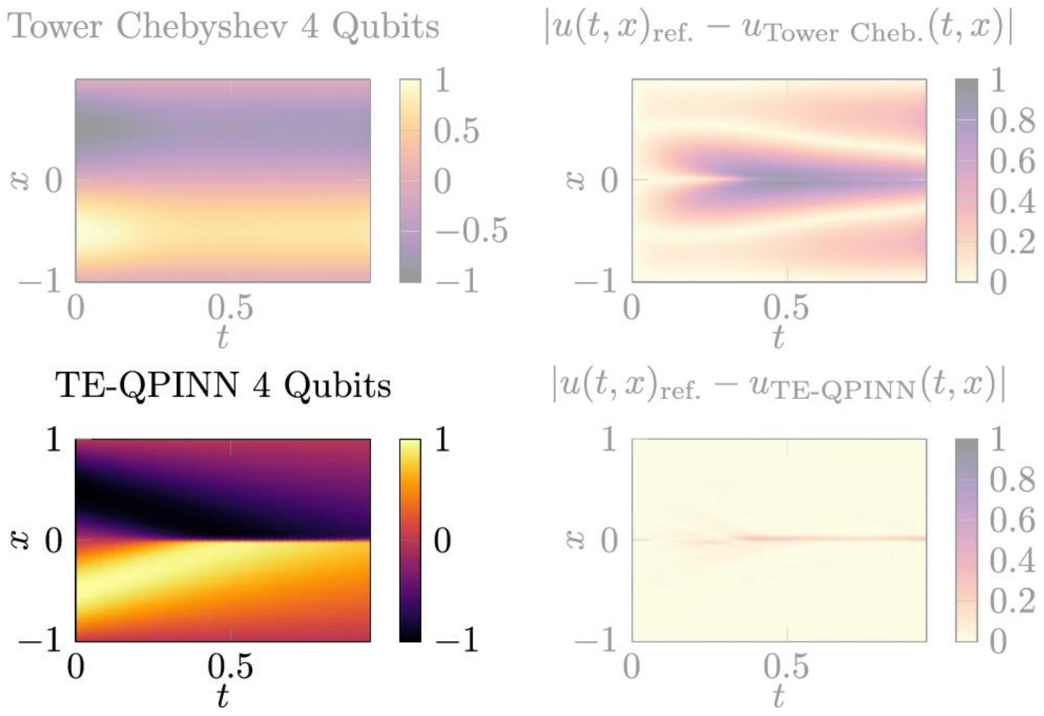

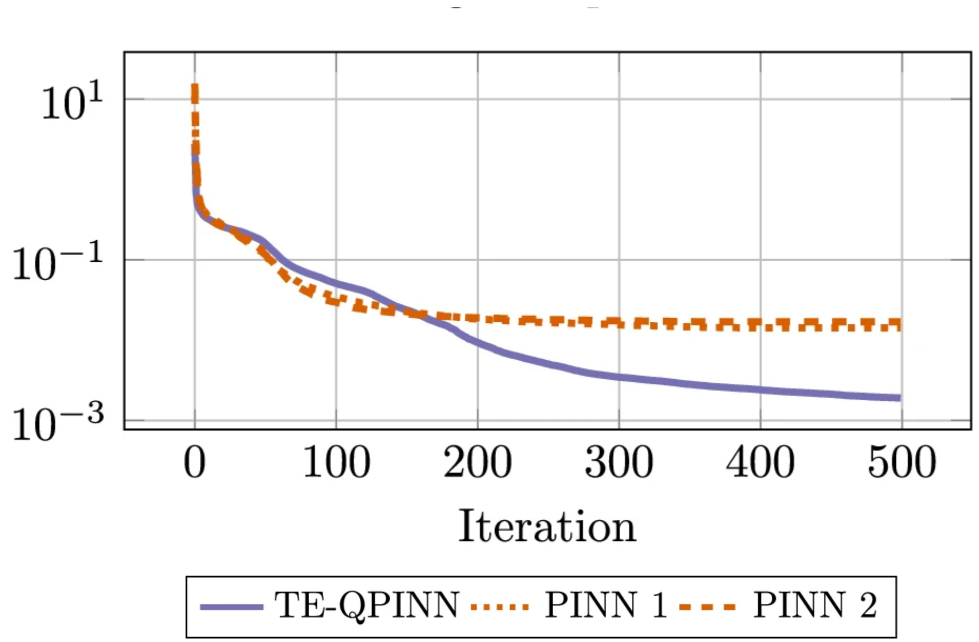

S. Berger *et al.*, Trainable embedding quantum physics informed neural networks for solving nonlinear PDEs, *Sci. Rep. 15 (2025)*

TE-QPINNs applied to incompressible NSE

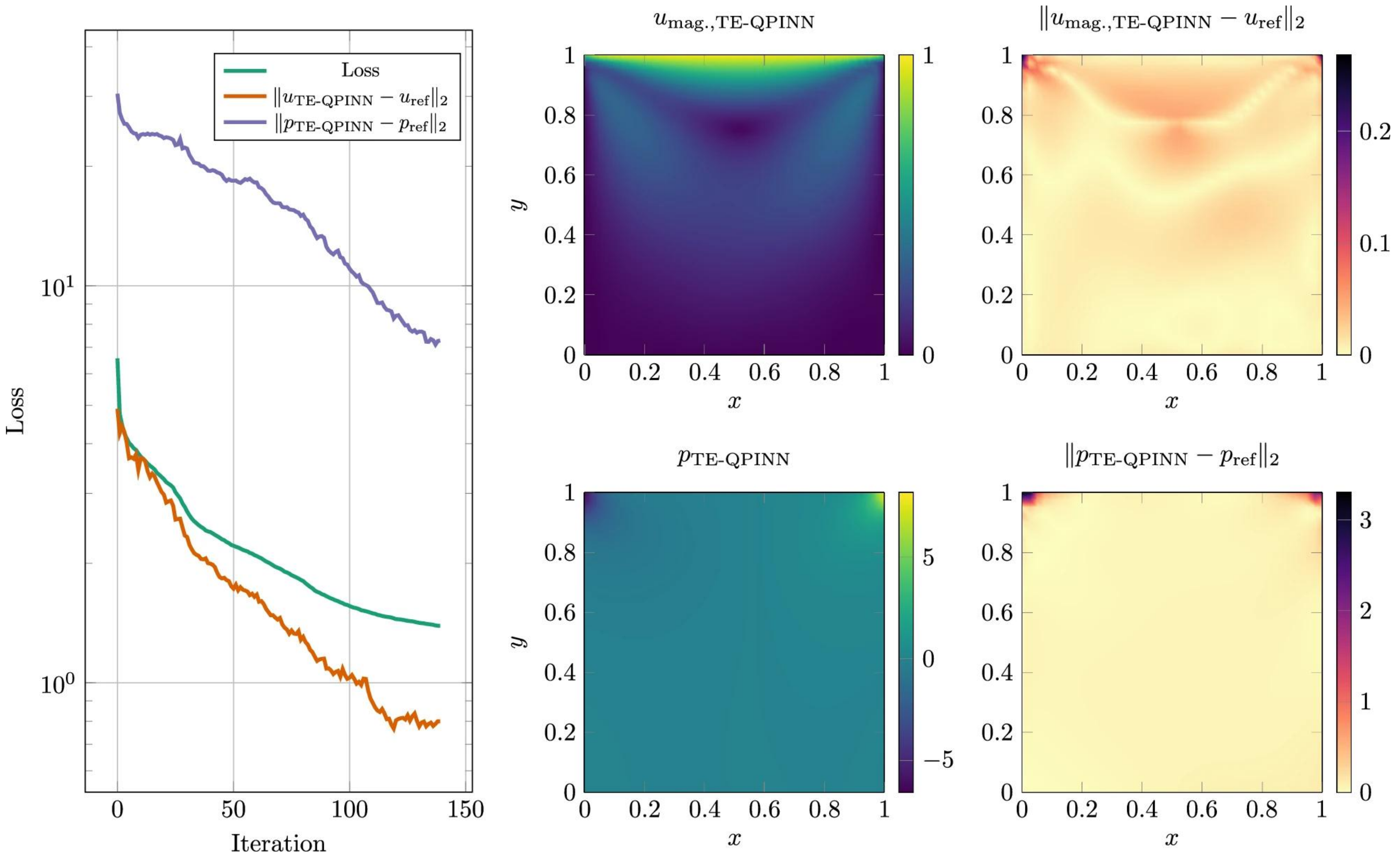

S. Berger et al., Trainable embedding quantum physics informed neural networks for solving nonlinear PDEs, *Sci. Rep. 15 (2025)*

TE-QPINNs applied to linear elasticity

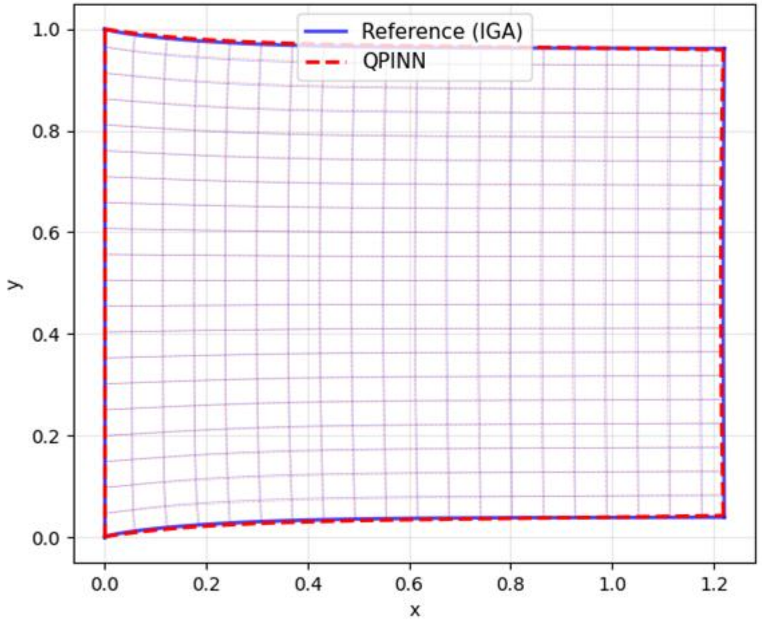

van Mises
stress ⇒

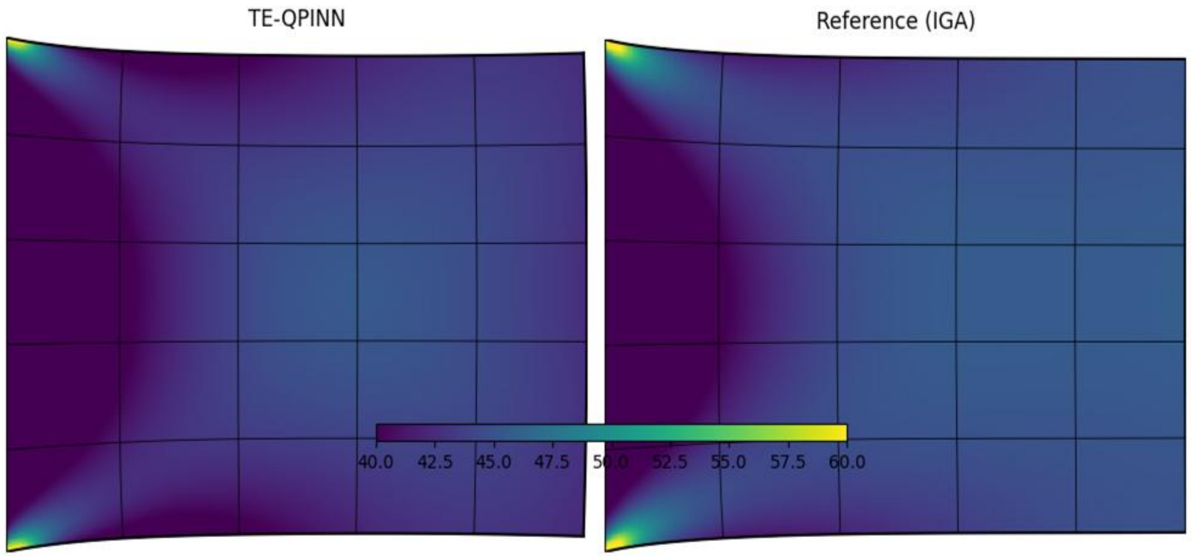

Error in
u and v ⇒

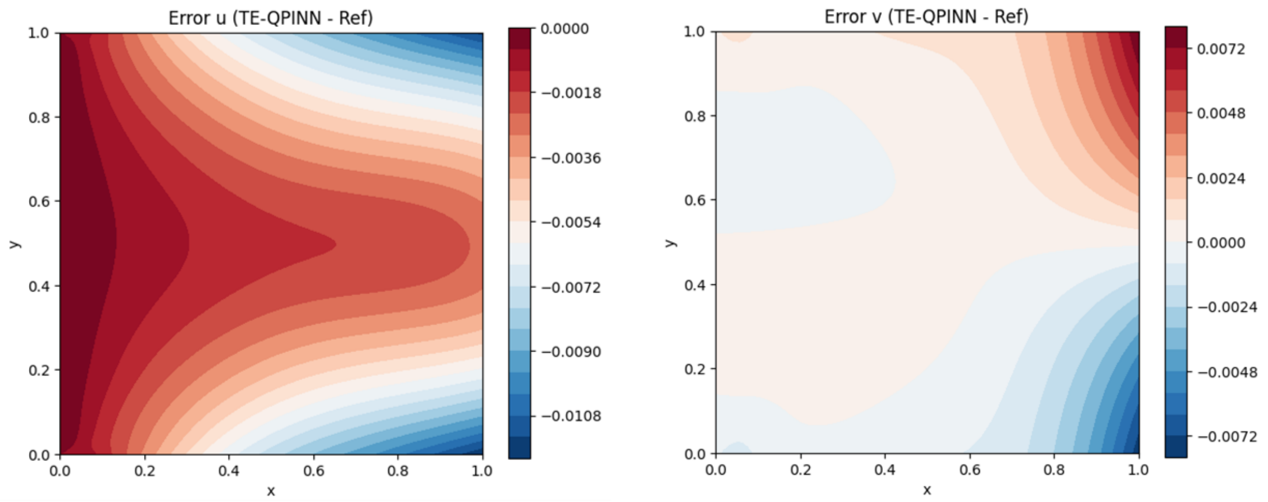

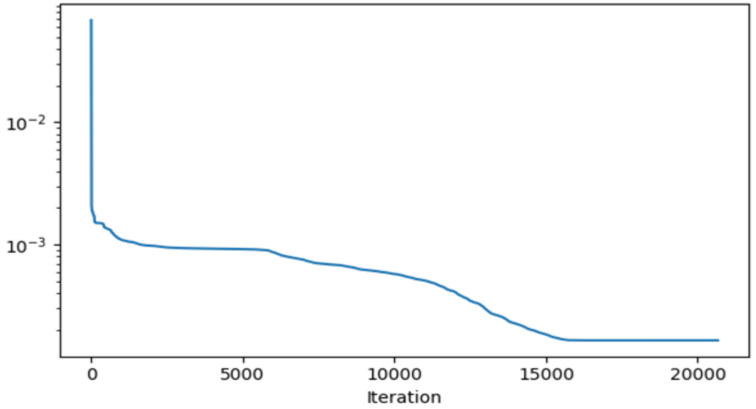

⇐ Loss
function